Isolation of neoantigen-specific T cell receptors for T cell receptor gene therapy

Inaugural-Dissertation

to obtain the academic degree

Doctor rerum naturalium (Dr.rer.nat)

submitted to the Department of Biology, Chemistry, Pharmacy
of Freie Universität Berlin

by

Corinna Grunert

2023

1st reviewer: PD Dr. med. Antonia Busse

2nd reviewer: Prof. Dr. med. Andreas Diefenbach

Date of defense: 29.04.2024

Acknowledgments

I would like to express my gratitude to my supervisor, PD Dr. med. Antonia Busse, for giving me the opportunity to be part of her team and pursuing this research. Thank you for your guidance, advice, and encouragement throughout my doctoral studies. I appreciate the support I received, and the trust placed in me to take on challenges and new tasks.

I would also like to extend my thanks to Prof. Antonio Pezzutto for his valuable feedback, scientific advice, and warm welcome into his research group. I am grateful to Prof. Thomas Blankenstein and Prof. Gerald Willimsky for their insightful discussions and collaboration on my research project. I would like to thank the members of the BIH Collaborative Research Grant "Targeting somatic mutations in human cancer by T cell receptor gene therapy" for their collaboration and support.
Additionally, I acknowledge Prof. Il-Kang Na and her group for allowing me to contribute to their research.

A special *thank you* to Caroline Peuker and Neşe Çakmak for their emotional support, scientific advice, and for being amazing company on late lab nights. Thank you for your friendship, both inside and outside the laboratory. I would also like to express my gratitude to all the wonderful colleagues and students I encountered in the Busse group.

Thank you, Maria and Tina, Amy, Bianka, Coco, Maria, Micha, Jens, Sarah, Sassy und Svenja for being an amazing family of friends.

I thank my entire family for supporting me throughout this time.
Ein ganz besonderes Dankeschön geht an meinen Bruder und an meine Tante.

Selbständigkeitserklärung

Hierdurch versichere ich, dass ich meine Dissertation selbstständig verfasst und keine anderen als die von mir angegeben Quellen und Hilfsmittel verwendet habe.

Corinna Grunert

Table of content

Summary

In recent years, adoptive T cell therapy has brought a revolutionary change in the treatment for B-cell leukemias, lymphomas and multiple myeloma. Along with T cells modified with chimeric antigen receptors (CARs), there is ongoing development of T cells modified with T cell receptors (TCRs). TCR-T cells are not restricted to recognizing surface antigens but can also recognize targets derived from intracellular antigens and specifically mutated antigens, including neoantigens. This increases the number of target antigens for developing precision immunotherapies with high tumor specificity and a favorable safety profile. Challenges in the development include identifying suitable tumor epitopes, isolating high-affinity TCRs, and expanding patient TCR-T cells in sufficient quantities with the preferred phenotype.

To tackle these questions, the first objective was to isolate neoepitope-specific TCRs from different repertoires in a side-by-side investigation. These repertoires included patients' peripheral blood lymphocytes (PBLs) and tumor-infiltrating lymphocytes (TILs), PBLs of healthy donors, and a humanized mouse model. Results of the study show the advantage and feasibility of stimulating healthy donor repertoires and humanized mice TCR repertoires to generate mutation-specific TCRs with different specificities, especially when patient material is sparse. It was also shown that no specific TCR was isolated for neoepitope used in this study from the patients' own repertoire.

Furthermore, it is desirable to target recurrent mutations. A high-affinity TCR specific to the HLA-B*07:02-restricted epitope of the common lymphoma-specific driver mutation MyD88 L265P was successfully isolated from the healthy donor repertoire. However, screening 24 donors was necessary to identify one high-avidity TCR that could recognize tumor cells endogenously expressing L265P. This highlights the influence of the individual TCR repertoire of the T cell donor, along with inherent immunogenicity of the epitope.

Lastly, the expansion of gene-modified T cells is a crucial part of the TCR-T cell manufacturing process. This is especially true for patients with insufficient numbers of T cells, or for T cells with insufficient expansion during the standard culture process. The feasibility of prolonging the T cell culture processes with minimal alteration to the standard process was demonstrated in the last presented study. These findings need to be confirmed on a GMP-compliant manufacturing platform but hold the promise to increase accessibility of adoptive T cell therapy (ATT) for certain patients.

Zusammenfassung

In den letzten Jahren hat die adoptive T-Zell-Therapie (ATT) einen revolutionären Wandel in der Behandlung von B-Zell-Leukämien, Lymphomen und multiplem Myelom gebracht. T-Zellen können mit T-Zellrezeptoren (TCRs) modifiziert werden und können neben Oberflächenantigenen auch intrazelluläre und spezifisch mutierte Antigene, wie zum Beispiel Neoantigene, erkennen. Dies erweitert das Spektrum möglicher Antigene für die Entwicklung von Präzisionsimmuntherapien mit hoher Tumorspezifität. Herausforderungen bei der Entwicklung dieser Therapien sind die Identifizierung geeigneter Tumorepitope, die Isolierung hochaffiner TCRs und die Vermehrung modifizierter T-Zellen in ausreichender Menge und mit gewünschtem Phänotyp.

Das erste Ziel dieser Arbeit war es verschiedene TCR-Repertoires zur Isolierung neoantigen-spezifischer TCRs nebeneinander zu vergleichen. Hierbei wurden periphere Lymphozyten (PBL) und tumorinfiltrierende Lymphozyten (TIL) von Patienten, PBLs von gesunden Spendern und ein humanisiertes Mausmodell untersucht. Die Ergebnisse zeigten, dass mutationsspezifische TCRs sowohl aus TCR-Repertoires gesunder Spender als auch humanisierter Mäuse isoliert werden können und diese Repertoires eine verfügbare TCR-Quelle darstellen, vor allem wenn Patientenmaterial begrenzt ist. Ebenfalls wurde gezeigt, dass für die in dieser Studie ausgesuchten Neoepitop-Kandidaten, kein spezifischer TCR aus dem eigenen Repertoire der Patienten generiert werden konnte.

Von Vorteil ist auch die Isolierung von TCRs, die gegen rekurrente Mutationen gerichtet sind. Hierfür wurde ein hochaffiner TCR aus dem gesunden Spenderrepertoire isoliert, welcher für das HLA-B*07:02-restringierte Epitop der Lymphom-spezifischen Treibermutation MyD88 L265P spezifisch ist. Ein Screening von 24 Spendern war erforderlich, um einen TCR mit hoher Avidität zu identifizieren, der Tumorzellen erkennen konnte, die L265P endogen exprimieren. Dies verdeutlicht den Einfluss des individuellen TCR-Repertoires des T-Zell-Spenders, sowie der inhärenten Immunogenität des Epitops auf den TCR-Isolierungserfolg.

Ein entscheidender Teil des TCR-T Herstellungsprozess ist die Expansion gentechnisch modifizierter T-Zellen. Dies trifft insbesondere für Patienten mit unzureichender Ausgangszahl an T-Zellen oder für T-Zellen, die während des Standard-Kulturverfahrens nicht ausreichend proliferieren, zu. In der vorgestellten Studie wurde gezeigt, dass die

Verlängerung des Standardherstellungsprozesses zu höheren TCR-T Zellausbeuten führt und zudem der Phänotyp der hergestellten Zellen vergleichbar mit dem der Zellen aus dem Standardprozess ist. Diese Ergebnisse müssen noch auf einer GMP-konformen Produktionsplattform bestätigt werden, versprechen aber, den Zugang zur ATT für bestimmte Patienten zu verbessern.

1 Introduction

1.1 The T cell receptor complex

T lymphocytes play an essential role in the cell-mediated adaptive immune response to pathogens, i.e., bacteria, viruses, and parasites. Additionally, they can recognize mutated peptide sequences and differentiate between self and non-self. The ability of T cells to detect foreign antigens is realized by the T cell receptor (TCR). Mutated peptide sequences are bound to the major histocompatibility complex (MHC) and presented on the cell surface of other host cells to circulating T cells.

Each TCR is a heterodimer, composed of two distinct transmembrane polypeptide chains. The majority of TCRs consist of an α and β chain (TCRα and TCRβ), and only very few T cells carry a TCR made up of a TCR γ and δ chain. Every chain consists of an immunoglobin-like variable - antigen-binding - region and a constant domain. The diversity of the variable region is realized by the combination of different variable (V), diversity (D), and joining (J) segments of the TCRβ chain, and the combination of V and J segments for the TCRα chain[1–3]. Further enzymatic modification at the junctions of different V(D)J regions increases the diversity of the TCR repertoire by random insertions or deletions of nucleotides. This junctional diversity leads to hypervariable regions, namely complementary determining regions 1-3 (CDR1-CDR3). The CDR3 region is responsible for antigen binding and determines the specificity of the TCR. An estimate of the theoretical diversity of the TCR repertoire is 10^{15}, however, the actual number of unique TCR clonotypes in the human body might range from 10^6 to 10^8 TCR sequences[4–7]. This great diversity of the TCR repertoire enables the recognition of a multitude of different antigens.

The TCRαβ-heterodimer is non-covalently associated with the CD3 chains δ, γ ε and ζ. While TCRαβ-chains have no intracellular signaling domains, TCR activation is transmitted intracellularly by the CD3ζζ homodimer. Signal transduction is realized via phosphorylation of immunoreceptor-based tyrosine activation motifs (ITAMs) on the intracellular domain of CD3ζ chains. Mature T cells are divided into two subsets by their expression of either CD8 or CD4 co-receptors, determining the ability to associate with either MHC class I or class II molecules, respectively.[8] These co-receptors stabilize the TCR-MHC complex by binding to the respective peptide-MHC (pMHC) and enhance the

TCR signaling. The function of CD4+ T cells is classically viewed as helper cells whereas CD8+ T cells are termed cytotoxic T cells. The CD4 monomer is composed of 4 domains, whereas the CD8 molecule is a heterodimer consisting of an α and a β chain. A schematic illustration of the TCR-CD3 complex of a CD8+ T cell interacting with a pMHC molecule on an antigen presenting cell (APC) is depicted in Figure 1.

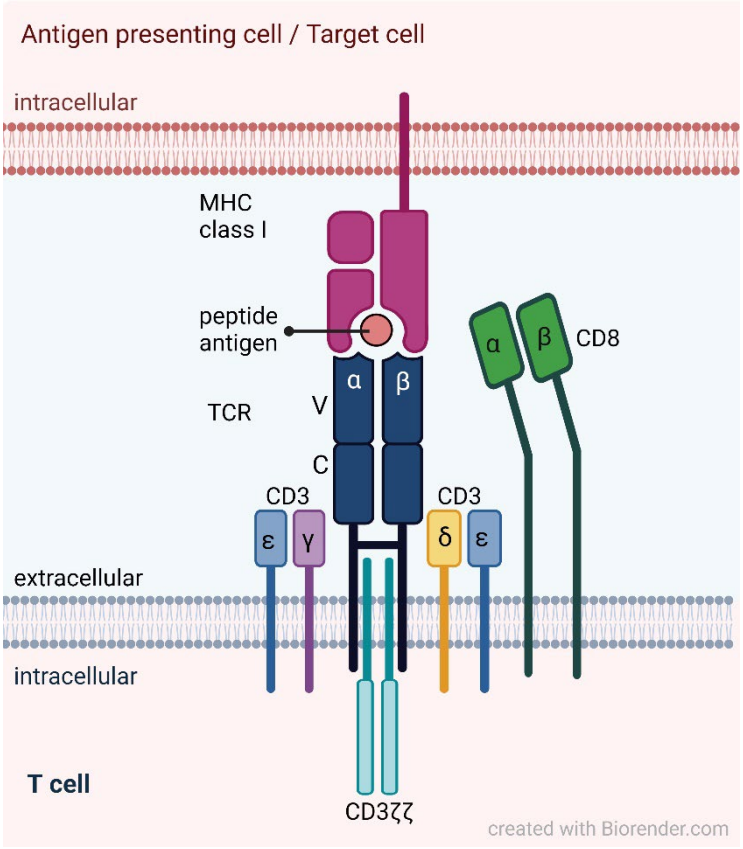

Figure 1: Schematic structure of the TCR-CD3 complex and MHC class I binding T cell receptor (TCR) A TCR-CD3 complex is depicted with co-stimulatory molecule CD8 binding a peptide-MHC class I complex (pMHC). TCR alpha and beta chains are composed of a variable (V) and a constant (C) region (dark blue). The CD3 complex is composed of CDR3 γ, δ and two ε chains, and the associated homodimer of CD3ζζ. The co-stimulatory heterodimer of CD8 is depicted in green. The TCR can bind pMHC complexes (magenta) via its variable regions.

1.2 T cell maturation and activation

Lymphocytes originate from hematopoietic precursor cells in the bone marrow and undergo T cell development and maturation in the thymus. This process involves a series of differentiation and selection events and is characterized by the expression of CD4 and CD8 co-receptors, or the lack thereof. Initially, T cells are negative for both co-receptors (termed double negative, DN) and undergo rearrangements of the TCR β gene to create

a functional TCR β chain. At this stage, a successfully rearranged TCR β chain is paired with an invariant α chain to form a pre-TCR and cells start becoming double positive for CD8 and CD4 (DP).[9] DP cells then undergo extensive expansion followed by the rearrangement of the TCR α chain. Thymocytes with a completely rearranged TCR will interact with thymic APCs which present self-antigens on MHC class I and class II molecules to the immature thymocytes. T cells that are able to interact with pMHC molecules with low affinity receive signals for proliferation and differentiation into either CD8+ (pMHC I interacting) or CD4+ (pMHC II interacting) single-positive T cells – a process called positive selection. T cells that fail to recognize MHC molecules will undergo apoptosis (death by neglect). Thymocytes carrying a TCR with an affinity above a certain threshold towards self-antigens are negatively selected in the thymic medulla. This clonal deletion eliminates potential autoreactive T cells. Matured, naïve T cells will then leave the thymus, circulate and migrate into peripheral lymphoid organs and are restricted to one single MHC molecule.[9–11]

T cell activation occurs when a foreign antigen bound to an MHC molecule is recognized. This process involves the binding of the TCR to the pMHC complex, followed by signal transduction into the cytoplasm and the initiation of a series of intracellular signaling pathways. For sufficient activation, T cells require three signals. The initial signal is the binding of the TCR to the pMHC complex. Co-stimulatory molecules provide the second signal that amplifies the activation signal in a non-specific manner.[12,13] T cell activation and expansion are further regulated by secreted cytokines, providing the third signal through cytokine receptor signaling[14]. Once activated, T cells undergo clonal expansion and differentiate into different subsets, such as effector or memory T cells.

1.3 The MHC class I complex and antigen presentation

The presentation of antigen fragments is a crucial process for the immune system to recognize foreign invaders. In complex with the MHC molecules short peptide sequences are displayed on the cell surface. MHC molecules are glycoproteins, subdivided into the two above mentioned classes: MHC class I and class II. CD8+ T cells interact with MHC class I molecules which present endogenous antigens, independent of their cellular localization, including tumor and viral antigens. MHC class II molecules present exogenous antigens, such as bacterial or fungal antigens, which are internalized by

phagocytosis or endocytosis and processed within the endocytic pathway and presented to CD4+ T cells.[11]

The MHC class I molecule is made up of a polymorphic α chain and is stabilized by a polypeptide chain, called β2 microglobulin[15]. Genes encoding for the MHC class I chain in humans are human leukocyte antigen (HLA) complex A, -B, and -C[16,17]. The α chain conformation enables the binding of peptide fragments of a length of 7 to 13 amino acids. These fragments are called epitopes and are anchored in the MHC groove via their N- and C-terminal amino acids and some central amino acid side chains. The conformation and folding of peptides in the binding groove depend on the amino acids composition, and therefore, different HLA haplotypes have preferences when binding peptide sequences[18]. MHC class I binding peptides are typically derived from cytosolic or nuclear proteins. In most cases, small peptide fragments are generated by proteasomal processing, followed by further degradation, particularly of the N-terminal end, by cytosolic proteases. Interferon y (IFNy) induces the expression of alternative catalytic subunits of the proteasome, now called immunoproteasome. Its cytolytic activity is slightly altered and produces increased amounts of polypeptides with hydrophobic residues, which in turn are preferred residues for anchoring to most MHC class I molecules.[19–21] Cleaved polypeptides are transported to the endoplasmic reticulum (ER) by transporter associated with antigen processing (TAP) proteins. Here, MHC class I molecules are loaded with polypeptides by chaperon proteins and transported to the cell surface by the Golgi-apparatus.[22,23]

1.4 Cellular immune response to cancer

Investigations in mice and rats first showed that the host immune system is able to respond to tumors[24–26], however, mechanisms of how this resistance is induced were not clear. Following the postulation of the existence of a putative antigen that provides protection from the outgrowth of transplanted tumors, termed tumor-specific transplantation antigen by Sjögren et al.[27], advances were made identifying T cells as a significant player in tumor and transplant rejections[28,29]. The ability of tumor recognition, rejection, and control was first termed immunosurveillance by Burnet[30] and later extended by the cancer immune-editing hypothesis[31]. This hypothesis has since been controversially discussed, especially in regard to spontaneous - in contrast to induced or

transplanted - tumors. It has later been challenged by reports of metastasis formation independent of the immune system and suppression of anti-tumor response in spontaneous tumors[32,33].

Primarily cytotoxic CD8+ T cells, but also CD4+ T helper cells play an essential role in the anti-tumor response. After the recognition of tumor antigens, antigen-specific CD8+ T cells are activated and can directly lyse target cells. Cytotoxicity is mediated by exocytosis of perforins and granzyme B, which is released into the tumor cell and induces apoptosis[34]. Additionally, cytokines such as IFNy, an activator of macrophages and a stimulator of MHC expression on APCs, are produced[35]. Activated CD4+ T cells assist the immune response by promoting CD8+ T cell activation. Differentiation of CD4+ T cells in different pro- or anti-inflammatory subtypes, such as TH1, TH2, or regulatory T cells, is influenced by the immediate cytokine composition of their environment.[36]

1.5 Tumor antigens

Tumor-associated and tumor-specific antigens

The first report of a human tumor antigen was published in 1991 by Thierry Boon and his peers demonstrating that melanoma cell lines were recognized by autologous cytotoxic T lymphocytes (CTLs). The MAGE-A1 antigen was identified to be presented on HLA-A*01 molecules and its expression was detected in several melanomas from different patients.[37] This finding was a milestone leading to the discovery of several other tumor rejection antigens, such as MAGE-A3 and NY-ESO-1[38–40]. Up to today, numerous antigens have been identified. They are classically seen to belong to two different categories, tumor-associated antigens (TAAs) and tumor-specific antigens (TSAs)[41].

TAAs are non-mutated self-antigens that are overexpressed in tumor cells, and to a lesser extent expressed in healthy tissue. TAAs can be derived from proteins of any subcellular compartment and presented to specific T cells on the cell´s MHC complex. TAAs which are expressed at significantly higher levels on tumor cells compared their cognate expression on healthy tissue are suitable targets for cell-based therapies. TAAs can be grouped into three main categories. Differentiation or lineage-specific antigens are characterized by their tissue specificity. Examples of lineage-specific antigens are Melan-A/MART-1[42], tyrosinase[43], or gp-100[42]. Secondly, cancer germline antigens or cancer-

testis antigens are restricted to adult reproductive tissue, such as testis and placenta, e.g. antigens of the MAGE family or NY-ESO-1, among many others. Overexpressed antigens belong to the third group of TAAs and are expressed in normal and tumor tissue. Examples of this group of TAAs are HER2, survivin, and mesothelin[44–47].

TSAs, on the other hand, are antigens confined to tumor tissue only. They include mutated antigens resulting from a genetic mutation or transcriptional alteration, e.g. mutated KRAS, PIK3CA, or MyD88, and antigens resulting from post-transcriptional, tumor-associated changes, for instance in glycosylation of transcribed peptides, for instance MUC1. Oncoviral antigens are derived from tumorigenic transforming viruses, such as EBV LMP1 and EBNA1, HPV E6 and E7, or HCV core protein. Idiotypic antigens in B-cell and T cell lymphomas and leukemias are antigens where clonal aberration leads to expansion of a clonal B-cell/T cell population with a unique idiotype. Neoantigens are TSAs that arise from somatic alterations in tumor cells which include single nucleotide variants (SNVs) - non-synonymous point mutations, insertion-deletion events, chromosomal rearrangements leading to fusion genes and altered gene expression, or viral integration.

Strategies targeting TSAs have several advantages over strategies targeting TAAs. Undesired on-target toxicity can occur when targeting TAAs, as seen in different studies. For example, severe cardiac toxicities were observed in two patients in a study targeting MAGE-A3 antigen with TCR-T cells, leading to the early termination of the trial. Severe adverse events have also been observed with other targets, highlighting the need for a comprehensive analysis to exclude on-target toxicities before transitioning a new T cell-based approach into the clinic.[48–51] Conversely, the absolute tumor specificity of TSAs minimizes the risk of undesired on-target toxicities. Neoantigens, therefore present a safer target. In contrast to TAAs, high-affinity TCRs can be isolated for neoantigens from the human repertoire as they are not subjected to central immune tolerance. Ideally, neoantigen targets are recurrent driver mutations, as a loss of the mutation would present a severe loss of tumor cell fitness and is therefore less likely to happen. However, the vast majority of cancer mutations are passenger mutations. These mutations bear the risk of being lost during targeted therapy. Moreover, they are unique to the patient which calls for a highly individualized treatment approach.

Neoantigen predictions and identification

Various algorithms have been developed to identify mutational events such as SNVs, indels or fusion of proteins from genomic sequencing data of cancers. Furthermore, prediction algorithms have been further developed to evaluate proteasomal digestion of proteins and binding affinities of peptide fragments to MHC molecules.[52–55] Some algorithms include predictions of the ability of the potential neoepitope to elicit an immune response, i.e. to activate T cells. However, for a more comprehensive prediction additional features of neoantigen candidates should be evaluated. The dissimilarity of the peptide fragment compared to self-peptides, and homology to known viral or pathogenic peptides is suggested to increase immunogenicity[56]. Evaluations should additionally include molecular features of neoantigens which might influence clinical outcome[57]. Now efforts are made to classify neoantigens by their functional impact – to identify potential recurrent and driver mutations[56,58]. However, a majority of predicted neoantigens might not be presented by the MHC on tumor cells. Despite significant progress in neoantigen prediction, the actual immunogenicity and the targetability of putative peptide fragments has to be verified experimentally.

Mass spectrometry (MS) can be applied to identify potential neoantigens which were eluted from MHC molecules, verifying the processing and presentation of predicted putative neoantigens[59–61]. Additionally, MS immunopeptidomics enables the identification of epitopes arising from post-translational modifications, aberrant splicing, or translational errors[62,63]. Identifying neoantigens by MS immunopeptidomics protocols is challenging due to the often low amount of patient material available for analysis and the complexity of the immunopeptidome. Advancements have been made by varying experimental conditions for the elution, fractioning, and detection of MHC-bound peptides, as well as improved instrument sensitivity and detection limits, however, some presented peptides might still be missed by this approach.[64] Additionally, new tools are being developed to predict neoantigens from splice variants[65].

1.6 T cell-based immunotherapy against cancer

Adoptive T cell therapy with unmodified T cells

Tumor-infiltrating lymphocytes (TILs) are potentially tumor-reactive cells that can be isolated and expanded ex vivo before reinfusing them into the patient. A pioneering study using TILs as an adoptive T cell therapy (ATT) was conducted in the late 1980s by Rosenberg et al. treating patients with advanced metastatic melanoma[66]. Results from this study were encouraging and paved the way for ATT approaches. First studies were conducted with expanded CD4+ and CD8+ TILs of heterogeneous and unknown antigen specificity and restriction to the patient's MHC complex[67,68]. The production of TIL products was further improved to obtain cell products with known specificities and a more homogeneous cell population by using tumor-reactive TIL clones for expansion. Alternative protocols were investigated to improve the production of TILs, obtain cell products with higher tumor reactivity, or improved phenotypic characteristics.[69–72] Treatment with TIL products has been most successful in advanced melanoma, nevertheless, isolation and ex vivo expansion of TILs was investigated for several other cancers. Most promising results were obtained in cervical cancers, and head and neck squamous cell cancers, in particular in combination with inhibition of checkpoint molecule PD-1[73–76].

Genetically engineered T cells

T cells can be genetically modified to express a specific TCR or a chimeric antigen receptors (CARs) to confer anti-tumor specificity[77–82]. Genetic modification can be achieved for instance by retroviral gene transfer. The natural function of T cells remains in engineered T cells, meaning that they can recognize and respond to foreign antigens, circulate the periphery, and home to inflamed (antigen-expressing) tissues. ATT with CD19-directed CAR-T cells was granted "Breakthrough therapy" status by the FDA in 2014, based on the success in B cell neoplasm, which produced long-lasting remissions in more than 50% of patients in the initial clinical trials[83,84]. As of April 2023, there are four CAR T cell products directed against the B cell lineage-specific antigen CD19 and two CAR T cell products directed against the BCMA antigen in multiple myeloma approved in Europe[85]. Further products are in development, mainly against B cell lineage-specific antigens, but also against (almost) tumor-specific antigens of solid tumors like claudin 6,

mesothelin, CD2, or MUC1[86–89]. First studies with gene-modified TCRs in metastatic solid tumors are promising and show response rates of up to 67 % [79].

Both, CAR- and TCR-T cells share some similarities but also have some distinct features, advantages, and disadvantages. CARs are engineered artificial receptors composed of an extracellular domain with a single-chain variable fragment (scFv) linked to a signaling domain of a TCR. The scFv is derived from an antibody specific to the targeted cell surface antigen. It conveys the antibody-like recognition of its target to the intracellular signaling domain, which is responsible for signal transduction and T cell activation. Different CAR generations have been developed containing one or more signaling and co-stimulatory domains enhancing T cell activation.[90,91] Target antigen recognition and T cell activation are not dependent on pMHC interaction and can theoretically recognize any cell surface antigen independent of the patient's specific HLA-composition. Conversely, this also poses a limitation to applicability since antigens must be expressed on the cell surface and targeted molecules are only tumor-associated, which causes higher toxicities. CAR-T cells can achieve fast and high levels of cancer cell killing and have proven their high efficacy in clinical studies[92–95]. In some patients, persisting CAR-T cells were correlated with reduced relapse and longer progression-free survival[96–99]. However, CD19-negative relapse was observed in several cases and presents a mechanism for tumor evasion[100–104].

TCR-engineered T cells are genetically modified to express a TCR, specific to a particular antigen, thereby redirecting the antigen-specificity of T cells towards that target antigen. In general, TCRs can detect target antigens independently of their protein location. Short peptide sequences derived from extracellular and intracellular proteins can be targeted equally. This enables T cells to recognize tumor specific antigens such as neoantigens. In contrast to CAR-T cell therapy approaches, loss of surface antigen expression or downregulation of protein expression on the tumor cell surface does not lead to the loss of target presentation for TCR-T cell therapy. Consequently, a wide range of antigens can be targeted theoretically.

The TCR-pMHC interaction is crucial for target recognition and it enables TCR-T cells to recognize and kill target cells with high specificity. Off-tumor toxicity is minimized,

especially when targeting TSA, off-tumor, on-target toxicity is not expected. However, target recognition can be lost when relying on MHC restriction for antigen recognition by downregulation or complete loss of MHC expression, which presents a mechanism of tumor escape[105–107] for TCR-T based therapy approaches.

2 Scientific Aim

The presented studies focus on the isolation of antigen-specific TCRs directed against patient specific and recurrent neoantigens. For this purpose, the in vitro stimulation of T cells from different TCR repertoires was optimized to compare isolation success from the patient`s own and the healthy donor TCR repertoire. Results were also compared to isolation success in the humanized murine system to evaluate suitable TCR repertoires for generating high-affinity TCRs.

Especially recurrent mutations are a desired target for TCR-T cell therapy. Hence, the aim of the second publication was to isolate a high-affinity TCR directed against the MyD88 L265P mutation from healthy human donors. Isolated TCRs were to be characterized and potential therapeutic effects tested.

Furthermore, focusing on a relevant clinical hurdle when TCR-T or CAR-T therapy is the selected therapeutic approach, namely study dropouts due to production failure, the extension of established TCR-T expansion protocols in vitro was investigated. Findings of long-term (LT) expansion of T cells from murine models were to be transferred to the human setting. Therefore, the effect of a long-term expansion culture on transduced human T cells was investigated.

3 Original Research Articles

The presented research investigated the generation, isolation, and characterization of mutation-specific TCRs, and the long-term expansion of TCR modified T cells for prospective clinical applications. The following publications 1 and 2 describe the process of isolating and characterizing neoantigen-specific TCRs directed against patient specific (private) mutations, as well as the recurrent driver mutation MyD88 L265P. Mutation-specific TCRs directed against private mutations were isolated from different TCR repertoires and isolation success was compared between these repertoires for eight putative neoantigens. A high-avidity TCR directed against the recurrent MyD88 L265P mutation was successfully isolated from healthy donor TCR repertoires following stimulation of multiple donors. Lastly, publication 3 demonstrates that the production protocol for T cell products can be minimally modified by extending the culturing process after TCR transduction to broaden the accessibility of ATT to patients with low initial T cells counts or insufficient T cell expansion after the standard manufacturing process.

3.1 Publication 1: Isolation of Neoantigen-Specific Human T Cell Receptors from Different Human and Murine Repertoires

Abstract: Mutation-specific T cell receptor (TCR)-based adoptive T cell therapy represents a truly tumor-specific immunotherapeutic strategy. However, isolating neoepitope-specific TCRs remains a challenge. We investigated, side by side, different TCR repertoires—patients' peripheral lymphocytes (PBLs) and tumor-infiltrating lymphocytes (TILs), PBLs of healthy donors, and a humanized mouse model—to isolate neoepitope-specific TCRs against eight neoepitope candidates from a colon cancer and an ovarian cancer patient. Neoepitope candidates were used to stimulate T cells from different repertoires in vitro to generate neoepitope-specific T cells and isolate the specific TCRs. We isolated six TCRs from healthy donors, directed against four neoepitope candidates and one TCR from the murine T cell repertoire. Endogenous processing of one neoepitope, for which we isolated one TCR from both human and mouse-derived repertoires, could be shown. No neoepitope-specific TCR could be generated from the patients' own repertoire. Our data indicate that the successful isolation of neoepitope-specific TCRs depends on various factors such as the healthy donor's TCR repertoire or the presence of a tumor microenvironment allowing

neoepitope-specific immune responses of the host. We show the advantage and feasibility of using healthy donor repertoires and humanized mouse TCR repertoires to generate mutation-specific TCRs with different specificities, especially in a setting when the availability of patient material is limited.

Cancers; 2022; volume 14, issue 7: 1842; DOI: 10.3390/CANCERS14071842

cancers

MDPI

Article

Isolation of Neoantigen-Specific Human T Cell Receptors from Different Human and Murine Repertoires

Corinna Grunert [1,2,*], Gerald Willimsky [3,4,5], Caroline Anna Peuker [1], Simone Rhein [2], Leo Hansmann [5,6], Thomas Blankenstein [2,7], Eric Blanc [8], Dieter Beule [8], Ulrich Keller [1,2,5], Antonio Pezzutto [1,2] and Antonia Busse [1,2,5,*]

1 Department of Hematology, Oncology and Cancer Immunology, Campus Benjamin Franklin, Charité–Universitätsmedizin Berlin, 12203 Berlin, Germany; caroline-anna.peuker@charite.de (C.A.P.); ulrich.keller@charite.de (U.K.); antonio.pezzutto@charite.de (A.P.)
2 Max Delbrück Center for Molecular Medicine in the Helmholtz Association, 13092 Berlin, Germany; simone.rhein@mdc-berlin.de (S.R.); tblanke@mdc-berlin.de (T.B.)
3 Institute of Immunology, Campus Buch, Charité–Universitätsmedizin Berlin, 13092 Berlin, Germany; gerald.willimsky@charite.de
4 German Cancer Research Center, 69120 Heidelberg, Germany
5 German Cancer Consortium (DKTK), Partner Site Berlin, CCCC (Campus Mitte), 10117 Berlin, Germany; leo.hansmann@charite.de
6 Department of Hematology, Oncology and Cancer Immunology, Campus Virchow-Klinikum, Charité–Universitätsmedizin Berlin, 13353 Berlin, Germany
7 Berlin Institute of Health at Charité, 10178 Berlin, Germany
8 Core Unit Bioinformatics, Berlin Institute of Health at Charité, 10117 Berlin, Germany; eric.blanc@bih-charite.de (E.B.); dieter.beule@bihealth.de (D.B.)
* Correspondence: corinna.grunert@charite.de (C.G.); antonia.busse@charite.de (A.B.)

Citation: Grunert, C.; Willimsky, G.; Peuker, C.A.; Rhein, S.; Hansmann, L.; Blankenstein, T.; Blanc, E.; Beule, D.; Keller, U.; Pezzutto, A.; et al. Isolation of Neoantigen-Specific Human T Cell Receptors from Different Human and Murine Repertoires. *Cancers* **2022**, *14*, 1842. https://doi.org/10.3390/cancers14071842

Academic Editor: Lisa Ebert

Received: 4 March 2022
Accepted: 31 March 2022
Published: 6 April 2022

Simple Summary: T cell-based immunotherapy has achieved remarkable clinical responses in patients with cancer. Neoepitope-specific T cells can specifically recognize mutated tumor cells and have led to tumor regression in mouse models and clinical studies. However, isolating neoepitope-specific T cell receptors (TCRs) from the patients' own repertoire has shown limited success. Sourcing T cell repertoires, other than the patients' own, has certain advantages: the availability of larger amounts of blood from healthy donors, circumventing tumor-related immunosuppression in patients, and including different donors to broaden the pool of specific T cells. Here, for the first time, a side-by-side comparison of three different TCR donor repertoires, including patients and HLA-matched allogenic healthy human repertoires, as well as repertoires of transgenic mice, is performed. Our results support recent studies that using not only healthy donor T cell repertoires, but also transgenic mice might be a viable strategy for isolating TCRs with known specificity directed against neoantigens for adoptive T cell therapy.

Abstract: (1) Background: Mutation-specific T cell receptor (TCR)-based adoptive T cell therapy represents a truly tumor-specific immunotherapeutic strategy. However, isolating neoepitope-specific TCRs remains a challenge. (2) Methods: We investigated, side by side, different TCR repertoires—patients' peripheral lymphocytes (PBLs) and tumor-infiltrating lymphocytes (TILs), PBLs of healthy donors, and a humanized mouse model—to isolate neoepitope-specific TCRs against eight neoepitope candidates from a colon cancer and an ovarian cancer patient. Neoepitope candidates were used to stimulate T cells from different repertoires in vitro to generate neoepitope-specific T cells and isolate the specific TCRs. (3) Results: We isolated six TCRs from healthy donors, directed against four neoepitope candidates and one TCR from the murine T cell repertoire. Endogenous processing of one neoepitope, for which we isolated one TCR from both human and mouse-derived repertoires, could be shown. No neoepitope-specific TCR could be generated from the patients' own repertoire. (4) Conclusion: Our data indicate that successful isolation of neoepitope-specific TCRs depends on various factors such as the heathy donor's TCR repertoire or the presence of a tumor microenvironment allowing neoepitope-specific immune responses of the host. We show the advantage and feasibility of using healthy donor repertoires and humanized mouse TCR repertoires to generate

mutation-specific TCRs with different specificities, especially in a setting when the availability of patient material is limited.

Keywords: neoantigens; T cell receptor (TCR) therapy; tumor-specific TCR; antigen-specific T cell; T cell receptor repertoire

1. Introduction

Remarkable clinical responses in patients with cancer have been achieved by T cell-based immunotherapy, especially in those with high mutational burden. Subsequent events of single point mutations may be sufficient to drive an oncogenic transformation in certain cancers [1]. Non-synonymous, somatic mutations can further accumulate in tumor cells over time, potentially resulting in the generation of targetable neoepitopes. Increasing evidence in mouse models and clinical settings has shown that T cells specific to neoepitopes can lead to tumor regression after receiving adoptive T cell therapy (ATT) [2–5], or immune checkpoint inhibitor therapy [6]. Neoantigens have the advantage of being truly tumor-specific, and thus are not associated with on-target toxicity. Moreover, by definition, they should be unable to have induced central tolerance. Redirecting patients' peripheral T cells by transferring mutation-specific TCRs, targeting a defined tumor-specific antigen, has the potential to become one of the most effective immunotherapeutic approaches. Yet, in addition to the identification of tumor-specific neoepitopes, this strategy requires the isolation of high-affinity neoepitope-specific TCRs. So far, successful isolation of neoepitope-specific T cells has only been achieved for a minority of potential neoepitopes. Although neoepitope-specific T cells can be found among TILs [7,8], they are not easy to isolate and expand [9]. Moreover, they do not necessarily contain the entire repertoire of possible neoantigen-specific T cells [10,11]. Notably, in epithelium-derived tumors most TILs are not tumor-specific but rather virus-specific and incapable of recognizing cognate tumors. Only about 10% of intratumoral CD8+ T cells were reported to recognize autologous tumor cells, and only a minority of reported somatic mutations induce T cell immune responses in epithelial cancers [12,13]. Even target antigens of predominantly TIL clones do not appear to be restricted to tumor tissue [14,15].

Often, the amount and availability of patient tumor material for isolating TILs is limited. In contrast, peripheral blood (PB) of cancer patients is easily accessible. The presence of a neoepitope-specific immune response can be detected in the memory T cell population provided that immunogenic neoepitopes are presented by the tumor and have resulted in successful T cell priming [16]. Furthermore, several studies have shown that PB from patients can be used to prime de novo neoantigen-specific T cells, presenting a useful source for the production of therapeutic T cell products [7]. Peripheral blood might contain a more diverse T cell repertoire in the naive T cell population as compared to TILs. However, so far T cells specific to predicted neoantigens could be isolated from PB only in a minority of cancer patients [11]. The failure to successfully identify tumor-specific T cells and isolate the specific TCRs, from both TILs and PB, could be due to tumor-related immunosuppression impeding the ability to build a potent immune response against neoepitopes during T cell priming at the tumor site. This hypothesis is supported by the observation of Strønen and colleagues, who successfully isolated neoantigen-specific T cell clones from PB of healthy donors, which were not detected in the patients' TIL [10]. Moreover, we and others have shown that an independent, non-tolerized T cell repertoire of an HLA-compatible healthy donor is a suitable alternative source for the isolation of neoantigen-specific T cells [10,17–19]. Although the risk of cross- and alloreactivity is increased when using donor TCR repertoires compared to the patient's own repertoire, this strategy has certain advantages: larger amounts of blood can be obtained from healthy donors than from most cancer patients, and the difficulty to isolate and expand cells from a presumably very low precursor frequency can be circumvented.

Using HLA-A*02:01-transgenic (ABabDII) mice [20], we succeeded in isolating high-affinity TCRs against self-antigens such as FLT3, against cancer testis antigens such as Mage-A1 and NY-ESO, and against viral antigens [21–23]. In these mice, mouse TCR α/β-gene loci are replaced with their human counterparts and mouse H2 molecules are exchanged for the human HLA-molecule HLA-A*02:01. The TCR repertoire of these mice has not been educated on normal human self-antigens and is therefore superior in generating and isolating TCRs for human self-antigens. The successful isolation of TCRs against viral antigens suggests that these mice might also be useful in generating neoantigen-specific T cells [24].

Here, we explored these different types of TCR repertoires to isolate specific TCRs directed against eight predicted HLA-A*02:01-restricted neoepitopes: patients' TILs and PB lymphocytes (PBLs), PBLs from HLA-A*02:01-matched healthy donors, and T cells from primed HLA-A*02:01-transgenic ABabDII mice. We isolated six TCRs from four healthy donors directed against four neoepitope candidates, and one TCRs from ABaaDII repertoire directed against one neoepitope candidate (for which a healthy donor-derived TCR was also isolated). Our data indicate that successful isolation of neoepitope-specific TCRs depends, at least in part, on the TCR repertoire of the donor.

2. Materials and Methods

2.1. Patients and Patient Material

Fresh tumor tissue, PB, and clinicopathological data of patients with localized solid tumors and at high risk of relapse were collected during surgery at initial diagnosis within a research project that aimed to develop mutation-specific T cells for ATT (ethics committee ID EA1/265/14, Charité–Universitätsmedizin Berlin: Collaborative Research Grant Project "Targeting somatic mutations in human cancer by T cell receptor gene therapy"). Two HLA-A*02:01-positive patients, one with colorectal and one with ovarian cancer, were selected for detailed T cell repertoire analysis.

2.2. Cell Cultures

All cell lines were cultured in RPMI 1640 medium (with stable Glutamine, Gibco), 10% FCS (Universität Heidelberg), 12.5 mM HEPES, 100 IU/mL penicillin, 100 µg/mL streptomycin (P/S), and 50 µg/mL gentamycin (complete medium, CM). Transduced PBLs were maintained in CM containing FCS purchased from PAN-Biotech (TCM). Cell line T2 and HEKT-GALV-g/p were kindly provided by the group of Prof. Uckert (Max Delbrück Center for Molecular Medicine, Berlin). Primary peripheral blood mononuclear cells (PBMCs) used for stimulations and expanded cytotoxic T lymphocytes (CTLs) were cultured in T cell medium containing 5% human serum type AB (hTCM, PAN-Biotec). Dendritic cells (DCs) were maintained in serum-reduced hTCM (1% human serum). Cytokine supplementation to the media is given in detail in the respective sections. All cytokines and growth factors, except for IL-2 (Proleukin®, Novartis, Basel, Switzerland), were purchased from PeproTech (Hamburg, Germany).

2.3. Identification of Neoepitope Candidates

Tumor and corresponding healthy tissue samples were analyzed by WES and RNA sequencing to identify expressed, non-synonymous somatic mutations. We have computed neoepitopes for all variants in protein-coding regions, that passed quality control filters, and variants showing at least one read from the mRNA sample (mRNA coverage, which covers the mutation locus (rna_coverage)). Additional filtration for higher mRNA level expression was not performed. The selection of candidate epitopes was based on high binding affinities to HLA-A*02:01 complex. Potential neoepitopes were predicted in silico for peptide-MHC (pMHC) binding using the artificial neural network algorithm NetMHCcon1.1a [25]. Neoepitopes were ranked according to their MHC-binding affinity. High-binding candidates were synthesized as short peptides (GenScript, Piscataway; NJ, USA) and encoded on tandem minigenes (TMG), ordered as gene-fragments (Gen-

eArt, Thermo Fisher Scientific, Waltham, MA, USA), and cloned into expression vector pcDNA3.1(-). Neoepitopes encoded on TMGs were flanked by 10 cognate amino acids, and multiple predicted neoepitopes were each separated by an alanine spacer to ensure proper proteasomal cleavage of the epitope. Enhanced-green fluorescent protein (eGFP) served as a reporter and was separated from the upstream minigene sequences via a GSG-p2A element. Transcription of the TMG plasmid results in one single RNA transcript. Individual epitopes are separated by an AAY sequence linker that ensures proteasomal cleavage [26]. TMGs were used for in vitro transcribed RNA (IVT-RNA) synthesis followed by nucleofection of APCs or direct plasmid nucleofection of target cell lines.

2.4. TIL Cultures and TMG Stimulation

TILs were isolated by dissecting tumor tissues, obtained after resection of the primary tumor, into small fragments and culturing 1–2 fragments in hTCM supplemented with IL-2 (50 IU/mL), IL-7, and IL-15 (both 5 ng/mL) for 12 days. Half-medium change was done every 2 to 3 days with supplemented interleukins. CD8+ TILs were separated from residual tumor tissue after days 12 of TIL culture with MACS CD8+ T cell isolation kit (Miltenyi Biotec, Bergisch-Gladbach, Germany) and cryopreserved until use. For the initial stimulation T cells, autologous DCs were generated from plastic-adherent monocytes with GM-CSF (800 IU/mL) and IL-4 (1000 IU/m) in serum-reduced hTCM over 3 days according to Dauer et al. [27]. For stimulations of T cells with TMG-derived IVT-RNA, immature DCs were nucleofected using Human Dendritic Cell Nucleofector™ kit (Lonza Group AG, Basel, Switzerland) according to the manufacturer's protocol. Cells were matured overnight with a cytokine-cocktail containing GM-CSF, IL-4, TNFa (10 ng/mL), IL-1ß (10 ng/mL), IL-6 (10 ng/mL), and PGE2 (1 µg/mL). Nucleofection efficiency was assessed by eGFP expression via flow cytometry 12 h after nucleofection. T cell stimulations were set up in wells of a 48-well plate, and 5×10^5 T cells/well were co-cultured with nucleofected DCs (TMG-DCs) at an effector to target ratio (E:T) of 10:1, calculated according to the nucleofection efficiency. IL-7 and IL-15 (each 5 ng/mL) were added to the medium on day 3, and cells were fed on day 6, 8, 10, and 12. Cytokine concentration was doubled on day 8, and expanding CTLs were transferred to the next larger well plate if necessary. TILs were restimulated with TMG-DCs twice, as described above, followed by an overnight co-culture and staining for CD8α (SK1, APC-H7-conjugated, BD Biosciences), CD3 (SK7, PerCP-conjugated, BD Biosciences, Franklin Lakes, NJ, USA) and CD137 (4B41, PE-conjugated, BioLegend®, San Diego, CA, USA) for single cell FACS sorting and TCR sequencing.

2.5. Generation of Neoepitope-Specific T Cells from PB

Patient and healthy donor CD8+ T cells were negatively selected from PBMCs using MACS CD8+ T cell Isolation Kit and frozen until further use. CD8-depleted PBMC were used for DC generation and maturation, as described above, after plastic adhesion or frozen for the following peptide stimulations. The neoantigen-specific T cell culture was adapted from Wölfl et al. [28]. Briefly, CD8+ T cells were thawed and rested overnight in hTCM containing IL-7 (5 ng/mL). Naive CD8+ T cell fractions were obtained by depletion of CD45RO+ and CD56+ cells (MACS microbeads, Miltenyi Biotec, Bergisch-Gladbach, Germany). Non-naive cells were recovered from the column. Autologous mature DCs were individually loaded with peptides at 2.5 µg/mL for 2 h in reduced hTCM. Peptide-pulsed, washed DCs were then pooled and used for T cell stimulation with an E:T of 10:1 for each peptide-loaded DC faction in wells of a 48-well plate at 5×10^5 cells/well. Expanding CTLs were maintained with IL-7/15 (5 ng/mL) as described above, and cytokine concentration was doubled on day 8 of co-culture. CTLs were restimulated once with irradiated, peptide-loaded, autologous, CD8-depleted PBMCs on day 14 of expansion culture. On day 10–12 after restimulation, peptide reactivity was screened for in an activation assay by measuring CD137 expression. Peptide-reactive CTLs were selected and sorted following a short co-culture with peptide-loaded T2 cells in the presence of monensin (GolgiPlug™, BD Biosciences, Franklin Lakes, NJ, USA) and an antibody against degranulation marker

CD107a (H4A3, PE-conjugated, BioLegend®, San Diego, CA, USA) for 3–4 h. Activated CD3+CD8+CD107+ CTLs were sorted for RNA isolation (RNeasy Micro Plus Kit, Qiagen, Hilden, Germany) into RLT buffer.

2.6. Immunization of ABabDII Mice

Animal experiments were performed according to institutional and national guidelines and regulations following approval by the responsible authority (Landesamt fuer Gesundheit und Soziales, Berlin, Germany). Mice were primed with synthesized predicted HLA-A*02:01-restricted peptides on day 0 with 150 µg of peptide in a 1:1 solution of Incomplete Freund's Adjuvant (IFA, Sigma-Aldrich, St. Louis; MO, USA) and 50 µg CpG1826 (Novus Biologicals) by subcutaneous injection. Mice were boosted three times, the earliest on day 21 after priming. Blood was collected 7 days after each boost, and mouse PBMCs were cultured with 1×10^{-6} M peptide overnight for Interferon-γ (IFN-γ) detection. Mice with IFN-γ-secreting CD8+ T cells in the periphery were sacrificed, and spleen and inguinal lymph nodes were collected. Splenocytes were isolated, and CD4+ cells were depleted. Splenocytes were expanded for 10 days in RPMI 1640 with 10% FBS, HEPES, NEAA, sodium pyruvate, 50 µM β-mercaptoethanol, 20 IU/mL IL-2, and 10^{-8} M peptide. After expansion, peptide-reactive cells were sorted in RLT buffer for RNA isolation following IFN-γ secretion assay (Miltenyi Biotech, Bergisch-Glattbach, Germany) and staining with antibodies against mouse CD3 (clone 17A2, APC-conjugated, BD Biosciences, Franklin Lakes, NJ, USA) and mouse CD8 (53-6.7, PerCP-conjugated, BD Biosciences, Franklin Lakes, NJ, USA).

2.7. TCRα/β Chain Identification

For single-cell (sc) TCR sequencing, expanded, single, viable CD3+CD8+ T cells were sorted into 96-well plates, and paired TCR sequencing was performed as previously described [29,30].

For bulk sorted CD3+CD8+CD107+ T cells, total RNA was extracted and 5′RACE-ready cDNA was synthesized using the SMARTer RACE kit (Takara Clonetech, Kusatsu, Japan). TCRα and β variable (TRAV/TRBV) chains were amplified as previously described [17] with TCRA (5′-CGGCCACTTTCAGGAGGAGGATTCGGACC-3′) or TCRB (TCRB: 5′-CCGTAGAACTGGACTTGACAGCGGAAGTGG-3′) gene-specific primers. Amplified PCR products were agarose-gel-purified, and corresponding bands were cloned using the Zero Blunt II TOPO vector (Invitrogen, Thermo Fisher Scientific, Waltham, MA, USA). A minimum of 20 bacterial clones were sequenced, and TRAV and TRBV chains were identified using the online IMGT.org vquest tool (http://www.imgt.org/IMGT_vquest/vquest, accessed between 24 February 2017 to 14 September 2021). The most frequent TRAV/TRBV chains were paired, and constant regions of identified TCRs were replaced by murine counterparts for expression in human PBLs. If more than one TRAV or TRBV sequence was dominant, all possible AV and BV chain combinations were assembled. TCRα and β chains were linked with a p2A element, and NotI and EcoRI restriction sites were added for restriction site cloning of the TCR cassettes into pMP71 γ-retroviral vector.

2.8. Virus Production and Transduction of PBLs

Packaging cell line HEKT-GALV-g/p, stably expressing MLV gag/pol and pALF-GALV, was transfected with 18 µg TCR-cassette-pMP71 vector to produce virus particle-containing culture supernatant. Culture supernatant was collected 48 h and 72 h after transfection. Healthy donor PBLs were activated on anti-hCD3/anti-hCD28 (clones HIT3a and CD28.2, respectively, BD Biosciences, Franklin Lakes, NJ, USA)-coated 24-well plates in 1 mL TCM supplemented with 400 IU/mL IL-2 at a density of 1×10^6 cells/mL for 48 h before transduction. Activated PBLs were spinoculated (800× *g*, 90 min, and 32 °C) with 1 mL cell-free virus supernatant 48 h after activation. Protamine sulfate was added to the medium at 4 µg/mL to aid transduction. A second transduction was performed on the following day by spinoculating virus supernatant onto RetroNectin® (Takara Clonetech,

Kusatsu, Japan)-coated 24-well plates (900× *g*, 90 min, 4 °C) and transferring PBLs on coated wells. Transduction efficiency was assessed by flow-cytometry 72 h after the second transduction by staining PBLs against murine TCRβ constant chain (H57-597, PE-conjugated, BioLegend®, San Diego, Ca, USA), CD3, and CD8α. TCR-transduced (TCR-td) PBLs were further expanded in TCM, containing 400 IU/mL IL-2 and 5 ng/mL IL-7/IL-15, for one week. Transduced, expanded PBLs were either frozen after expansion phase or maintained in culture in TCM supplemented with 40 IU/mL IL-2 and 5 ng/mL IL-7/IL-15.

2.9. Transfection of Cell Lines

Multiple myeloma cell line U266 (purchased from DSMZ-German Collection for Microorganisms) was transfected with neoepitope-encoding TMG-constructs in pcDNA3.1(+) plasmid by nucleofection with the Amaxa Nucleofector 4D device. One million cells were washed once with PBS, resuspended in 20 µL OptiMEM (Lonza Group AG, Basel, Switzerland), and transferred to the 4D Nucleofection strip. Two microgram plasmid DNA in 5 µL OptiMEM were added to the cell suspension, mixed, and nucleofected with the preset nucleofection program for cell line HL60. Viability and reporter expression were analyzed prior to coculture set-up by flow-cytometry.

2.10. CTL Screening and Functional Assays

CTLs were screened for peptide-reactivity after an overnight co-culture with peptide-loaded (1×10^{-6} M) target cells and staining for T cell activation marker CD137 by flow cytometry. Cells were stained against CD8α and CD137 (4B41, PE-conjugated, and BioLegend®, San Diego, CA, USA). Peptide recognition of TCR-td PBLs was confirmed in co-culture assays of peptide-loaded target cells and PBLs in an overnight culture. Target cells were HLA-A2-positive cell lines T2 and U266. To assess the functional avidity of isolated TCRs, titration assays were performed on TAB-deficient T2 cells loaded with decreasing peptide concentrations. Secreted IFN-γ from cell-free supernatant was detected by ELISA (OptEIA™ sets, BD Biosciences, Franklin Lakes, NJ, USA) after an overnight co-culture. Tyrosinase peptide YMD (YMDGTMSQV) served as a peptide-loading control for T2 cells, and cells were pulsed at 1×10^{6} M and incubated with YMD-specific TCR T58-td PBLs. The mean functional avidity of TCRs was determined by measuring IFN-γ secretion to declining peptide concentrations of target cell, and the peptide dose at which the half-maximum of T cell activity was achieved (EC50) was determined.

For FACS analysis of T cell activation, cells were stained against CD8α, mTCRβ (PerCP-Cy5.5-conjugated, BioLegend®, San Diego, CA, USA), and CD137. For analysis of cytotoxicity, TCR-td PBLs and target cells were incubated for 3-4 h in the presence of monensin and anti-CD107α antibody followed by staining for CD8α and mTCRβ. CD107α-surface expression was assessed as a marker of degranulation via flow cytometry.

2.11. Statistical Analysis

Data visualization and statistical analysis was performed using GraphPad Prism 7.0 (GraphPad Software, Version 7.00, GraphPad Software, La Jolla, CA, USA). EC50 values were calculated from peptide titration assays at the peptide dose at which the half-maximum of T cell activity was achieved. The data were normalized to the percentage of maximal (plateauing value) of response before curve fitting. Titration data were analyzed using 4PL model.

3. Results

3.1. Identification of Candidate Neoepitopes for an Ovarian Cancer Patient and Colon Cancer Patient

WES and RNA sequencing were performed on tumor and healthy tissue for colon carcinoma patient BIH146 and patient BIH56 with advanced ovarian carcinoma. Patients' characteristics are summarized in Table S1. The WES of tissue samples was performed with an average sequencing depth of 681.6×/374.5× for BIH56 and 458.4×/234.4× for

BIH146 and revealed 48 and 182 missense mutations for BIH56 and BIH146, respectively. Binding affinities of transcribed mutated peptide sequences for patient's HLA alleles were predicted with NetMHCcons1.1a, and neoantigen candidates were selected according to their predicted MHC class I binding affinity (IC_{50}). Identified somatic variants and a list of identified potential epitopes for HLA-A*02:01 are given in the Table S2. For BIH146, seven HLA-A*02:01-restricted potential neoantigens were selected for further investigation, six of which had high (IC_{50} < 50 nM) and one of which had low (IC_{50} 653 nM) binding affinity. For BIH56, neoantigen candidates were restricted to five of the patient's HLA-alleles, and IC_{50} ranged from 36 to 5720 nM with only one predicted candidate for HLA-A*02:01 (IC_{50} 63 nM). Selected neoantigen candidates are summarized in Table 1. For each patient, a TMG was constructed encoding for all selected candidates. TMG-constructs were used for IVT-RNA synthesis for stimulation of T cells, or for nucleofection of target cell lines to be used for testing endogenous epitope processing.

Table 1. Summary of neoantigens selected for TMG-construction for patients BIH146 and BIH56. Mutated amino acids of the respective epitopes are indicated in red. HLA-binding predictions were performed with NetMHC4.0; threshold rank for strong binders was 0.5, and for weak binders it was 2.00.

Patient	TMG Name	Epitope	Gene/ Mutation	HLA Restriction	% Rank	IC_{50} (nM)
146	TMG146	ILISYIGMV	$SLC35D1_{T324S}$	A2:01	0.12	9.76
		RLNGYFAQL	$CDH2_{D660Y}$	A2:01	0.6	44.92
		FLTEGERSPYL	$PIGM_{V62L}$	A2:01	0.12	10.64
		MLFTIGQSKV	$TBC1D1_{E299K}$	A2:01	0.6	43.62
		SLFPEILLRV	$ATP11C_{I1108R}$	A2:01	0.15	12.01
		FLGTSTLLVSV	$MCOLN2_{W390S}$	A2:01	0.5	36.71
		QLMEHSENGAV	$CADPS2_{E695Q}$	A2:01	3.5	653.37
56	TMG56	HILSFVYPI	$SLC27A4_{R408H}$	A2:01	0.8	62.41
		SPSRPPGPT	$PLCB3_{R918S}$	B7:02	0.25	50.2
		LAVDTDEIEKY	$NBPF_{M674T}$	B35:01	2.00	1356.1
		HSHELNGPY	$CRYBB2_{C38Y}$	B35:01	0.2	36.43
		WLDGKHVVF	$PPIAL4G_{A128V}$	C4:01	0.03	1679.01
		TKFDVQVLK	$INF2_{E670Q}$	C4:01	0.4	4893.37
		YRQQAGRELL	$IGSF9B_{E63Q}$	C7:02	0.01	48.03
		RRNPTGSVVM	$PDXK_{A305T}$	C7:02	1.2	3589.15
		YRRDVHHVACY	$KLHL22_{Q281H}$	C7:02	1.9	5719.99

3.2. TCRs Identified from TIL or Patients' PB Repertoire Did Not Show Reactivity against Selected Neoantigens

As a potential source of neoepitope-specific T cells, TILs and PB were analyzed in patient BIH146. The number of CD8+ cells isolated from TIL and PBMC was very limited for this study. We isolated a total of 1.15×10^7 CD8+ T cells from TIL cultures of BIH146. Only $0.5–1 \times 10^6$ CD8+ T cells from PBMCs for both patients could be used for each. Expanded CD8+ T cells, stimulated with autologous TMG-DCs, were sorted for single-cell TCR sequencing, and T cell clone frequencies were calculated where both α and β chains were detected. One dominant T cell clone was detected in stimulated TIL but not in stimulated patient-derived PBMCs. The identified TCR rearrangement 16A4 (Table S3), expanded from a frequency of 2.3% (3/133 complete α/β rearrangements) before stimulation to 14.7% (10/68) after stimulation. Some expanded T cell clones were also present in mock-stimulated T cells and were thus not TMG-specific (Figure 1A). There was no clonal expansion in TMG-stimulated T cells derived from PB. Additionally, we stimulated TILs and PBMC-derived CD8+ cells with peptide-loaded APCs. Peptide stimulations of TILs (about 1×10^6 cells per peptide) were carried out with single-peptide loaded APCs, which reduced the number of cells available for each individual peptide stimulation, compared to

TMG stimulations, where all neoepitope candidates are encoded on one TMG-construct. Peptide stimulated T cells did not expand and could not be sorted for scTCR-sequencing.

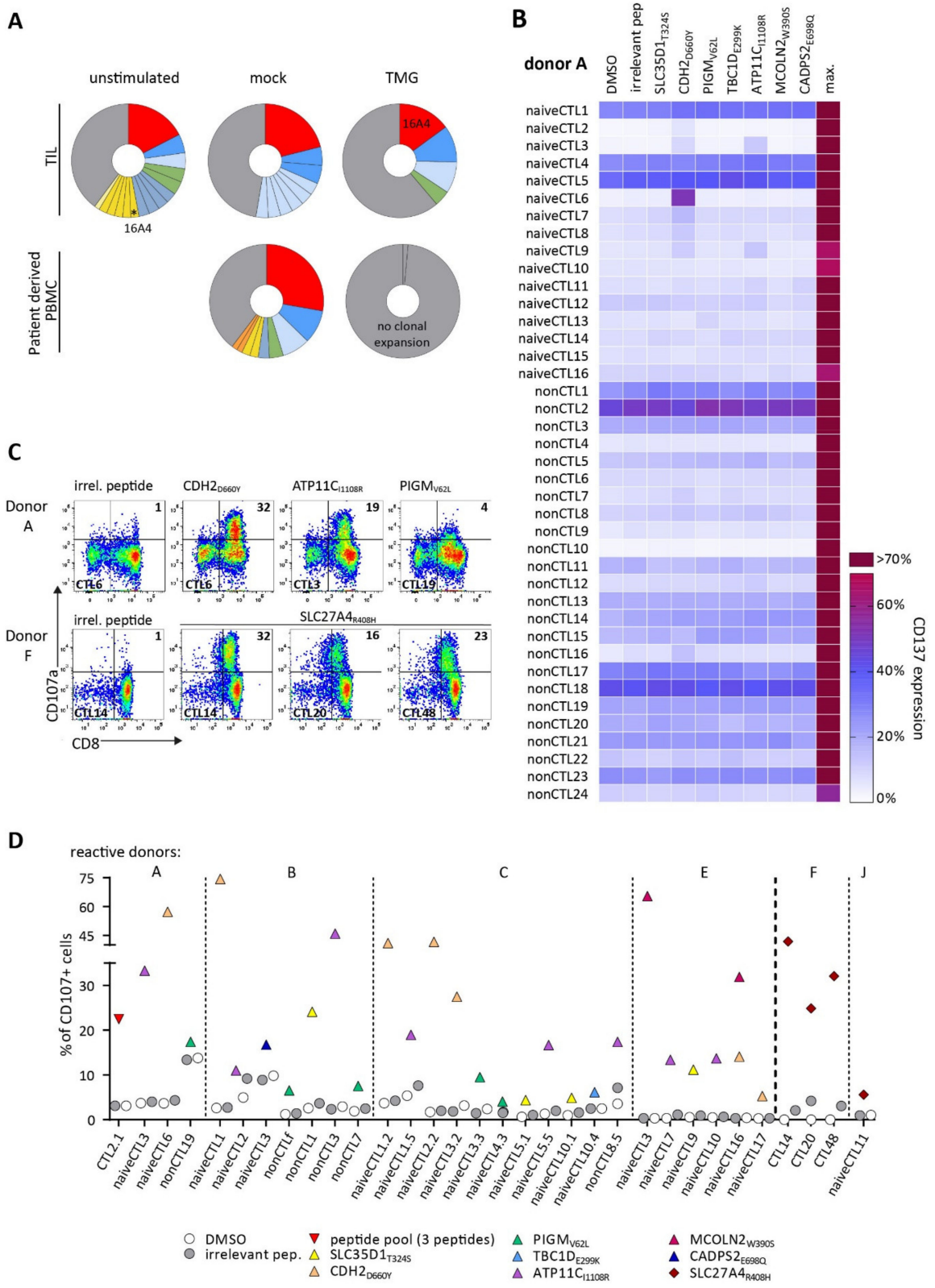

Figure 1. Stimulation and identification of patient- and donor-derived peptide-reactive T lymphocytes (CTLs). (**A**) Single-cell sequencing of TILs and PBMCs for patient BIH146. Pie charts show relative frequencies of detected TCRα/β sequences. The most frequent clone in TMG-stimulated TIL is indicated

(16A4). Grey segments represent all TCRα/β rearrangements, which were detected only once per sample. (**B**) Peptide-expanded CTL lines were generated in a peptide stimulation containing all seven neoantigen candidates identified for patient BIH146. Each CTL line was screened for peptide recognition of individually loaded T2 cells, and T cell activation was measured by CD137 surface expression after 20 h. Representative results are shown for donor A-derived CTL lines, which were generated from naive-enriched (naiveCTL) and non-naive (nonCTL) CD8+ T cells. CD137 expression is depicted as a heatmap of the percentage of CD8+ cells. For each patient, five donors were stimulated twice. Max: maximal activation induced by PMA and Ionomycin activation. (**C**) CTL lines identified by screening assays were stimulated with their specific peptide. T2 cells were pulsed with peptide at 1×10^6 µg/mL and used as target cells in a degranulation assay for 4h in the presence of monensin. Degranulation marker CD107a-positive cells were sorted. Representative FACS plots show CTL lines, which were generated from stimulations of naive and non-naive CD8+ T cells (donor A, upper panel) with a peptide pool of all seven peptides for BIH146 and bulk CD8+ T cells stimulated with one neoantigen candidate for BIH56 (lower panel, donor F). To estimate background activation, T2 cells were loaded with an irrelevant peptide and DMSO control. A representative control is shown (first row). (**D**) Summary of degranulation assays of all identified CTLs of all reactive donors (n = 6 reactive donors). Alive, single, CD3+CD8+ cells were gated for CD107a expression. Dotted lines separate donors, and the dashed line separates stimulations for patients BIH146 and BIH56.

The identified expanded TCR 16A4 was cloned and expressed on donor PBLs. Following a co-culture with peptide-loaded target cells, recognition of neoantigen candidates by 16A4-td PBLs was assessed by measuring the expression of activation marker CD137. However, 16A4-td PBLs failed to recognize neoepitope candidates (Figure S1A) when loaded onto target cells.

For BIH56, only patient-derived PBMCs but not TILs were available to isolate CD8+ T cells for stimulation with autologous peptide-loaded APCs. Expanded T cell clones were sorted and identified, and two TCRs were constructed (TCR 1C4 and 1A6, Table S3). PBLs transduced with TCR 1C4 did not recognize peptide-loaded target cells, and TCR 1A6 showed unspecific activation by target cell line T2 independent (Figure S1B,C) of peptide loading.

In summary, although expansion of T cell clones from patients' PBMCs and TILs could be detected, no neoepitope-reactive TCR was identified. An overview of all isolated TCRs, stimulation methods, and TCR repertoire used is given in Table S4.

3.3. Detection of Neoantigen-Reactive CTLs after Stimulation of Healthy HLA-Matched Donor CD8+ T Cells

We used T cell repertoires of multiple healthy HLA-A*02:01-matched donors to stimulate neoantigen-specific T cells. HLA haplotypes of healthy donors are summarized in Table S5. We were able to generate CTLs from a peptide pool of three predicted neoepitope candidates ($CDH2_{D660Y}$, $SLC35D1_{T324S,}$ and $PIGM_{V62L}$), identified for patient BIH146, from the CD8+ T cells (bulk population containing naive and non-naive T cells) from donor A. Three expanded CTL lines specifically recognized target cells loaded with the peptide pool (Figure S2).

Aiming to generate further CTL lines against neoepitope candidates of patient BIH146, T cell stimulation was repeated with the same donor as well as twice with four additional healthy donors. Here, we used a peptide pool of all seven predicted neoepitope candidates. Furthermore, to minimize the risk of unspecific T cell expansion, CD8+ lymphocytes were purified for naive T cells by sequential 'untouched' enrichment for CD8+ and naive cells. Both fractions, naive-enriched and non-naive CD8+ cells, were used for stimulations. Peptide recognition was assessed of expanded CTL lines in a screening assay measuring CD137 upregulation. A representative screening assay of all expanded CTL for donor A is shown in Figure 1B. Additional donors were treated accordingly (donors A-E). For patient BIH56, five HLA-A*02:01-matched donors (donors F-J) were stimulated with one

predicted HLA-A*02:01-restricted neoepitope, $SLC27A4_{R408H}$. Reactive CTL lines were then stimulated in a degranulation assay with the respective peptide, and cells were sorted for CD107a expression. Representative staining plots of CD8+CD107α+ CTLs are shown in Figure 1C for donors A and F. Expression of CD107α of reactive CTL lines are summarized in Figure 1D for all reactive donors.

Overall, peptide-reactive CTLs could be generated from 4/5 donors for patient BIH146 directed against the seven predicted epitopes. For patient BIH56, 2/5 donors showed reactivity against the predicted neoepitope candidate. From one reactive donor, more than one CTL line could be generated, recognizing different neoantigen candidates. Interestingly, peptide $CDH2_{D660Y}$ induced repeated and robust expansions of peptide-reactive CTLs in all reactive donors, whereas other peptides (e.g., $MCOLN2_{W390S}$, $TBC1D_{E299K}$, and $CADPS2_{E698Q}$) induced expansion of specific CTL populations in only one donor. This suggests that the generation of peptide-specific CTLs is dependent on both the characteristics of the peptide and the donor repertoire.

3.4. Identified TCRs from the Human Repertoire Exhibit Reactivity against Neoantigen Candidates

In order to identify the TCR sequences of peptide-reactive CTLs, TCRα and β chains of selected CD107α+ sorted CTL lines were identified. Most abundant TCRα/β chains were paired and cloned for expression in primary PBLs. We were able to identify highly prevalent TCRα/β variable regions for some, but not every, sorted CTL line. A summary of all identified TCRα/β rearrangements from a healthy donor repertoire, which were cloned and used for transduction of donor PBLs, is given Table S3. TCR transduction efficiencies and IFNγ secretion of reactive TCRs after a co-culture with peptide-loaded target cells is shown in Figure 2A,B. TCRs 1628 and 6.2, isolated from donor A, were specific to predicted neoepitope candidate $CDH2_{D660Y}$. Furthermore, TCR 56.11 and 56.48, isolated from two different donors, recognized the potential neoepitope candidate $SLC27A4_{R408H}$, and TCR 3.6 and 5.1, isolated from two different donors, were specific to peptides $MCOLN2_{W390S}$ and $SLC35D1_{T324S}$, respectively.

In a peptide titration assay, EC_{50} values for TCR 1628 (5.4×10^{-9} M) and for TCR 6.2 (2.0×10^{-7} M) were determined. Peptide titration for TCRs 56.48 and 56.11 revealed -EC_{50} values of 1.1×10^{-9} M and 1×10^{-6} M, and EC_{50} values for TCR 3.6 and 5.1 were 4.9×10^{-9} M and 2.1×10^{-9}, respectively, showing that we were able to identify high-avidity TCRs from the healthy human TCR repertoire (Figure 2C).

Four reactive TCRs originated from naive-enriched CD8+ T cell fractions, and in the cases of TCR 1628 and 56.48, from the bulk CD8+ T cell fraction.

3.5. Immunization of ABabDII Transgenic Mice Led to the Isolation of a High-Affinity TCR

ABabDII mice, transgenic for human TCRα/β gene loci and the HLA-A*02:01 molecule, were immunized four times with HLA-A2-restricted peptides, and three mice were immunized per peptide. Peptide-reactive T cells were sorted via IFN-γ capture assay from splenocyte cultures after reactivity was observed in PB. Most abundant TCRα and β sequences of reactive T cells were paired. The TCRα/β rearrangements are summarized in Table S6. TCR mb11a4 showed only minimal recognition of its peptide ($ATP11C_{I1108R}$) after incubation of TCR-td PBLs with peptide-loaded target cells at high peptide concentrations ($\geq 10^{-6}$ M). We identified one high-affinityy TCR, TCR m875 (sorting plot Figure S3), and TCR-td PBLs recognized target cells loaded with peptide $MCOLN2_{W390S}$ down to concentrations of 1×10^{-11} M with an EC_{50} of 6×10^{-9} M (Figure 2C).

Taken together, likewise to the human repertoire, only a small fraction of the isolated TCRs from the mouse repertoire were specific to the predicted neoepitopes. One high-affinity TCR (m875) was specific against predicted neoepitope candidate $MCOLN2_{W390S}$, for which one specific TCR (3.6) could also be generated from the human TCR repertoire.

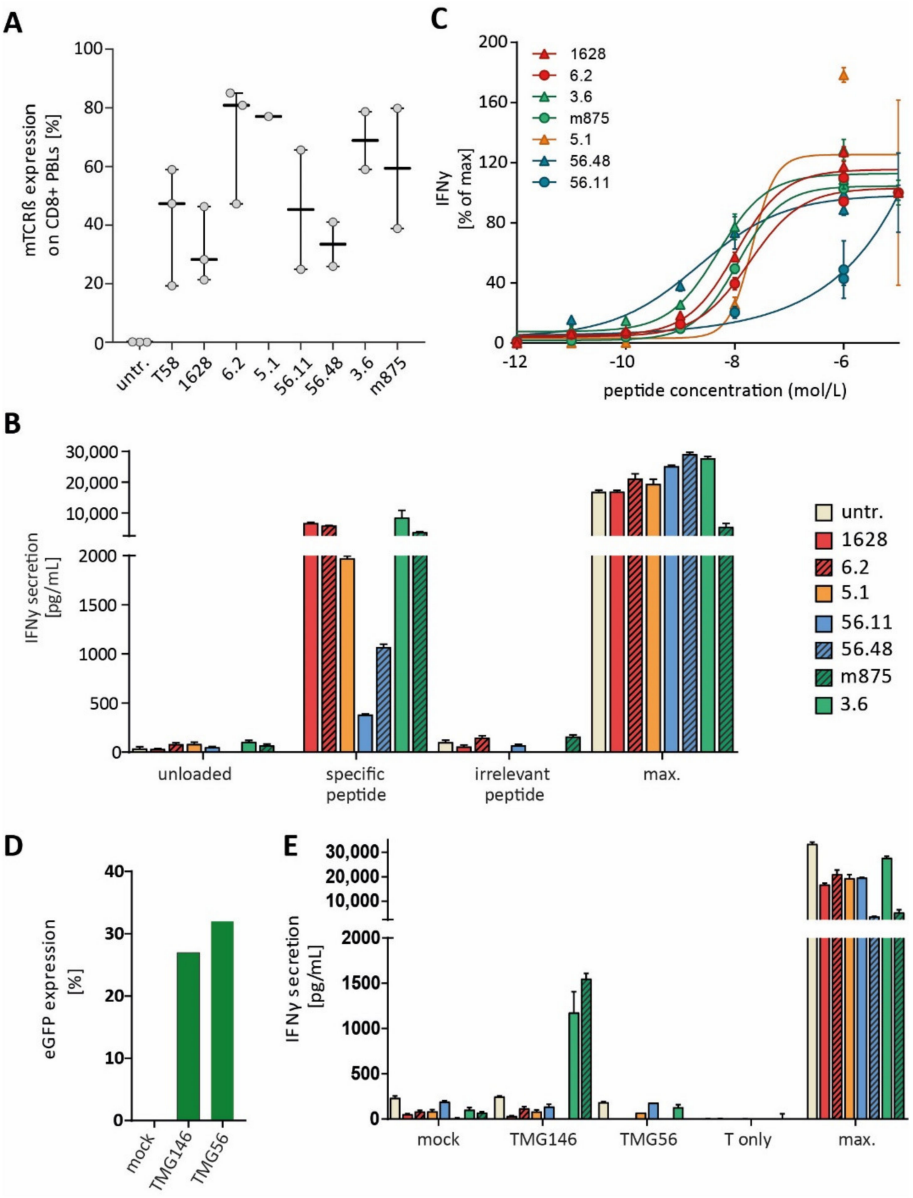

Figure 2. TCR specificity and endogenous processing of predicted neoepitope candidates. (**A**) TCR-cassettes were expressed in different donor PBLs (minimum n = 2), and expression of engineered TCRs was measured by staining for mouse TCRß constant region (mTCRß). Transduction efficiencies varied between 20 and 85% of CD8+ T cells. (**B**) The HLA-A2+ target cell line U266 was loaded with neoepitope candidates at 1×10^{-6} M and incubated with TCR-transduced (td) PBLs. Peptide-recognition was measured by IFNγ-secretion after overnight incubation. Representative data from one donor are shown, and samples were analyzed in duplicates. (**C**) Decreasing concentrations of peptides from 1×10^{-5}–1×10^{-12} M were loaded onto T2 cells and co-cultured with TCR-transduced (TCR-td) PBLs. IFNγ secretion was measured from culture supernatant. (**D**) Nucleofection of tandem minigenes (TMG) encoding for neoepitope candidates into U266 cells. Nucleofection efficiency was assessed by eGFP-expression by flow cytometry. The graph shows nucleofection efficiency for the U266 cell, which was used for co-culture with TCR-transduced PBLs shown in graph (**E**). (**E**) Recognition of TMG-expressing U266 cells by TCR-td PBLs. IFN-γ secretion was detected by ELISA after overnight incubation. Representative data are shown for one donor, and experiments were carried out in duplicates and for at least two different donors. Irrelevant peptide: non-specific or wildtype peptide; max: T cell activation cocktail, and untr.: untransduced. The same-colored bars/lines indicate specificity for the same neoepitope candidate; red: $CDH2_{D660Y}$, yellow: $SLC35D1_{T324S}$; blue: $SLC27A4_{R408H}$, and green: $MCOLN2_{W390S}$.

3.6. Endogenous Processing of Predicted Neoepitope Candidates

Multiple myeloma cell line U266, which naturally expresses HLA-A*02:01 and has been shown to be able to present internally processed, electroporated peptides [31], was nucleofected with TMG-constructs to confirm endogenous processing and presentation of candidate neoepitopes, for which specific TCRs were identified. Nucleofection efficiencies ranged from 14–45% (Figure S4). Figure 2D shows nucleofection efficiencies from TMG-nucleofected U266, which were used in a co-culture experiment with TCR-td PBLs (Figure 2E). TMG146-nucleofected U266 was recognized by PBLs expressing human-derived TCR 3.6 and murine-derived TCR m875, both specific to $MCOLN2_{W390S}$. PBLs transduced with TCR 1628 and 6.2, however, did not recognize the nucleofected target cells, suggesting a lack of processing of the neoepitope candidate $CDH2_{D660Y}$. The same is true for neoepitope candidate $SLC35D1_{T324S}$ and TCR 5.1. Similarly, target cells nucleofected with TMG56, containing the HLA-A*02:01-restricted neoantigen candidate $SLC27A4_{R408H}$, were not recognized by TCR 56.48-td and 56.11-td PBLs. Representative results from transduced PBLs of one donor are shown. Thus, endogenous processing of neoepitope candidates can be confirmed for 1/4 candidate epitopes, for which peptide-specific TCRs have been isolated.

4. Discussion

Adoptive transfer of neoantigen-specific T cells is considered one of the most attractive immunotherapeutic strategies. However, the optimal source of a TCR repertoire for their isolation is yet to be defined. Here, we exploited different types of TCR repertoires to isolate specific TCRs directed against predicted HLA-A*02:01-restricted neoepitopes from a colon and an ovarian cancer patient. Included TCR repertoires were the patients' TIL and PB, the repertoire of different healthy HLA-A*02:01-matched donors, and the TCR repertoire of humanized AabDII mice.

In total, we isolated six different TCRs from the healthy donor repertoire, which were specific to 4/8 predicted neoepitope candidates. The predicted neoepitope $MCOLN2_{W390S}$ led to the generation of a specific TCR in both the human and the murine-derived TCR repertoire (TCRs 3.6 and m875). Additionally, endogenous processing was confirmed only for $MCOLN2_{W390S}$. Some neoepitope candidates, for which we were able to isolate specific TCRs in one donor repertoire, did not result in the generation of dominant specific TCRs in other donor repertoires, indicating that the ability to generate specific TCRs is, in part, dependent on the donor TCR-repertoire.

The patient's own TCR repertoire would presumably be the ideal source for isolating individual neoantigen-specific TCRs. Tumor growth may already induce an immune response that leads to tumor-specific T cell expansion, at least in the immediate tumor environment. Furthermore, a successfully isolated TCR from the patient's own repertoire would not raise safety concerns. However, we were not able to isolate a specific TCR for the predicted HLA-A*02:01-restricted neoepitopes from the patients' own TCR repertoire.

Limited success rates in detecting neoantigen-reactive T cells and isolating corresponding specific TCRs from patients' repertoire have been observed before in several tumors, initially in melanoma [11]. This may be primarily due to the low frequency of neoantigen-specific T cells in TILs. Isolation of tumor-specific TCRs might be even more challenging in epithelial cancers, which frequently have immune-excluded or immune-desert phenotypes that hamper efficient T cell priming. Nonetheless, it has been shown that neoantigen-specific CD8+ and CD4+ T cells can indeed be isolated from TILs or from the PB T cell repertoires in metastatic epithelial cancers of some individual patients [32]. These tumor-specific T cells can be found exclusively in the memory T cell population.

The limited number of T cells from TIL cultures in the patients analyzed in this study presented a major limitation considering the low frequency of neoantigen-specific T cells in TILs [11]. Infiltrating and peripheral neoantigen-specific T cell frequencies are estimated to be as low as 0.002% in cancer patients [7], which is up to two magnitudes lower compared to the EBV-specific T cell in seronegative donors (ranging from 0.3–0.8%), and almost

four magnitudes lower compared to EBV seropositive donors, which range from 2.1 to 9.8% (with an average of 4.7%) [33]. Hence, it is desirable to expand specific T cells to higher frequencies or apply highly sensitive strategies for the detection and enrichment of neoepitope-specific T cells. In addition to using cultures of tumor fragments to enrich neoepitope-specific T cells, immediate identification of tumor-reactive T cells from the bulk TIL population after tumor resection is another way to isolate neoepitope-specific TCRs. This can be accomplished by sorting T cells expressing activation markers such as PD1, ideally combined with CD134/CD137, and followed by single-cell sequencing [34,35]. This approach would reduce the effort required to pair the a/ß TCR chains, as well as yield more sequencing depth. In addition, one would not risk losing tumor-specific T cells in the expansion cultures due to overgrowth of nonspecific T cell clones because exhausted tumor-specific T cells would not persist as well in culture. Regardless of which approach is used to isolate neoantigen-specific T cells, it would be desirable to collect tumor fragments from different locations from the resected tissue to account for tumor heterogeneity. Using the latter approach, TCR specificity would subsequently need to be determined using in silico predicted peptides. Moreover, it has been recently shown that most infiltrating lymphocyte clones, which are predominantly detected in the tumor tissue, are not necessarily tumor-specific [14].

Interestingly, most of the reported identified TCRs are not directed against HLA-A*02:01-restricted epitopes [3,16,36]. In another study, neoantigen-reactive T cell lines expanded for seven different HLA class I-restricted neoepitopes from PB of an ovarian cancer patient, but only one recognized an HLA-A*02:01-restricted neoepitope [37]. Since we have solely investigated the isolation of TCRs against potential HLA-A*02:01-restricted neoepitopes, the possibility remains that specific TCRs against neoepitopes, other than the here predicted ones, could potentially be isolated. Indeed, we have been successful in generating high-affinity TCRs specific to the HLA-B*07:02-restricted $MyD88_{L265P}$ mutation [17].

In principle, it is possible to expand T cells against peptides of candidate neoepitopes from the naive T cell repertoire of cancer patients. However, limitations remain that influence the stimulation and priming success, namely, the low T cell precursor frequency and the often-limited amount of patient's T cells available for neoantigen-specific in vitro priming, as was the case with the patient material in this study. To circumvent these limitations, we successfully used PB from HLA-A*02:01-matched healthy donors as a TCR repertoire source. Additionally, the use of HLA- and TCR repertoire-transgenic mice to isolate high-affinity TCRs, targeting tumor-associated or cancer germline antigens, circumvents mechanisms of tolerance and has allowed us to generate several useful TCRs [21–23] against self-antigen-specific TCRs.

The limited success of inducing specific TCRs in transgenic mice against the here-predicted neoepitope candidates other than $MCOLN2_{W390S}$ may be due to different factors, such as binding affinities of predicted epitopes to the human MHC-complex, or the immunogenic properties of the predicted candidates. Additionally, immunizing more animals (three mice per candidate were used) might have led to the generation of more specific TCRs.

In general, the incidence of processed and immunogenic neoepitopes among predicted candidates is very low [38]. In this study, endogenous processing and the presentation of neoepitope candidates was confirmed for only one of the four predicted candidates, for which high-affinity TCRs were isolated. It cannot be excluded that neoepitope candidates with a predicted lower binding affinity, and thus not prioritized by our in-silico prediction approach, are possibly more immunogenic in vivo. A plethora of cumulative effects eventually determines which peptides function as immunogenic epitopes. This includes factors involved in antigen processing and presentation, which regulate the amount and quality of peptides presented on the cell surface, as well as factors that determine whether the presented peptide is recognized by T cells and is able to induce an immune response that renders the presented peptide immunogenic [39–41]. Besides inherent neoepitope properties, the individual donor TCR repertoire has a significant influence on the successful

isolation of neoepitope-specific TCRs. TCR repertoires are not only affected by age and possibly the presence of acute or chronic infections but also by HLA polymorphisms [42,43]. The individual composition of HLA haplotypes of different donors might be another influencing factor considering the isolation success of neoantigen-specific TCRs. In this study, all stimulated donors were matched for HLA-A*02:01 only. It has been shown that TCR repertoire diversity is positively associated with polymorphisms in the HLA class I loci. While the effects of age and chronic viral infections negatively affect the TCR repertoire in general, HLA diversity may rather influence the ability to generate individual antigen-specific TCRs [42,44]. Recently, we have been able to isolate a specific high-affinity TCR for the recurrent $MyD88_{L265P}$ mutation. In this case, we screened about 20 donors and were able to isolate 13 TCR sequences, from which seven high-affinity TCRs were identified from five donors [17]. Here, we tested five different donors for the potential neoepitopes of two patients. Including more donors might have led to the identification of more specific TCRs.

5. Conclusions

This study, as well as our experience with cancer-testis and other mutation-specific epitopes, suggest that, despite possible disadvantages in terms of safety, the generation of TCRs from allogeneic, partially matched healthy donors, or from humanized transgenic mice, might be a viable strategy for the development of mutation-specific ATT with defined specificity directed against cancer-specific mutations, especially in settings with limited patient material available. Here, we isolated specific TCR for the same neoepitope candidates from multiple healthy donors and the humanized mouse model. Our results also highlight the need for adequate predictions for neoepitope processing and immunogenicity.

Thus, to identify high-affinity TCRs, it might be necessary to screen multiple, up to 20, donor repertoires [17]. TCRs identified by this approach offer an ATT treatment option for patients with relapsed or refractory disease after revalidation of the presence of the identified neoepitope. Ideally, to prevent immune escape by loss of target antigen or HLA alleles, transfer of TCR-T cells directed against several neoantigens, restricted to different HLA alleles, would be beneficial.

Supplementary Materials: The following supporting information can be downloaded at: https://www.mdpi.com/article/10.3390/cancers14071842/s1, Supplementary Figures (Figures S1–S4). Table S1: patients characteristics; Table S2: somatic variants; Table S3: healthy donor TCR rearrangement; Table S4: overview of TCR repertoire stimulation method and TCR reactivity; Table S5: donor haplotypes; and Table S6: ABabDII TCR rearrangement.

Author Contributions: Conceptualization, A.B., G.W., A.P. and T.B.; methodology, A.B., A.P.; formal analysis and investigation, C.G.; clinical sample collection and data curation, C.A.P.; patient sequencing data curation and analysis, E.B., D.B.; single-cell TCR sequencing and analysis, L.H.; animal experiments, G.W., writing—original draft preparation, C.G, A.B. and C.A.P.; writing—review and editing, U.K., S.R.; visualization, C.G.; supervision, A.B., A.P.; and funding acquisition, A.B., C.G. All authors have read and agreed to the published version of the manuscript.

Funding: This research was funded by the Berlin Institute of Health (BIH) at Charité–Universitätsmedizin Berlin. CG has received funding for her research from BSIO—Berlin School of Integrated Oncology and Berliner Krebsgesellschaft e.V. Research funding was given to LH by Deutsche Krebshilfe e.V. (70113355). UK received funding from Deutsche Forschungsgemeinschaft (DFG, grant SFB1335/P3, Deutsche Krebshilfe (grants 70114425 and 70114724, Stiftung Charité, and Wilhelm-Sander Foundation (2017.048.2). GW received funding from Deutsche Krebshilfe (111546).

Institutional Review Board Statement: The study was conducted in accordance with the Declaration of Helsinki and approved by the Ethics Committee of Charité-Universitätsmedizin Berlin (ID EA1/265/14, date of approval 23 September 2014). All animal experiments were performed according to institutional and national guidelines and regulations. The animal study protocol was approved by the governmental authority Landesamt für Gesundheit und Soziales, Berlin (LaGeSo, H0086/16).

Informed Consent Statement: Written informed consent was obtained from all subjects involved in the study. Written informed consent was obtained from the patients to publish this paper.

Data Availability Statement: Generated data presented in this study on somatic variation and epitope predictions for the patients are available in the Supplementary Material. Further information on methods and data are available on request from the corresponding author.

Acknowledgments: The authors wish to thank the patients who participated in the Collaborative Research Grant Project "Targeting somatic mutations in human cancer by T cell receptor gene therapy". We also thank Kerstin Dietze for expert technical assistance for single-cell sequencing experiments.

Conflicts of Interest: The authors declare no conflict of interest. The funders had no role in the design of the study; in the collection, analyses, or interpretation of data; in the writing of the manuscript; or in the decision to publish the results.

References

1. Anandakrishnan, R.; Varghese, R.T.; Kinney, N.A.; Garner, H.R. Estimating the Number of Genetic Mutations (Hits) Required for Carcinogenesis Based on the Distribution of Somatic Mutations. *PLoS Comput. Biol.* **2019**, *15*, e1006881. [CrossRef] [PubMed]
2. Zacharakis, N.; Chinnasamy, H.; Black, M.; Xu, H.; Lu, Y.-C.; Zheng, Z.; Pasetto, A.; Langhan, M.; Shelton, T.; Prickett, T.; et al. Immune Recognition of Somatic Mutations Leading to Complete Durable Regression in Metastatic Breast Cancer. *Nat. Med.* **2018**, *24*, 724–730. [CrossRef] [PubMed]
3. Tran, E.; Robbins, P.F.; Lu, Y.-C.; Prickett, T.D.; Gartner, J.J.; Jia, L.; Pasetto, A.; Zheng, Z.; Ray, S.; Groh, E.M.; et al. T-Cell Transfer Therapy Targeting Mutant KRAS in Cancer. *N. Engl. J. Med.* **2016**, *375*, 2255–2262. [CrossRef]
4. Rosenberg, S.A.; Yang, J.C.; Sherry, R.M.; Kammula, U.S.; Hughes, M.S.; Phan, G.Q.; Citrin, D.E.; Restifo, N.P.; Robbins, P.F.; Wunderlich, J.R.; et al. Durable Complete Responses in Heavily Pretreated Patients with Metastatic Melanoma Using T-Cell Transfer Immunotherapy. *Clin. Cancer Res.* **2011**, *17*, 4550–4557. [CrossRef]
5. Leisegang, M.; Engels, B.; Schreiber, K.; Yew, P.Y.; Kiyotani, K.; Idel, C.; Arina, A.; Duraiswamy, J.; Rweichselbaum, R.; Uckert, W.; et al. Eradication of Large Solid Tumors by Gene Therapy with a T Cell Receptor Targeting a Single Cancer-Specific Point Mutation. *Clin. Cancer Res.* **2016**, *22*, 2734. [CrossRef] [PubMed]
6. Merhi, M.; Zhang, X.; Wang, S.; Hu, Y.; Liu, L.; Wu, D.; Liu, Y.; Li, X.; Liu, Y.; Yang, Q.; et al. Identification of Clonal Neoantigens Derived From Driver Mutations in an EGFR-Mutated Lung Cancer Patient Benefitting From Anti-PD-1. *Front. Immunol.* **2020**, *1*, 1366. [CrossRef]
7. Cohen, C.J.; Gartner, J.J.; Horovitz-Fried, M.; Shamalov, K.; Trebska-McGowan, K.; Bliskovsky, V.V.; Parkhurst, M.R.; Ankri, C.; Prickett, T.D.; Crystal, J.S.; et al. Isolation of Neoantigen-Specific T Cells from Tumor and Peripheral Lymphocytes. *J. Clin. Investig.* **2015**, *125*, 3981–3991. [CrossRef]
8. Robbins, P.F.; Lu, Y.C.; El-Gamil, M.; Li, Y.F.; Gross, C.; Gartner, J.; Lin, J.C.; Teer, J.K.; Cliften, P.; Tycksen, E.; et al. Mining Exomic Sequencing Data to Identify Mutated Antigens Recognized by Adoptively Transferred Tumor-Reactive T Cells. *Nat. Med.* **2013**, *19*, 747–752. [CrossRef]
9. Dudley, M.E.; Wunderlich, J.R.; Shelton, T.E.; Even, J.; Rosenberg, S.A. Generation of Tumor-Infiltrating Lymphocyte Cultures for Use in Adoptive Transfer Therapy for Melanoma Patients. *J. Immunother.* **2003**, *26*, 332–342. [CrossRef]
10. Stronen, E.; Toebes, M.; Kelderman, S.; Van Buuren, M.M.; Yang, W.; Van Rooij, N.N.; Donia, M.; Boeschen, M.-L.; Lund-Johansen, F.; Olweus, J.; et al. Targeting of Cancer Neoantigens with Donor-Derived T Cell Receptor Repertoires. *Sci. Rep.* **2016**, *352*, 1337–1341. [CrossRef] [PubMed]
11. Gros, A.; Parkhurst, M.R.; Tran, E.; Pasetto, A.; Robbins, P.F.; Ilyas, S.; Prickett, T.D.; Gartner, J.J.; Crystal, J.S.; Roberts, I.M.; et al. Prospective Identification of Neoantigen-Specific Lymphocytes in the Peripheral Blood of Melanoma Patients. *Nat. Med.* **2016**, *22*, 433–438. [CrossRef] [PubMed]
12. Tran, E.; Ahmadzadeh, M.; Lu, Y.-C.; Gros, A.; Turcotte, S.; Robbins, P.F.; Gartner, J.J.; Zheng, Z.; Li, Y.F.; Ray, S.; et al. Immunogenicity of Somatic Mutations in Human Gastrointestinal Cancers. *Science* **2015**, *350*, 1387–1390. [CrossRef] [PubMed]
13. Scheper, W.; Kelderman, S.; Fanchi, L.F.; Linnemann, C.; Bendle, G.; J Rooij, M.A.; Hirt, C.; Mezzadra, R.; Slagter, M.; Dijkstra, K.; et al. Low and Variable Tumor Reactivity of the Intratumoral TCR Repertoire in Human Cancers. *Nat. Med.* **2018**, *25*, 89–94. [CrossRef]
14. Penter, L.; Dietze, K.; Ritter, J.; Lammoglia Cobo, M.F.; Garmshausen, J.; Aigner, F.; Bullinger, L.; Hackstein, H.; Wienzek-Lischka, S.; Blankenstein, T.; et al. Localization-Associated Immune Phenotypes of Clonally Expanded Tumor-Infiltrating T Cells and Distribution of Their Target Antigens in Rectal Cancer. *Oncoimmunology* **2019**, *8*, e1586409. [CrossRef]
15. Oliveira, G.; Stromhaug, K.; Klaeger, S.; Kula, T.; Frederick, D.T.; Le, P.M.; Forman, J.; Huang, T.; Li, S.; Zhang, W.; et al. Phenotype, Specificity and Avidity of Antitumour CD8 + T Cells in Melanoma Cell State of CD8 + TIL-TCR Clonotypes. *Nature* **2021**, *596*, 119. [CrossRef]
16. Cafri, G.; Yossef, R.; Pasetto, A.; Deniger, D.C.; Lu, Y.C.; Parkhurst, M.; Gartner, J.J.; Jia, L.; Ray, S.; Ngo, L.T.; et al. Memory T Cells Targeting Oncogenic Mutations Detected in Peripheral Blood of Epithelial Cancer Patients. *Nat. Commun.* **2019**, *10*, 449. [CrossRef] [PubMed]
17. Çınar, Ö.; Brzezicha, B.; Grunert, C.; Kloetzel, P.M.; Beier, C.; Peuker, C.A.; Keller, U.; Pezzutto, A.; Busse, A. High-Affinity T-Cell Receptor Specific for MyD88 L265P Mutation for Adoptive T-Cell Therapy of B-Cell Malignancies. *J. Immunother. Cancer* **2021**, *9*, 2410. [CrossRef]

18. Ali, M.; Foldvari, Z.; Giannakopoulou, E.; Böschen, M.-L.; Strønen, E.; Yang, W.; Toebes, M.; Schubert, B.; Kohlbacher, O.; Schumacher, T.N.; et al. Induction of Neoantigen-Reactive T Cells from Healthy Donors. *Nat. Protoc.* **2019**, *14*, 1926–1943. [CrossRef]
19. Kato, T.; Matsuda, T.; Ikeda, Y.; Park, J.-H.; Leisegang, M.; Yoshimura, S.; Hikichi, T.; Harada, M.; Zewde, M.; Sato, S.; et al. Effective Screening of T Cells Recognizing Neoantigens and Construction of T-Cell Receptor-Engineered T Cells. *Oncotarget* **2018**, *9*, 11009. [CrossRef]
20. Li, L.; Lampert, J.C.; Chen, X.; Leitão, C.; Popović, J.; Müller, W.; Blankenstein, T. Transgenic Mice with a Diverse Human T Cell Antigen Receptor Repertoire. *Nat. Med.* **2010**, *16*, 1029–1034. [CrossRef]
21. Çakmak-Görür, N.; Radke, J.; Rhein, S.; Schumann, E.; Willimsky, G.; Heppner, F.L.; Blankenstein, T.; Pezzutto, A. Intracellular Expression of FLT3 in Purkinje Cells: Implications for Adoptive T-Cell Therapies. *Leukemia* **2019**, *33*, 1039–1043. [CrossRef] [PubMed]
22. Obenaus, M.; Leitão, C.; Leisegang, M.; Chen, X.; Gavvovidis, I.; van der Bruggen, P.; Uckert, W.; Schendel, D.J.; Blankenstein, T. Identification of Human T-Cell Receptors with Optimal Affinity to Cancer Antigens Using Antigen-Negative Humanized Mice. *Nat. Biotechnol.* **2015**, *33*, 402–407. [CrossRef] [PubMed]
23. Poncette, L.; Chen, X.; Lorenz, F.K.M.; Blankenstein, T. Effective NY-ESO-1-Specific MHC II-Restricted T Cell Receptors from Antigen-Negative Hosts Enhance Tumor Regression. *J. Clin. Investig.* **2019**, *129*, 324–335. [CrossRef] [PubMed]
24. Cho, Y.-B.; Lee, I.-G.; Joo, Y.-H.; Hong, S.-H.; Seo, Y.-J. Molecular Sciences TCR Transgenic Mice: A Valuable Tool for Studying Viral Immunopathogenesis Mechanisms. *Int. J. Mol. Sci.* **2020**, *21*, 9690. [CrossRef] [PubMed]
25. Karosiene, E.; Lundegaard, C.; Lund, O.; Nielsen, M. NetMHCcons: A Consensus Method for the Major Histocompatibility Complex Class i Predictions. *Immunogenetics* **2012**, *64*, 177–186. [CrossRef] [PubMed]
26. Spiotto, M.T.; Yu, P.; Rowley, D.A.; Nishimura, M.I.; Meredith, S.C.; Gajewski, T.F.; Fu, Y.X.; Schreiber, H. Increasing Tumor Antigen Expression Overcomes "Ignorance" to Solid Tumors via Crosspresentation by Bone Marrow-Derived Stromal Cells. *Immunity* **2002**, *17*, 737–747. [CrossRef]
27. Dauer, M.; Schad, K.; Herten, J.; Junkmann, J.; Bauer, C.; Kiefl, R.; Endres, S.; Eigler, A. FastDC Derived from Human Monocytes within 48 h Effectively Prime Tumor Antigen-Specific Cytotoxic T Cells. *J. Immunol. Methods* **2005**, *302*, 145–155. [CrossRef]
28. Wölfl, M.; Greenberg, P.D. Antigen-Specific Activation and Cytokine-Facilitated Expansion of Naive, Human CD8+ T Cells. *Nat. Protoc.* **2014**, *9*, 950–966. [CrossRef]
29. Han, A.; Glanville, J.; Hansmann, L.; Davis, M.M. Linking T-Cell Receptor Sequence to Functional Phenotype at the Single-Cell Level. *Nat. Biotechnol.* **2014**, *4*, 684–692. [CrossRef]
30. Penter, L.; Dietze, K.; Bullinger, L.; Westermann, J.; Rahn, H.-P.; Hansmann, L. FACS Single Cell Indexsorting Is Highlyreliable Anddetermines Immunephenotypes of Clonallyexpanded T Cells. *Eur. J. Immunol.* **2018**, *8*, 1248–1250. [CrossRef]
31. Campillo-Davo, D.; Versteven, M.; Roex, G.; De Reu, H.; Van Der Heijden, S.; Anguille, S.; Berneman, Z.N.; Van Tendeloo, V.F.I.; Lion, E. Rapid Assessment of Functional Avidity of Tumor-Specific T Cell Receptors Using an Antigen-Presenting Tumor Cell Line Electroporated with Full-Length Tumor Antigen MRNA. *Cancers* **2020**, *12*, 256. [CrossRef] [PubMed]
32. Bobisse, S.; Genolet, R.; Roberti, A.; Tanyi, J.L.; Racle, J.; Stevenson, B.J.; Iseli, C.; Michel, A.; Le Bitoux, M.A.; Guillaume, P.; et al. Sensitive and Frequent Identification of High Avidity Neo-Epitope Specific CD8+ T Cells in Immunotherapy-Naive Ovarian Cancer. *Nat. Commun.* **2018**, *9*, 1092. [CrossRef] [PubMed]
33. Bhaduri-McIntosh, S.; Rotenberg, M.J.; Gardner, B.; Robert, M.; Miller, G. Repertoire and Frequency of Immune Cells Reactive to Epstein-Barr Virus–Derived Autologous Lymphoblastoid Cell Lines. *Blood* **2008**, *111*, 1334–1343. [CrossRef] [PubMed]
34. Pasetto, A.; Gros, A.; Robbins, P.F.; Deniger, D.C.; Prickett, T.D.; Matus-Nicodemos, R.; Douek, D.C.; Howie, B.; Robins, H.; Parkhurst, M.R.; et al. Tumor- and Neoantigen-Reactive T-Cell Receptors Can Be Identified Based on Their Frequency in Fresh Tumor. *Cancer Immunol. Res.* **2016**, *4*, 734–743. [CrossRef]
35. Yossef, R.; Tran, E.; Deniger, D.C.; Gros, A.; Pasetto, A.; Parkhurst, M.R.; Gartner, J.J.; Prickett, T.D.; Cafri, G.; Robbins, P.F.; et al. Enhanced Detection of Neoantigen-Reactive T Cells Targeting Unique and Shared Oncogenes for Personalized Cancer Immunotherapy. *JCI Insight* **2018**, *3*, e122467. [CrossRef]
36. Tran, E.; Turcotte, S.; Gros, A.; Robbins, P.F.; Lu, Y.; Dudley, M.E.; Wunderlich, J.R.; Somerville, R.P.; Hogan, K.; Hinrichs, C.S.; et al. Cancer Immunotherapy Based on Mutation-Specific CD4+ T Cells in a Patient with Epithelial Cancer. *Science* **2014**, *344*, 641–645. [CrossRef]
37. Martin, S.D.; Wick, D.A.; Nielsen, J.S.; Little, N.; Holt, R.A.; Nelson, B.H. A Library-Based Screening Method Identifies Neoantigen-Reactive T Cells in Peripheral Blood Prior to Relapse of Ovarian Cancer. *Oncoimmunology* **2018**, *7*, e1371895. [CrossRef]
38. Popović, J.; Li, A.P.; Kloetzel, P.M.; Leisegang, M.; Uckert, W.; Blankenstein, T. The Only Proposed T-Cell Epitope Derived from the TEL-AML1 Translocation Is Not Naturally Processed. *Blood* **2011**, *118*, 946–954. [CrossRef]
39. Sgourakis, N.G.; Bradley, P.; Riemer, A.B.; Riley, T.P.; Baker, B.M.; J Keller, G.L.; Smith, A.R.; Davancaze, L.M.; Arbuiso, A.G.; Devlin, J.R. Structure Based Prediction of Neoantigen Immunogenicity. *Front. Immunol.* **2019**, *10*, 2047. [CrossRef]
40. Fritsch, E.F.; Rajasagi, M.; Ott, P.A.; Brusic, V.; Hacohen, N.; Wu, C.J. HLA-Binding Properties of Tumor Neoepitopes in Humans. *Cancer Immunol. Res.* **2014**, *2*, 522–529. [CrossRef]
41. Wei, J.; Kishton, R.J.; Angel, M.; Conn, C.S.; Dalla-Venezia, N.; Marcel, V.; Vincent, A.; Catez, F.; Ferré, S.; Ayadi, L.; et al. Ribosomal Proteins Regulate MHC Class I Peptide Generation for Immunosurveillance. *Mol. Cell* **2019**, *73*, 1162–1173.e5. [CrossRef] [PubMed]

42. Krishna, C.; Chowell, D.; Gönen, M.; Elhanati, Y.; Chan, T.A. Genetic and Environmental Determinants of Human TCR Repertoire Diversity. *Immun. Ageing* **2020**, *17*, 26. [CrossRef] [PubMed]
43. Britanova, O.V.; Putintseva, E.V.; Shugay, M.; Merzlyak, E.M.; Turchaninova, M.A.; Staroverov, D.B.; Bolotin, D.A.; Lukyanov, S.; Bogdanova, E.A.; Mamedov, I.Z.; et al. Age-Related Decrease in TCR Repertoire Diversity Measured with Deep and Normalized Sequence Profiling. *J. Immunol.* **2014**, *192*, 2689–2698. [CrossRef] [PubMed]
44. Chowell, D.; Morris, L.G.T.; Grigg, C.M.; Weber, J.K.; Samstein, R.M.; Makarov, V.; Kuo, F.; Kendall, S.M.; Requena, D.; Riaz, N.; et al. Patient HLA Class I Genotype Influences Cancer Response to Checkpoint Blockade Immunotherapy. *Science* **2018**, *359*, 582–587. [CrossRef]

3.2 Publication 2: High-affinity T cell receptor specific for MyD88 L265P mutation for adoptive T cell therapy of B-cell malignancies.

Abstract: Adoptive transfer of engineered T cells has shown remarkable success in B-cell malignancies. However, the most common strategy of targeting lineage-specific antigens can lead to undesirable side effects. Also, a substantial fraction of patients have refractory disease. Novel treatment approaches with more precise targeting may be an appealing alternative. Oncogenic somatic mutations represent ideal targets because of tumor specificity. Mutation-derived neoantigens can be recognized by T cell receptors (TCRs) in the context of MHC–peptide presentation. Here we have generated T cell lines from healthy donors by autologous in vitro priming, targeting a missense mutation on the adaptor protein MyD88, changing leucine at position 265 to proline (MyD88 L265P), which is one of the most common driver mutations found in B-cell lymphomas.

Generated T cell lines were selectively reactive against the mutant HLA-B*07:02-restricted epitope but not against the corresponding wild-type peptide. Cloned TCRs from these cell lines led to mutation-specific and HLA-restricted reactivity with varying functional avidity. T cells engineered with a mutation-specific TCR (TCR-T cells) recognized and killed B-cell lymphoma cell lines characterized by intrinsic MyD88 L265P mutation. Furthermore, TCR-T cells showed promising therapeutic efficacy in xenograft mouse models. In addition, initial safety screening did not indicate any sign of off-target reactivity.

Taken together, our data suggest that mutation-specific TCRs can be used to target the MyD88 L265P mutation, and hold promise for precision therapy in a significant subgroup of B-cell malignancies, possibly achieving the goal of absolute tumor specificity, a long sought-after dream of immunotherapy.

Journal for ImmunoTherapy of Cancer (JITC); 2021; volume 9; issue 7; 9:e002410;
DOI: 10.1136/jitc-2021-002410

Contribution to the publication

In the presented publication, T2304-T cells were produced and expanded for in vivo animal experiments. In vivo experiments were designed and conducted in cooperation with Özcan Cinar and EPO (Experimental Pharmacology & Berlin Buch), monitoring of animals during the course of the experiment was conducted in cooperation with EPO. Organ preparation, cell staining, and flow-cytometry analysis of sacrificed mice was carried out. Additionally, repetition of TCR safety relevant in vitro assays was carried out and reviewing of the manuscript.

Journal for ImmunoTherapy of Cancer

High-affinity T-cell receptor specific for MyD88 L265P mutation for adoptive T-cell therapy of B-cell malignancies

Özcan Çınar ,[1,2] Bernadette Brzezicha,[3] Corinna Grunert,[1,2] Peter Michael Kloetzel,[4] Christin Beier,[4] Caroline Anna Peuker,[1] Ulrich Keller ,[1,2] Antonio Pezzutto,[1,2] Antonia Busse[1,2]

To cite: Çınar Ö, Brzezicha B, Grunert C, *et al*. High-affinity T-cell receptor specific for MyD88 L265P mutation for adoptive T-cell therapy of B-cell malignancies. *Journal for ImmunoTherapy of Cancer* 2021;**9**:e002410. doi:10.1136/jitc-2021-002410

► Additional supplemental material is published online only. To view, please visit the journal online (http://dx.doi.org/10.1136/jitc-2021-002410).

AP and AB contributed equally.

Accepted 09 July 2021

For numbered affiliations see end of article.

Correspondence to
Dr Özcan Çınar;
oezcan.cinar@charite.de

ABSTRACT

Background Adoptive transfer of engineered T cells has shown remarkable success in B-cell malignancies. However, the most common strategy of targeting lineage-specific antigens can lead to undesirable side effects. Also, a substantial fraction of patients have refractory disease. Novel treatment approaches with more precise targeting may be an appealing alternative. Oncogenic somatic mutations represent ideal targets because of tumor specificity. Mutation-derived neoantigens can be recognized by T-cell receptors (TCRs) in the context of MHC–peptide presentation.

Methods Here we have generated T-cell lines from healthy donors by autologous in vitro priming, targeting a missense mutation on the adaptor protein MyD88, changing leucine at position 265 to proline (MyD88 L265P), which is one of the most common driver mutations found in B-cell lymphomas.

Results Generated T-cell lines were selectively reactive against the mutant HLA-B*07:02-restricted epitope but not against the corresponding wild-type peptide. Cloned TCRs from these cell lines led to mutation-specific and HLA-restricted reactivity with varying functional avidity. T cells engineered with a mutation-specific TCR (TCR-T cells) recognized and killed B-cell lymphoma cell lines characterized by intrinsic MyD88 L265P mutation. Furthermore, TCR-T cells showed promising therapeutic efficacy in xenograft mouse models. In addition, initial safety screening did not indicate any sign of off-target reactivity.

Conclusion Taken together, our data suggest that mutation-specific TCRs can be used to target the MyD88 L265P mutation, and hold promise for precision therapy in a significant subgroup of B-cell malignancies, possibly achieving the goal of absolute tumor specificity, a long sought-after dream of immunotherapy.

INTRODUCTION

Recently, clinical studies of adoptive T-cell therapy (ATT) using chimeric antigen receptor T (CAR-T) cell therapy against the B-cell antigen CD19 have achieved remarkable success and have shown response in around 50% of refractory and relapsed patients with diffuse large B-cell lymphoma (DLBCL).[1 2] Similar strategies have been developed targeting other B-cell lineage antigens such as CD20, CD22 and BCMA (B-cell maturation antigen).[3–5] However, tumor escape by modulating surface expression of the target antigen is a limitation of this strategy, leading to relapse in up to 50% of patients treated with CD19 CAR-T cells.[6 7] Furthermore, although being much more specific than standard chemotherapy, CD19 CAR-based ATT is lineage-specific rather than truly cancer-specific, as major parts of the B-cell compartment including normal B lymphocytes are eliminated. This frequently leads to severe B-cell aplasia that may cause morbidity or requirement for long-term immunoglobulin substitution and/or antibiotic prophylaxis.[8]

Surface antigens druggable by antibodies or antibody derivatives are only rarely tumor-specific, as oncogenic mutations occur mostly in intracellular proteins regulating cell proliferation and survival.[9] In contrast to CAR-based strategies, T-cell receptor (TCR)-based ATT relies on classical TCR recognition of processed antigen-derived epitopes presented in the context of MHC (major histocompatibility complex) molecules. The ability to target any protein independent of cellular localization greatly widens the spectrum of target antigens including truly cancer-specific mutant antigens, so called 'neoantigens', derived from somatic mutations that are acquired in the course of tumor development.[10]

Among all cancer-associated somatic mutations, oncogenic driver mutations are obviously the most attractive targets for TCR gene therapy. A prerequisite for TCR-based therapies is that the mutation leads to generation of peptides presented on MHC molecules with high affinity.[11 12] Selection of antigen-loss variants within the tumor is unlikely, if a driver mutation is targeted that is crucial for

oncogenic transformation. However, many driver mutations such as common p53 mutations occur at many variable positions of a given protein, creating a large number of potential target epitopes, which would need to be addressed individually. In contrast, a missense mutation almost consistently changing leucine in position 265 to proline (L265P) in the MyD88 adaptor protein is one of the most common driver mutations found in about one-fifth of all lymphoid malignancies. MyD88 L265P is the hallmark mutation in Waldenström macroglobulinemia, but it is also frequently found in aggressive B-cell lymphomas, for example, 30% of activated B cell (ABC)-like DLBCL, 45%–60% of central nervous system lymphomas and testicular lymphomas,[13–16] diseases with a huge need for novel specific and well-tolerated therapies.

In this study, we developed high-affinity TCRs recognizing the mutant peptide sequence in MyD88 L265P with specific killing capacity towards the mutant malignant B-cell population. Targeting cancer-specific genetic alterations with highly specific immunotherapies represents a huge step towards precision cellular therapy in oncology.

MATERIALS AND METHODS

In vitro antigen processing and mass spectrometry

Before trying to generate TCRs specific for mutated MyD88, we checked whether a peptide spanning the mutation is processed by the proteasome and potentially presented by the MHC complex. The polypeptide substrate MyD88 $L265P_{256–281}$ was synthesized by the core facility of the Institute of Biochemistry using standard Fmoc (*N*-(9-fluorenyl) methoxycarbonyl) methodology (0.1 mmol) on an Applied Biosystems 433A automated synthesizer. The peptide was purified by high-performance liquid chromatography and analyzed by mass spectrometry (ABI Voyager DE PRO). 20S proteasomes were purified from human red blood cells, in principle following the procedure as previously described by Textoris-Taube *et al*.[17] Proteasome digests of the synthetic MyD88 $L265P_{256–281}$ polypeptide were performed in 100 µL of TEAD buffer (20 mM Tris, 1 mM EDTA, 1 mM NaN_3, 1 mM Dithiothreitol, pH 7.2) over time at 37°C. For establishing a full-scale cleavage map, processing times were 48 hours. Proteasomal processing of the synthetic of polypeptides was performed at a substrate concentration of 40 µM in the presence of 4 µg 20S proteasome. Digested samples of 10 µL were loaded for 5 min onto a trap column (PepMap C18, 5 mm×300 µm×5 µm, 100 Å; Thermo Fisher Scientific, Massachusetts, USA) with 2:98 (v/v) acetonitrile:water containing 0.1% (v/v) Trifluoroacetic acid at a flow rate of 20 µL/min and analyzed by nanoscale LC-MS/MS using an Ultimate 3000 and LTQ Orbitrap XL mass spectrometer (Thermo Fisher Scientific). The system comprises a 75 µm inner diameter ×250 mm nano LC column (Acclaim PepMap C18, 2 µm; 100 Å; Thermo Fisher Scientific) or a 200 mm PicoFrit analytical column (PepMap C18, 3 µm, 100 Å, 75 µm; New Objective). The mobile phase (A) is 0.1% (v/v) formic acid in water, and (B) is 80:20 (v/v) acetonitrile:water containing 0.1% (v/v) formic acid. For elution, a gradient 3%–45% B in 85 min with a flow rate of 300 nL/min was used. Full MS spectra (m/z 300–1800) were acquired on an Orbitrap instrument at a resolution of 60,000 (FWHM). At first, the most abundant precursor ion was selected for either data-dependent collision-induced dissociation (CID) fragmentation with parent list (1^+, 2^+ charge state included). Fragment ions were detected in an ion trap instrument. Dynamic exclusion was enabled with a repeat count of 2 and 60 s exclusion duration. Additionally, the theoretically calculated precursor ions of the expected spliced peptides were pre-elected for two Orbitrap CID (resolution 7500) and higher-energy collisional dissociation (HCD) (resolution 15,000) fragmentation scans. The maximum ion accumulation time for MS scans was set to 200 ms and that for tandem mass spectra (MS/MS) scans was set to 500 ms. Background ions at m/z 371.1000 and 445.1200 act as lock mass.

For LC-MS/MS runs using a Q Exactive Plus mass spectrometer coupled with an Ultimate 3000 RSLC-nano (Thermo Fisher Scientific), samples were trapped as described previously and then analyzed by the system that comprised a 250 mm nano LC column (Acclaim PepMap C18, 2 µm; 100 Å; 75 µm Thermo Fisher Scientific). A gradient of 3%–40% B (alternatively 3%–45% B) in 85 min was used for elution. Mobile phase A was 0.1% (v/v) formic acid in water, and mobile phase B was 80% acetonitrile in water containing 0.1% (v/v) formic acid. The Q Exactive Plus instrument was operated in the data-dependent mode to automatically switch between full scan MS and MS/MS acquisition. Full MS spectra (m/z 200–2000) were acquired at a resolution of 70,000 (FWHM) followed by HCD MS/MS fragmentation of the top 10 precursor ions (resolution 17,500, 1^+, 2^+, 3^+, charge state included, isolation window of 1.6 m/z, normalized collision energy of 27%). The ion injection time for MS scans was set to a maximum of 50 ms, automatic gain control (AGCs) target value of 1×10^6 ions and that for MS/MS scans was set to 100 ms, AGCs 5×10^4; dynamic exclusion was set to 20 s. Background ions at m/z 391.2843 and 445.1200 act as lock mass.

Peptides were identified by PD2.1 software (Thermo Fisher Scientific) based on their merged MS/MS of CID and HCD. Based on the results, further work focused on the 10 mer peptide RPIPIKYKAM (figure 1).

Cell lines and generation of target cells

K562 leukemic cell line was cultured in RPMI with 10% fetal bovine serum (FBS) and 100 U/mL penicillin/streptomycin. Non-Hodgkin's lymphoma cell lines SU-DHL-6, OCI-Ly3 and TMD8 were cultured in RPMI with 20% FBS and 100 U/mL penicillin/streptomycin. OCI-Ly3 and TMD8 cells were kindly supplied by groups of Professor Clemens Schmitt and Dr Martin Janz (Max-Delbruck-Center for Molecular Medicine, Berlin, Germany).

SU-DHL-6, OCI-Ly3, TMD8 and K652 cells do not naturally express HLA-B*07:02. To generate

A

	Monoiso., m/z Da			Charge (Positive)	Sequence	RT (min)	Monoiso., m/z Da		
	Detected	Calculated	Δ	z			detected	calculated	Δ
1.	362.5664	362.561	0.0054	3	R[9-17]A	24.1	1084.6992	1084.683	0.0162
2.	406.2462	406.2411667	0.005033333	3	R[9-18]M	25.4	1215.7386	1215.7235	0.0151
3.	419.2325	419.22885	0.00365	2	L[1-8]K	20.4	836.465	836.4577	0.0073
4.	491.6313	491.6256667	0.005633333	3	Q[7-18]M	25.5	1471.8939	1471.877	0.0169
5.	672.9127	672.9092	0.0035	2	K[8-18]M	25.3	1343.8254	1343.8184	0.007
6.	961.574	961.5717	0.0023	1	K[19-26]L	43.1	960.574	960.5717	0.0023

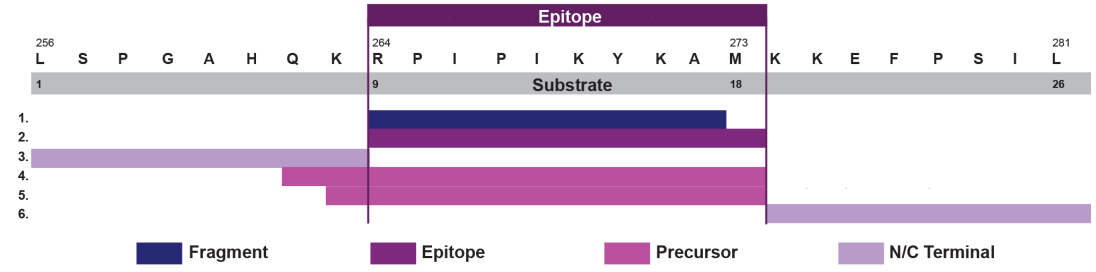

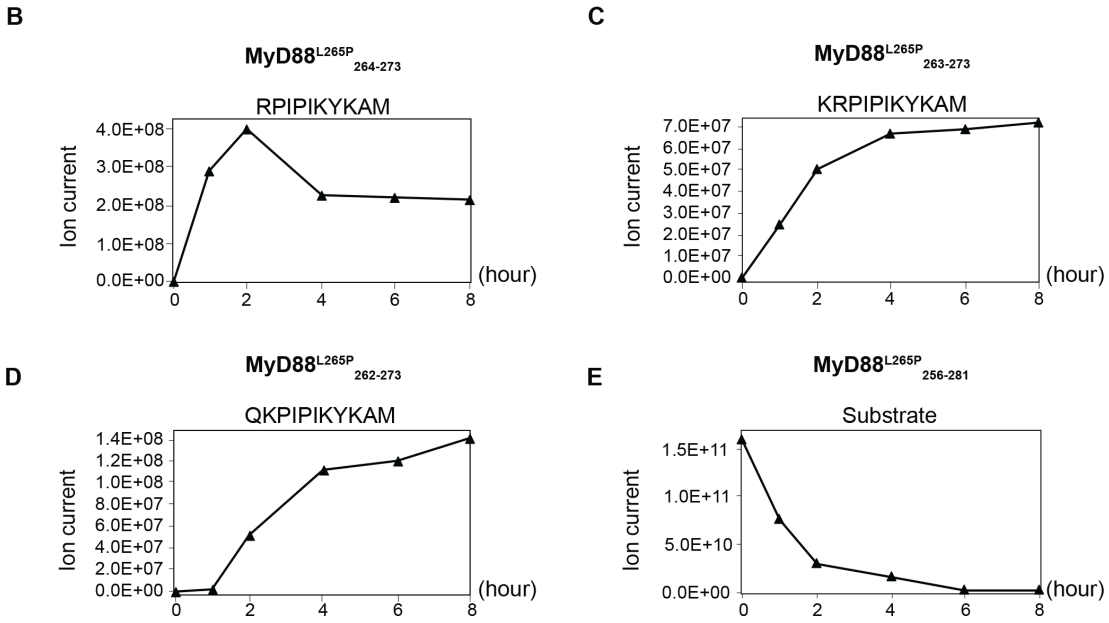

Figure 1 In vitro generation of the MyD88 L265P$_{264–273}$ neoepitope. Kinetic proteasomal antigen processing experiments were performed using the synthetic polypeptide substrate MyD88 L265P$_{256–281}$. (A) Summary of the peptides generated by the proteasome from the polypeptide substrate MyD88 L265P$_{256–281}$ in an in vitro digest. The complete list can be found in online supplemental table 4. (B–D) The generation kinetics of the MyD88 L265P-derived 10 mer neoepitope and its potential N-terminally extended precursor peptides are shown. (E) Kinetics of the degradation of the MyD88 L265P-derived polypeptide substrate MyD88 L265P$_{256–281}$.

HLA-B*07:02-positive target cells, we transduced the cell lines with HLA-B*07:02-coding gamma-retroviral vector MP71.[18] Moreover, K562 cells with or without HLA-B*07:02 were virally transduced to express the complete length wild-type or mutant (L265P) *MYD88*—coupled to the expression marker green florescent protein (GFP) via p2A—and used as artificial target cells.

Generation of mutation-specific T cells

All mutation-specific TCRs were cloned from peripheral blood mononuclear cells (PBMCs), isolated from HLA-B7-positive healthy donors. Monocytes were separated by plastic adherence for generation of dendritic cells (DCs). Following 3 days of culture with 800 IU/mL granulocyte-macrophage colony-stimulating factor (GM-CSF) and 10 ng/mL interleukin (IL)-4 in RPMI with 1% human serum, immature DCs were cultured overnight with addition of 10 ng/mL LPS and 50 ng/mL interferon gamma (IFN-γ) for maturation. Mature DCs were then loaded with mutant peptide (RPIPIKYKAM) and used for priming autologous CD8+ naive T cells. After 10 days, cells from each well were stained with a streptamer (HLA*B07:02-RPIPIKYKAM; IBA GmbH, Germany) or stained for T-cell

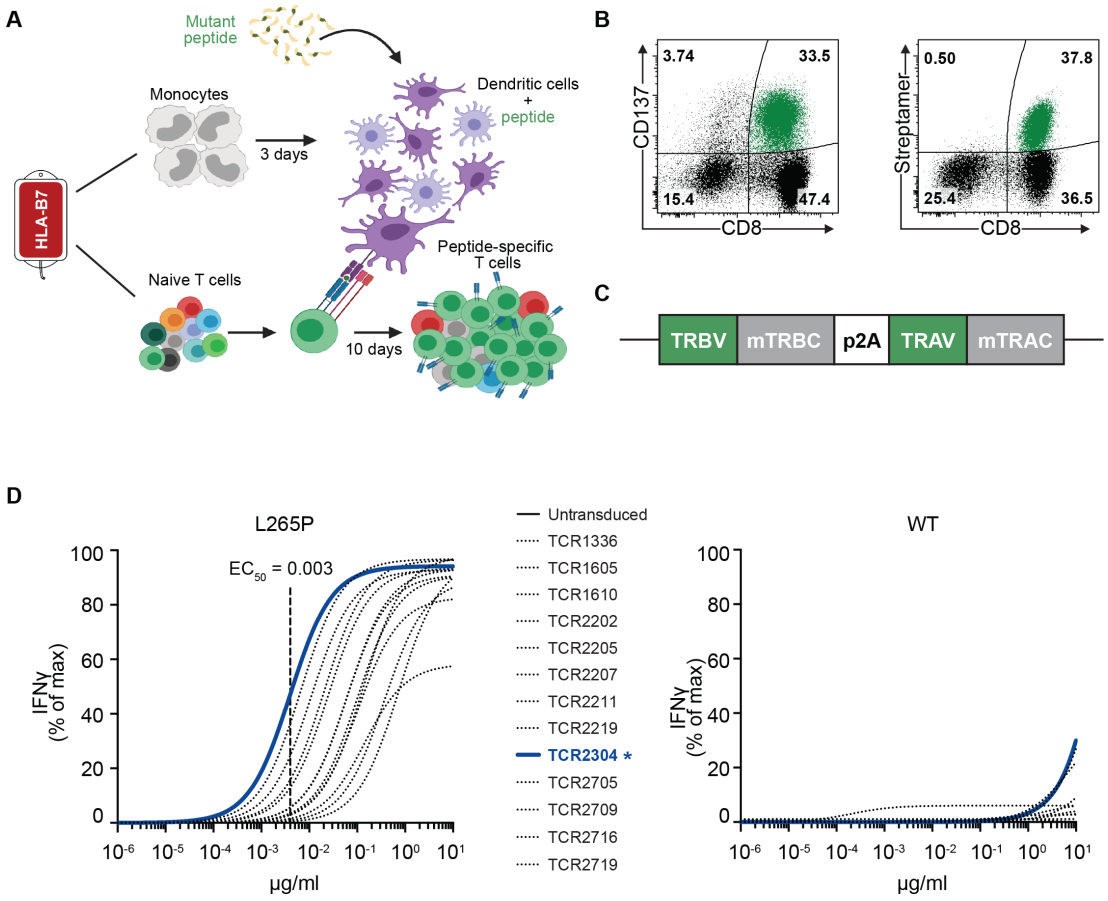

Figure 2 Generation of mutation-specific TCRs. (A) Schematic explanation of methodology for generation of mutation-specific T-cell lines. (B) Representative CD137 staining on 6 hours of restimulation with peptide, or streptamer staining for FACS isolation of peptide-specific T cells. (C) Construction of TCR gene cassettes. (D) Non-linear curve analysis of IFN-γ response by TCR-transduced CD8+ T cells from healthy donors, following coculture with K562 cells that were transduced with HLA*B07:02 and loaded with different concentrations of the mutant peptide (R**P**IPIKYKAM) or the corresponding WT peptide (RLIPIKYKAM). Response to the mutant peptide was detectable down to the concentration of 10^{-4} μg/mL with EC50 values within the nano molar (high affinity) range. Mutation-specific TCRs showed more than 10,000-fold higher affinity to the mutant peptide. IFN-γ response was measured by ELISA. FACS, fluorescence-activated cell sorting; IFN-γ, interferon gamma; TCR, T-cell receptor; WT, wild type.

activation markers such as CD137 (4-1BB) following a peptide restimulation. Positively stained wells were restimulated with peptide-loaded autologous PBMCs for expansion, in case it was necessary to obtain enough cells for fluorescence-activated cell sorting (FACS) isolation. The methodology for generating mutation-specific T cells is shown in figure 2A. This protocol was largely adapted from Wölfl and Greenberg.[19]

Identification of mutation-specific TCRs

Viable, CD8+ and streptamer-positive cells were sorted by FACS for total RNA isolation. A representative FACS plot is shown in figure 2B. TCR alpha and beta genes were amplified via 5′-RACE PCR (SMARTER RACE cDNA Amplification Kit; Clontech, Japan) and cloned (Zero Blunt TOPO Cloning Kit; Invitrogen/Thermo Fisher Scientific, Massachusetts, USA) in competent *Escherichia coli* cells. Multiple bacterial clones from each TCR chain were sequenced to analyze T-cell clonality, and dominant sequences were matched to create alpha-beta (αβ) TCRs for further characterization. Online supplemental table 1 shows CDR3 sequences and gene subtypes of MyD88 L265P mutation-specific TCRs. Identified variable domains (TRBV and TRAV) were combined with murine constant domain sequences (mTRBC and mTRAC) for experimental characterization of TCRs and synthesized on codon optimization (GeneArt, Thermo Fisher Scientific) for expression in human cells. TCR gene cassettes encoding the TRBV in combination with a murine TRBC and the TRAV in combination with a murine TRAC, separated by a p2A signal, were constructed as shown in figure 2C. TCR cassettes were cloned into the vector pMP71 by restriction site cloning. CD8+ T cells from healthy donors transduced with the TCRs were again stained with streptamer to test surface expression of the TCRs and functionality of αβTCR pairing (online supplemental figure 1).

T-cell activation and cytotoxicity analysis

Peripheral CD8+ T cells from HLA-B7-positive (not typed for HLA-B7 subtypes) healthy donors were transduced to express mutation-specific TCRs. Staining for murine TRBC (PE anti-mouse TCR β chain antibody; BioLegend, California, USA) was performed to check transduction efficiency before every experiment, which ranged between 25% and 65% of CD8+ T cells. Target cell lines were cocultured with TCR-transduced or control T cells for 16 hours. IFN-γ secretion was measured by ELISA (OptEIA Human IFN-γ ELISA Set; BD Biosciences, New Jersey, USA). Cytotoxicity was evaluated by flow cytometry analysis after staining of target cells for active caspase-3 (AF647 Rabbit Anti-Active Caspase-3, BD Biosciences) and fixable dead cell stain (LIVE/DEAD Fixable Violet Dead Cell Stain, Thermo Fisher Scientific). Target cells were gated on GFP-positive as reporter of wild-type or mutant MyD88 expression.

Xenograft models

All animal experiments were performed according to the institutional protocols and the national laws and regulations. Adult female NOG mice (NOD.Cg-*Prkdc*^{scid} *Il2rg*^{tm1Sug}/JicTac) and hIL2-NOG (NOD.Cg-*Prkdc*^{scid} *Il2rg*^{tm1Sug} Tg(CMV-IL2)4-2Jic/JicTac) mice, which due to their production of human IL-2 provide better support for the growth of adoptively transferred human T cells, were acquired from Taconic Biosciences (New York, USA). In short, mice were inoculated subcutaneously with 5×10^6 OCI-Ly3 or luciferase-expressing TMD8 cells. Once the tumors reached the predetermined volume of 100 mm^3 (~2 weeks after injection), OCI-Ly3 tumor-bearing mice were treated with intravenous injection of 1×10^7 TCR-T cells, or mock T cells (untransduced) of the same donor, or phosphate buffered saline (PBS) as control. TMD8-bearing mice were treated similarly on day 7 after tumor cell injection. Caliper and bioluminescence measurements were used to monitor tumor growth. Tumor volume was calculated with the formula: length×width^2/2. Mice were sacrificed when tumor size exceeded 1500 mm^3 or signs of distress was observed as determined in the animal experimentation protocol.

Alanine scan for cross-reactivity

To define the TCR-binding motif, a list of peptides was created, in which every amino acid residue in the mutant epitope was exchanged one by one with alanine. All peptides were separately loaded on HLA-B*07:02-expressing K562 cells in the concentration of 10 µg/mL and cocultured with TCR-T cells for 16 hours. Response was measured via IFN-γ ELISA. Results were then analyzed using the online tool Expitope[20] to screen for motif similarities in the human proteome. Peptides identified to have a binding-motif similarity to the original epitope were loaded on HLA-B*07:02-expressing K562 cells in the concentration of 10 µg/mL for coculture with TCR-T cells from three different healthy donors. Reactivity was measured via IFN-γ ELISA.

Lymphoblastoid cell line (LCL) scan for alloreactivity

TCR-T cells from three different healthy donors were cocultured for 16 hours with immortalized B-LCLs expressing a variety of frequent HLA haplotypes (online supplemental table 2), with or without prior peptide loading. Response was measured via IFN-γ ELISA.

Data sharing

For further information, please contact oezcan.cinar@charite.de. Supplemental files can be found in the online version of this article. Complete length nucleic acid and amino acid sequences of TCRs can be found in the published patent application: WO 2020/152161 A1.

RESULTS

Mutation-encompassing peptide is processed by human proteasome and binds to HLA-B*07:02 with high affinity

We used NetMHC V.4.0[21] and NetMHCpan V.4.0[22] for screening of peptides spanning the mutation region on MyD88 for candidate epitopes, restricted to HLA haplotypes commonly found in the European population. A 10 mer peptide (RPIPIKYKAM) harboring a proline residue at position 2 which is highly preferred by HLA-B*07:02,[23] the most common HLA-B allele found in Europe and North America, was predicted to be a strong binder, while the wild-type sequence had very low predicted HLA binding affinity (online supplemental table 3). Since it is established that the in vitro generation of epitopes by 20S proteasomes reflects the in vivo situation with high fidelity,[24] we performed kinetic in vitro proteasome digestion experiments to study the generation of the predicted MyD88 L265P$_{264–273}$ neoepitope from the synthetic 26 mer polypeptide substrate MyD88 L265P$_{256–281}$. A summary of the different peptides generated by the proteasome in an in vitro digest is shown in figure 1A; the whole list can be found in online supplemental table 4. Giving confidence that the predicted 10 mer neoepitope is indeed generated, mass-spectrometric analysis of the proteasomal digests identified the generation of the predicted neoepitope MyD88 L265P $_{264–273}$ as well as the generation of two N-terminally extended neoepitope precursor peptides MyD88 L265P$_{263–273}$ and MyD88 L265P$_{262–273}$ requiring trimming by endoplasmic reticulum resident aminopeptidases. The kinetic generation of the three peptides is shown in figure 1B–D, while the degradation of the 26mer substrate is shown in figure 1E.

Isolated TCRs yielded mutation-specific and HLA-restricted T-cell activity

Next, we generated peptide-specific T-cell lines against this neoepitope by priming naive T cells with autologous peptide-loaded DCs from healthy HLA-B7-positive donors (figure 2A). These peptide-specific T-cell lines recognized the mutant peptide when restimulated as shown by CD137 expression and stained with custom MHC-peptide streptamer (figure 2B). We cloned 13 unique TCR alpha and beta genes from peptide-specific T cells

of five individual donors (first two digits in TCR names indicate donor number; eg, TCR1605 and TCR1610 are cloned from the same donor) into the gamma-retroviral vector MP71, for expression on primary CD8+ T cells (figure 2C). T cells transduced with these TCRs (TCR-T) recognized HLA-B*07:02-positive K562 cells loaded with mutant peptide with varying functional avidity, while the corresponding wild-type peptide was not recognized (figure 2D). In addition, the 11 and 12 mer precursor peptides (MyD88 L265P$_{263–273}$ and MyD88 L265P$_{262–273}$) detected in mass-spectrometric analysis were also recognized by TCR-T cells (online supplemental figure 2).

To further assess specificity and functionality, we cocultured TCR-T cells with engineered HLA-B*07:02-positive or HLA-B*07:02-negative K562 target cells expressing the complete wild-type or mutant *MYD88* gene. Flow cytometric analysis showed mutation-specific and HLA-restricted recognition of target cells without exogenous peptide loading, proving that the epitope can be generated from endogenously expressed MyD88 and presented by HLA-B*07:02 at the cell surface (figure 3A). Seven out of 13 peptide-specific TCRs showed strong reactivity against target cells (figure 3C). In addition, the amount of IFN-γ secreted by TCR-T cells on target recognition correlated with previously measured TCR avidity. The highly specific recognition of target cells observed here has also led to cytotoxic T-cell activity (figure 3B,D). The TCR with the highest overall activity in the comparative assessment was TCR2304. TCR2304 was thus chosen for further development. Hereafter, TCR-T cells refer to TCR2304-transduced T cells.

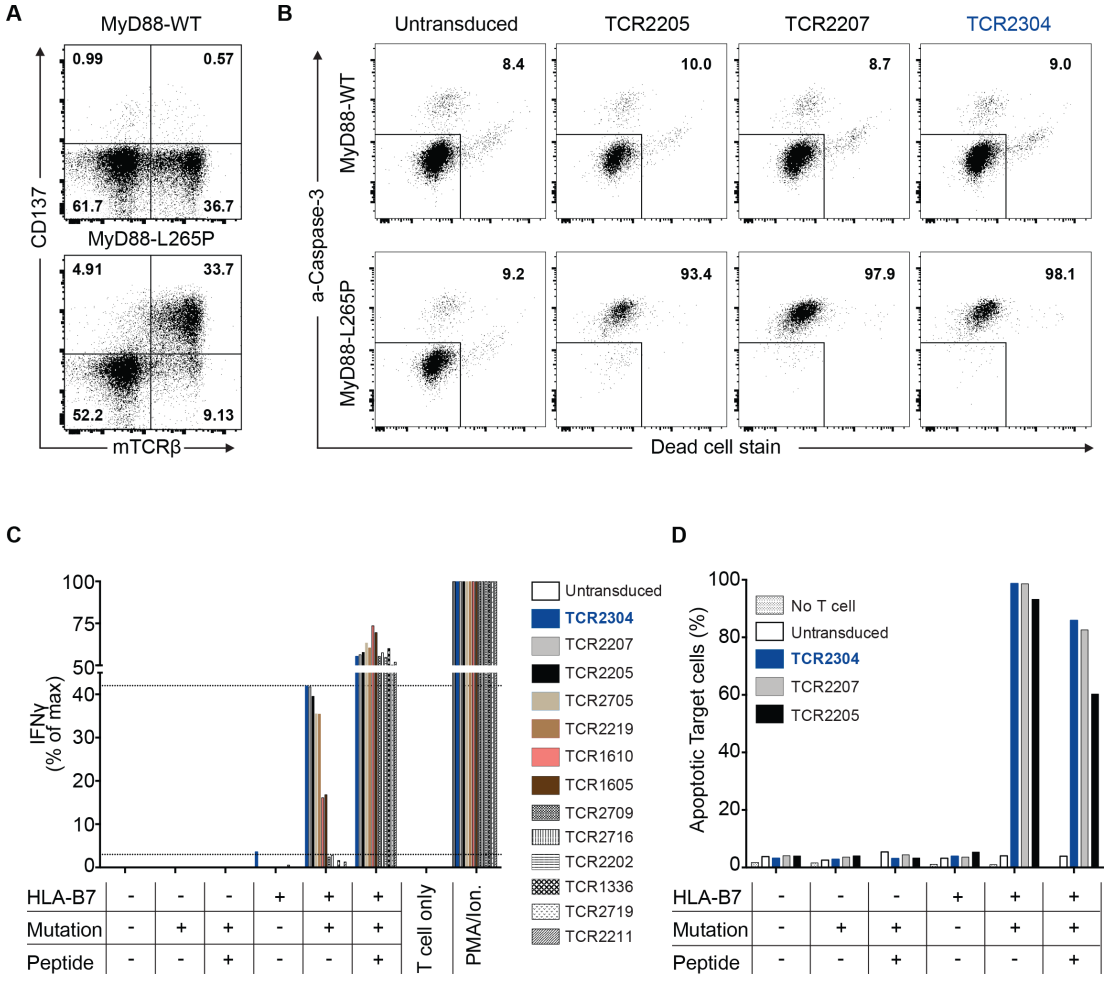

Figure 3 Mutation-specific activity of TCR-T cells. (A) Mutation-specific activation of TCR-T cells against K562 target cells—virally transduced to express complete length wild-type or mutant (L265P) MyD88 and HLA*B07:02, shown by flow cytometry analysis performed after 16 hours of coculture. (B) Viability of HLA*B07:02-positive target K562 cells that were cocultured for 16 hours with T cells expressing one of the three highest avidity TCRs, analyzed by flow cytometry. The proportions of apoptotic/dead cells are given in the upper right quadrant. (C) Comparative TCR-T cell response against target K562 cells. IFN-γ response measured by ELISA after coculture with K562 cells virally transduced to express complete length WT or mutant (L265P) MyD88 (mutation+) and/or HLA*B07:02 (HLA-B7+) as indicated. K562 cells loaded with the mutant peptide served as control (peptide+). Thirteen different TCRs were listed according to their respective EC50 values to the mutant peptide titration, from highest to the lowest. (D) Viability of target cells for cytotoxicity analysis of T cells transduced with three highest avidity TCRs. Strength of cytotoxicity as well as IFN-γ response against target cells strongly correlated with TCR avidity, previously measured by IFN-γ response to peptide titration. IFN-γ, interferon gamma; TCR, T-cell receptor; WT, wild type.

T cells engineered to express TCR2304 recognize and kill MyD88 L265P expressing lymphoma cells

To investigate the functional potential of TCR2304 when MyD88 L265P is expressed at natural expression levels, we analyzed the T-cell response against B-cell lymphoma cell lines. We used SU-DHL-6 (GCB-like DLBCL, wild-type MyD88), OCI-Ly3 (ABC-like DLBCL, homozygous L265P mutation) and TMD8 (ABC-like DLBCL, heterozygous L265P mutation) (figure 4A). Since all three cell lines originated from HLA-B7-negative patients, they were transduced to stably express the *HLA*B07:02* gene. Surface expression of HLA*B07:02 measured by flow cytometry was comparable to primary peripheral blood cells and to the HLA-B*07:02-positive B-LCL STA01 (figure 4B).

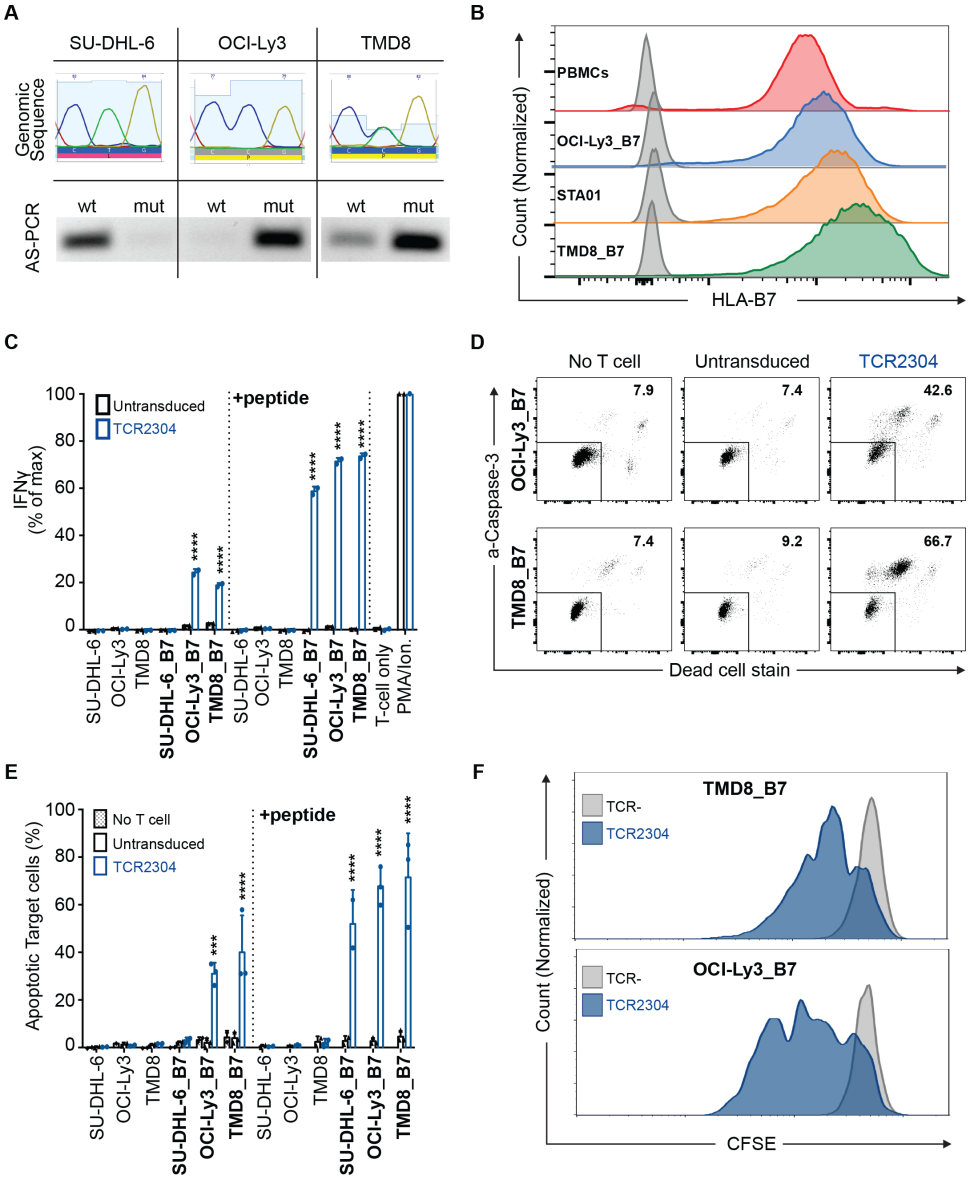

Figure 4 Mutation-specific activity of TCR-T cells against DLBCL cell lines with intrinsic MyD88 L265P expression. (A) Genomic sequence and allele-specific (AS) PCR analysis of lymphoma cell lines: SU-DHL-6 (GBC-like DLBCL, WT MyD88), OCI-Ly3 (ABC-like DLBCL, homozygous MyD88 L265P) and TMD8 (ABC-like DLBCL, heterozygous MyD88 L265P). (B) Side-by-side comparison of HLA*B07:02 expression of virally transduced lines versus natural expression in PBMCs isolated from an HLA*B07:02-positive donor and an HLA*B07:02-positive B-LCL line (STA01) measured by flow cytometric staining. (C) Activation analysis of TCR2304-transduced T cells via IFN-γ ELISA, after 16 hours of coculture with lymphoma cells. Cell lines virally transduced to express HLA*B07:02 are shown as 'cell line_B7'. Results from two different blood donors plotted with error bars showing SD significance analysis by two-way ANOVA: ****p<0.0001. (D) Representative flow cytometric viability analysis of lymphoma cells expressing HLA*B07:02 after 16 hours of coculture with T cells (as explained in figure 3). (E) Viability analysis of lymphoma cells with or without HLA*B07:02 expression. T cells of three different donors were used, error bars with SD significance analysis by two-way ANOVA: ***p<0.001, ****p<0.0001. (F) Antigen-induced proliferation of TCR2304-transduced T cells following 72 hours of coculture with HLA*B07:02-positive OCI-Ly3 and TMD8 cells. T cells were labeled with CFSE to trace proliferation prior to coculture. ANOVA, analysis of variance; DLBCL, diffuse large B-cell lymphoma; IFN-γ, interferon gamma; PBMC, peripheral blood mononuclear cell; TCR, T-cell receptor; WT, wild type.

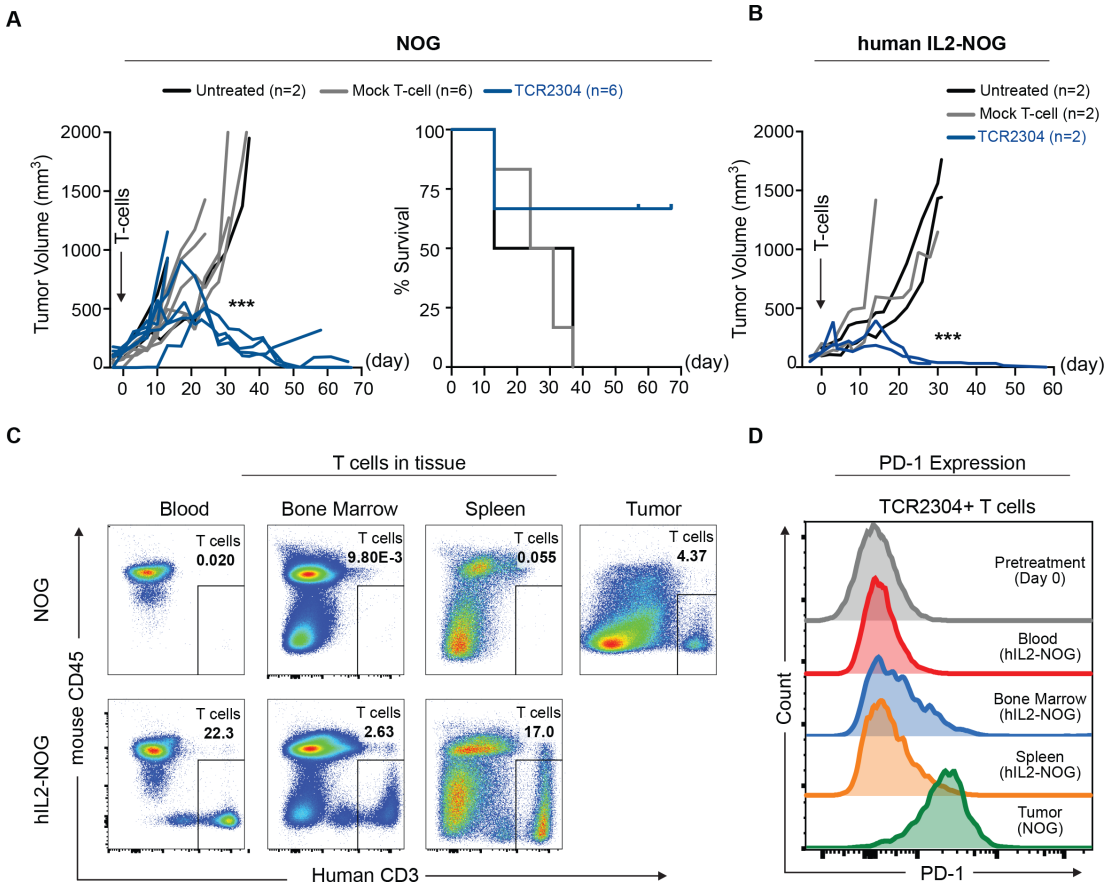

Figure 5 Therapeutic efficacy of TCR-T cells in OCI-Ly3 xenograft mouse models. NOG and hIL2-NOG mice were subcutaneously injected with 5×10^6 HLA*B07:02 expressing OCI-Ly3 cells. Treatment with 1×10^7 T cells was given by intravenous injection after tumors reached the predetermined size of 100 mm^3. (A) Change of tumor volume (significance analysis by two-way ANOVA, showing difference of tumor volume on day 31: ***p<0.001) and survival after treatment start in NOG mice. (B) Change of tumor volume after treatment start in hIL2-NOG mice. Significance analysis by two-way ANOVA, showing difference on day 30: *p<0.05, **p<0.01, ***p<0.001, ****p<0.0001. (C) Flow cytometric analysis of T cells in tissues of TCR-T cell-treated common NOG and hIL2-NOG mice, 58 days after treatment. (D) PD-1 expression in TCR-T cells in tissues of hIL2-NOG and common NOG mice on day 58 after treatment start, analyzed by flow cytometry. ANOVA, analysis of variance; IL, interleukin; TCR, T-cell receptor.

Overnight coculture with these lymphoma cells led to activation of TCR-T cells (figure 4C), which was accompanied by mutation-specific cytotoxicity (figure 4D,E) and T-cell proliferation (figure 4F). Specific T-cell response and cytotoxicity against naturally mutant lymphoma cells provided further evidence for the functional potential of TCR2304.

Myd88 L265P-redirected TCR-T cells induce durable regression of human lymphoma xenografts in mice

Having observed a strong specific T-cell response against MyD88 L265P mutant B-cell lymphoma lines in vitro, we tested TCR2304 in vivo for further assessment of its therapeutic potential. For this purpose, we generated a xenograft model by subcutaneously injecting HLA-B*07:02-expressing OCI-Ly3 cells into immunodeficient NOG mice. After tumors reached the predetermined size of 100 mm^3, mice were randomly treated with a single intravenous injection of 1×10^7 TCR-T or mock T cells, or PBS as untreated control. All untreated or mock-treated mice showed progressive tumor growth that required sacrificing the mice between days 13 and 37 (figure 5A). Four of the six mice that received TCR2304-T cells showed complete remission of the tumor, with tumor shrinking beginning between days 18 and 25 after T-cell application, although in one of these mice the tumor started to regrow around day 40. Two mice needed to be sacrificed early in the experiment due to rapid tumor progression and severe symptoms of disease before TCR-T cells could take effect. Since human T cells grow poorly without support from human cytokines, we also used the same tumor model in hIL2-NOG (immunodeficient NOG mouse expressing human IL-2 cytokine). This model is expected to have an enhanced T-cell engraftment and has been shown to improve the outcome from T-cell therapy.[25] Indeed, tumors in hIL2-NOG mice that received TCR-T cells disappeared completely after 3 weeks and did not relapse after up to 2 months following treatment (figure 5B).

To evaluate the mechanisms leading to tumor regrowth after initial response, the NOG mouse that had shown

tumor regrowth starting on day 40 was sacrificed on day 58 together with a mouse that had continuing response from the hIL2-NOG TCR-T treated group. We observed that the hIL2-NOG mouse still had a high amount of human T cells in blood, bone marrow and spleen, while the NOG mouse had only some T cells remaining in the tumor (figure 5C). TCR-T cells from tissues of the hIL2-NOG mouse did not show any significant change in the exhaustion marker PD-1 (programmed cell death protein 1), while TCR-T cells remaining in the growing tumor of the NOG mouse showed increased PD-1 staining in flow cytometric analysis (figure 5D).

However, in a second series of experiments using hIL2-NOG mice, some of the animals died independently of the size of the tumor. We had hints that these mice were developing severe graft-versus-host disease (GvHD) by proliferating human T cells, as reported by Ito *et al*.[26] The amount of GvHD-related toxicity indeed varied significantly using different human donors; therefore, we decided to stop further experiments in this model.

To validate our findings in a second model, luciferase-expressing HLA-B*07:02-positive TMD8 cells were subcutaneously injected into NOG mice, yet it caused some mice to die early due to strong systemic dissemination and aggressive tumor progression before treatment could be administered. Therefore, we decided to treat TMD8 bearing NOG mice 7 days after tumor inoculation. Indeed, on these experimental conditions, the T-cell treatment led to a significant reduction in tumor size starting at day 24 (figure 6A,B). Furthermore, TCR-T cell treatment prevented systemic dissemination of TMD8 cells (figure 6C,D and online supplemental figure 3).

Again, data in hIL2-NOG mice were complicated by T-cell toxicity caused by human versus mouse GvHD, which differed from experiment to experiment depending on different human donors, and although these experiments largely confirmed activity of transduced T cells in controlling tumor growth, they are not presented here.

TCR2304 is highly specific for the MyD88 L265P mutation without off-target reactivity

Even though all TCRs described in this study were isolated from healthy HLA-B7- positive donors and thus passed thymic selection, the risk of cross-reactivity against other human proteins is still potentially present. Peptides generated in the alanine scan were loaded separately on HLA-B*07:02-expressing K562 cells and cocultured with TCR-T cells to define the amino acids that are essential for the recognition (binding motif) by different TCRs (online supplemental figure 4). The proline in position 2, which reflects the amino acid substitution L265P in mutant MyD88, as well as the tyrosine in position 7, turned out to be essential for all TCRs, demonstrating the specificity of the TCRs for the mutation. Following detection of the binding motif (online supplemental figure 5A), we assessed the possibility of cross-reactivity to other human proteins, which might be caused by binding-sequence similarity, using the online tool Expitope.[20] In the case of TCR2304, the screen revealed 26 human peptides exhibiting motif similarity (xPxxIxYxxx) with up to five amino acid mismatches: 12 of these had some predicted binding affinity to HLA-B*07:02 on NetMHC V.4.0 and/or NetMHCpan V.4.0 (online supplemental figure 5). We tested TCR-T cells against all 12 peptides loaded on HLA-B*07:02-positive K562 cells in high concentration (10 µg/mL) in a coculture. However, no meaningful response was observed (online supplemental figure 5B).

For assessment of alloreactivity, we cocultured TCR-T cells with a panel of 16 Epstein-Barr virus-immortalized B-LCLs, which covered a broad spectrum of HLA haplotypes and most of the frequent HLA alleles found in Europe (Online supplemental table 2). When compared with untransduced control T cells, overnight coculture only demonstrated significant TCR-T cell response when HLA-B7-positive cell lines were externally loaded with mutant peptide (online supplemental figure 5C). Thus, we did not observe any sign of alloreactivity in this setting.

DISCUSSION

Contrary to CAR-T cell-based approaches, TCR-based cellular therapy has not yet led to breakthrough clinical results. However, because of the promise of cancer specificity, targeting tumor-specific neoepitopes by TCR gene therapy is continuing to attract attention. In solid tumors, TCRs directed against patient-individual mutations but also against a few recurrent mutations have been successfully isolated. First trials targeting mutant KRAS are currently recruiting.[27 28]

In this study, we present strong preclinical evidence that the lymphoma-associated L265P point mutation of MyD88 creates suitable neoepitopes for HLA-presentation, eliciting an efficient mutation-specific T-cell response. We have isolated a high-affinity TCR targeting a 10 mer neoepitope restricted to HLA-B*07:02, which mediates strong in vitro T-cell response against lymphoma cells with both homozygous and heterozygous L265P mutations. Adoptive transfer of gene-modified TCR-T cells shows promising therapeutic effect in preclinical experiments using human xenografts in immune-deficient mice. Our data indicate that the mutant epitope can indeed serve as a rejection antigen. In addition, preliminary safety screening does not indicate off-target activity of the TCR.

In a previous study by Nelde *et al* in 2017,[29] potential peptides derived from MyD88 L265P had been analyzed and shown to generate T-cell responses restricted to HLA-B*07:02 and HLA-B*15:01. Peptide-specific T cells reported in their study showed cytotoxic reactivity against peptide-loaded target cells, and it was suggested that these peptides may be used for a peptide-based immunotherapy approach, in case the peptides are naturally processed and presented. A separate study by Nielsen *et al*[30] in the same year confirmed that one of the mentioned peptides restricted to HLA-B*07:02 induced a mutation-specific T-cell response, and data suggested that the target epitope is endogenously processed. Peptide-specific T

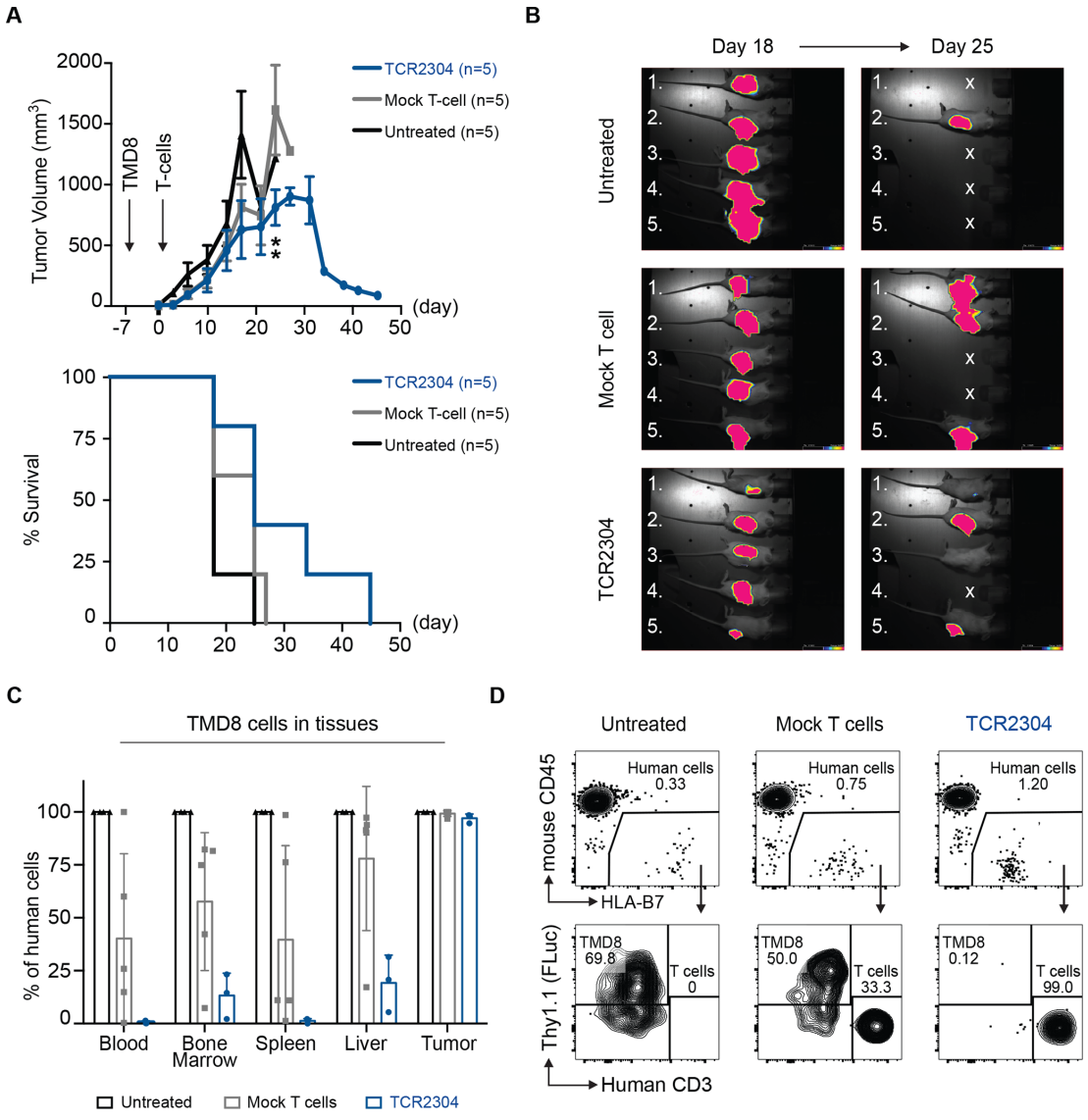

Figure 6 Therapeutic efficacy of TCR2304-T cells in TMD8 xenograft mouse model. NOG mice were suncutaneously injected with 5×10^6 TMD8 cells that are stably transduced with HLA*B07:02 and firefly luciferase. Tumor growth was detectable via bioluminescence imaging in all mice as early as day 2. (A) Change of tumor volume over time (error bars plotted with SEM significance analysis by two-way analysis of variance, showing difference on day 24: **p<0.01) and survival of NOG mice after treatment start. (B) Bioluminescence images of tumor-bearing mice at days 18 and 25 after treatment. Exposure: 60 s. (C) Flow cytometric analysis of systemic dissemination: proportion of TMD8 cells in tissues of tumor-bearing NOG mice. Human cells meaning sum of TMD8 lymphoma cells and human T cells. (D) Representative staining of blood samples from tumor-bearing NOG mice. Shown plots were pregated on single, viable cells.

cells against this HLA-B*07:02-restricted epitope were only detected in one out of six donors, hinting that a peptide-based immunotherapy approach may not elicit autologous immunity in the majority of patients.

In vitro antigen processing experiments, generating linear non-spliced peptides, are accepted to mirror the in vivo situation with high fidelity.[24] In our work, we show that the HLA-B*07:02 10 mer neoepitope is generated in vitro and that we also could generate strong T-cell responses in 5 out of 24 donors. However, only a few of 13 isolated and cloned TCRs from these five donors showed high affinity for the mutated peptide—demonstrating reactivity in the nanomolar range, which is thought to be crucial to achieve a therapeutic antitumor effect.[31] Our high-affinity TCR elicited strong therapeutic activity in a preclinical mouse model, suggesting that the sequence of a high-affinity TCR could be used 'off the shelf' to generate a highly specific, individualized yet broadly applicable ATT product usable in all HLA-B*07:02-positive patients whose tumors carry the L265P mutation. In our opinion, such a treatment could fulfill in an ideal way the criteria for precision cancer therapy.

A main limitation to TCR gene therapy is the impaired MHC–peptide presentation in cancer cells. Mutations in the processing and presentation machinery, or downregulation of MHC molecules on the cell surface, is described in solid cancers and also in lymphomas.[32 33] However, this rarely affects all malignant cells in a tumor and rarely

results in a total loss of HLA antigens. IFN-γ secretion by even a few specific T cells engaging tumor might be able to transform the tumor microenvironment,[34] inducing MHC upregulation and possibly enhancing the susceptibility of tumor cells to further TCR-T cells migrating into the tumor.[35]

In this respect, the difference we observed between hIL2-NOG and normal NOG mice is remarkable: NOG mice, in which T-cell proliferation is not supported by IL-2, showed some T-cell infiltration in tumors after adoptive transfer of MyD88 L265P-specific TCR-T cells, but tumors in some mice eventually regrew. Thus, it appears that besides lack of cytokine support for T-cell proliferation, upregulation of checkpoint inhibitory signals in T cells may have contributed to this result. Recent studies[36 37] have shown that MyD88-mutant lymphomas exhibit high level expression of the immune-checkpoint mediator PD-L1, thus possibly preventing their efficient clearance by adaptive host immunity. Conversely, these mutant-specific dependencies were therapeutically exploitable by anti-PD1 checkpoint blockade. On the other hand, mice where T-cell growth is supported by IL-2 stay in remission. Experiments in human IL-2 transgenic mice, however, are complicated by strong GVHD effect of human T cells with strong variations in the severity of GVHD from donor to donor; therefore, only a limited number of experiments were performed using this model. We think that in an appropriate clinical setting where autologous transduced T cells likely encounter cytokine support—particularly if administered after lymphodepletion—escape mechanisms could be avoided. A combination of adoptive transfer of mutation-specific TCR-T cells with immune-checkpoint blockade[38] might also be considered in a second phase of a pilot study.

We have tested our TCR in xenografted tumors but considered using a syngeneic lymphoma model with conditional MyD88 L265P mutation.[39] However, these mice would have to be crossed to humanized HLA-B*07:02 mice,[40] which is time consuming. More importantly, the information provided by such a model would be limited with respect to issues of safety and toxicity of the TCR in a clinical context, which is eventually crucial before moving to a clinical trial. This being our prior issue, we have extensively evaluated our TCR for potential toxicity. Based on our experience with generation of TCRs for ATT, we are confident that major reactivities can be excluded based on our LCL reactivity and alanine scan experiments. Moreover, while a number of TCRs are generated in transgenic mice for other targets with some of them already being approved by regulatory authorities for testing in clinical trials,[41 42] TCRs described in this study were generated from healthy humans—without further modifications to enhance affinity—and had undergone thymic selection, thus at least theoretically further reducing the risk of unwanted recognition of self-proteins. Further safety testing, such as reactivity studies using larger cell line and tissue libraries or the use of amino acids other than alanine in amino acid replacements,[43] has been proposed and will be discussed with safety authorities if required in preparation of a clinical trial.

We believe that besides CAR-T cell therapy, which has become a tremendous tool for the treatment of poor prognosis lymphomas and leukemias, there is a great potential in the use of TCR-T cell therapy. Our study provides a strong base for such a highly tumor-specific, molecularly defined TCR-based immunotherapy in selected hematological malignancies.

Author affiliations
[1]Department of Hematology, Oncology and Tumor Immunology, Charité – Universitätsmedizin Berlin, corporate member of Freie Universität Berlin, Humboldt-Universität zu Berlin, and Berlin Institute of Health, Berlin, Germany
[2]Max-Delbrück-Center for Molecular Medicine in the Helmholtz Association, Berlin, Germany
[3]Experimental Pharmacology and Oncology Berlin-Buch GmbH (EPO), Berlin, Germany
[4]Institute of Biochemistry, Charité – Universitätsmedizin Berlin, corporate member of Freie Universität Berlin, Humboldt-Universität zu Berlin, and Berlin Institute of Health, Berlin, Germany

Twitter Özcan Çınar @cinar_ozcan

Acknowledgements The authors thank Professor Dr Thomas Blankenstein (Charité–Universitätsmedizin Berlin, Germany) for constructive suggestions during the experimental phase and for reading the manuscript. The authors acknowledge Professor Dr Gerald Willimsky (Charité–Universitätsmedizin Berlin, Berlin, Germany) and Dr Armin Rehm (Max-Delbrück-Center for Molecular Medicine, Berlin, Germany) for helpful discussion through the study. The authors also thank Dr Simone Rhein (Max-Delbrück-Center for Molecular Medicine, Berlin, Germany) for technical advice and Dr Dilansu Guneykaya (Harvard Medical School, Boston, Massachusetts, USA) for experimental support and for helping the preparation of the manuscript.

Contributors ÖÇ designed and implemented studies, acquired, analyzed and interpreted data, and wrote the manuscript; BB designed and implemented animal studies and acquired and analyzed data; CG, CB and CAP acquired data; PMK interpreted the biochemistry data and reviewed and revised the manuscript; UK reviewed and revised the manuscript; AP designed and supervised the studies, interpreted the data, and reviewed and revised the manuscript; AB designed the studies, interpreted the data, and reviewed and revised the manuscript.

Funding This study was supported by SPARK/Validation Fund from Berlin Institute of Heath (BIH). ÖÇ was supported by fundings provided by Berlin School of Integrative Oncology (Charité–Universitätsmedizin Berlin) and The German Academic Exchange Service.

Competing interests AP and ÖÇ are inventors on a filed patent application for the T-cell receptors described in the study (WO 2020/152161 A1).

Patient consent for publication Not required.

Provenance and peer review Not commissioned; externally peer reviewed.

Data availability statement Data are available upon reasonable request. All data relevant to the study are included in the article or uploaded as supplementary information. For further information, please contact oezcan.cinar@charite.de. Supplementary files can be found in the online version of this article. Complete length nucleic acid and amino acid sequences of T-cell receptors can be found in the published patent application: WO 2020/152161 A1.

ORCID iDs
Özcan Çınar http://orcid.org/0000-0001-5297-127X
Ulrich Keller http://orcid.org/0000-0002-8485-1958

REFERENCES

1 Kochenderfer JN, Dudley ME, Kassim SH, *et al*. Chemotherapy-refractory diffuse large B-cell lymphoma and indolent B-cell malignancies can be effectively treated with autologous T cells expressing an anti-CD19 chimeric antigen receptor. *J Clin Oncol* 2015;33:540–9.
2 Neelapu SS, Locke FL, Bartlett NL, *et al*. Axicabtagene ciloleucel CAR T-cell therapy in refractory large B-cell lymphoma. *N Engl J Med* 2017;377:2531–44.
3 Zhang W-Y, Wang Y, Guo Y-L, *et al*. Treatment of CD20-directed chimeric antigen receptor-modified T cells in patients with relapsed or refractory B-cell non-Hodgkin lymphoma: an early phase IIA trial report. *Signal Transduct Target Ther* 2016;1:1–9.
4 Fry TJ, Shah NN, Orentas RJ, *et al*. CD22-targeted CAR T cells induce remission in B-ALL that is naive or resistant to CD19-targeted CAR immunotherapy. *Nat Med* 2018;24:20–8.
5 Raje N, Berdeja J, Lin Y, *et al*. Anti-BCMA CAR T-cell therapy bb2121 in relapsed or refractory multiple myeloma. *N Engl J Med* 2019;380:1726–37.
6 Sotillo E, Barrett DM, Black KL, *et al*. Convergence of acquired mutations and alternative splicing of CD19 enables resistance to CART-19 immunotherapy. *Cancer Discov* 2015;5:1282–95.
7 Braig F, Brandt A, Goebeler M, *et al*. Resistance to anti-CD19/CD3 bite in acute lymphoblastic leukemia may be mediated by disrupted CD19 membrane trafficking. *Blood* 2017;129:100–4.
8 Brudno JN, Kochenderfer JN. Chimeric antigen receptor T-cell therapies for lymphoma. *Nat Rev Clin Oncol* 2018;15:31–46.
9 Futreal PA, Coin L, Marshall M, *et al*. A census of human cancer genes. *Nat Rev Cancer* 2004;4:177–83.
10 Blankenstein T, Leisegang M, Uckert W, *et al*. Targeting cancer-specific mutations by T cell receptor gene therapy. *Curr Opin Immunol* 2015;33:112–9.
11 Tran E, Robbins PF, Lu Y-C, *et al*. T-Cell transfer therapy targeting mutant KRAS in cancer. *N Engl J Med* 2016;375:2255–62.
12 Malekzadeh P, Pasetto A, Robbins PF, *et al*. Neoantigen screening identifies broad TP53 mutant immunogenicity in patients with epithelial cancers. *J Clin Invest* 2019;129:1109–14.
13 Ngo VN, Young RM, Schmitz R, *et al*. Oncogenically active MYD88 mutations in human lymphoma. *Nature* 2011;470:115–21.
14 Rovira J, Karube K, Valera A, *et al*. MYD88 L265P mutations, but no other variants, identify a subpopulation of DLBCL patients of activated B-cell origin, extranodal involvement, and poor outcome. *Clin Cancer Res* 2016;22:2755–64.
15 Lee J-H, Jeong H, Choi J-W, *et al*. Clinicopathologic significance of MYD88 L265P mutation in diffuse large B-cell lymphoma: a meta-analysis. *Sci Rep* 2017;7:1–8.
16 Xu L, Hunter ZR, Yang G, *et al*. MYD88 L265P in Waldenström macroglobulinemia, immunoglobulin M monoclonal gammopathy, and other B-cell lymphoproliferative disorders using conventional and quantitative allele-specific polymerase chain reaction. *Blood* 2013;121:2051–8.
17 Textoris-Taube K, Kuckelkorn U, Beier C, *et al*. Analysis of proteasome-generated antigenic peptides by mass spectrometry. *Methods Mol Biol* 2019;1988:15–29.
18 Engels B, Cam H, Schüler T, *et al*. Retroviral vectors for high-level transgene expression in T lymphocytes. *Hum Gene Ther* 2003;14:1155–68.
19 Wölfl M, Greenberg PD. Antigen-specific activation and cytokine-facilitated expansion of naive, human CD8+ T cells. *Nat Protoc* 2014;9:950–66.
20 Jaravine V, Mösch A, Raffegerst S, *et al*. Expitope 2.0: a tool to assess immunotherapeutic antigens for their potential cross-reactivity against naturally expressed proteins in human tissues. *BMC Cancer* 2017;17:1–9.
21 Andreatta M, Nielsen M. Gapped sequence alignment using artificial neural networks: application to the MHC class I system. *Bioinformatics* 2016;32:511–7.
22 Jurtz V, Paul S, Andreatta M, *et al*. NetMHCpan-4.0: improved peptide-MHC class I interaction predictions integrating eluted ligand and peptide binding affinity data. *J Immunol* 2017;199:3360–8.
23 Sidney J, Southwood S, del Guercio MF. Specificity and degeneracy in peptide binding to HLA-B7-like class I molecules. *J Immunol* 1996;157:3480–90.
24 Sijts EJAM, Kloetzel PM. The role of the proteasome in the generation of MHC class I ligands and immune responses. *Cell Mol Life Sci* 2011;68:1491–502.
25 Forsberg EMV, Lindberg MF, Jespersen H, *et al*. HER2 CAR-T cells eradicate uveal melanoma and T-cell therapy-resistant human melanoma in IL2 transgenic NOD/SCID IL2 receptor knockout mice. *Cancer Res* 2019;79:899–904.
26 Ito R, Katano I, Kawai K, *et al*. A novel xenogeneic graft-versus-host disease model for investigating the pathological role of human $CD4^+$ or $CD8^+$ T cells using immunodeficient NOG mice. *Am J Transplant* 2017;17:1216–28.
27 Administering peripheral blood lymphocytes transduced with a murine T-cell receptor recognizing the G12D variant of mutated Ras in HLA-A*11:01 patients. Available: https://clinicaltrials.gov/ct2/show/NCT03745326 [Accessed 19 Nov 2018].
28 National Library of Medicine (US), ClinicalTrials.gov [Internet]. Administering peripheral blood lymphocytes transduced with a murine T-cell receptor recognizing the G12V variant of mutated Ras in HLA-A*11:01 patients. Available: https://clinicaltrials.gov/ct2/show/NCT03190941 [Accessed 19 Jun 2017].
29 Nelde A, Walz JS, Kowalewski DJ, *et al*. HLA class I-restricted *MYD88* L265P-derived peptides as specific targets for lymphoma immunotherapy. *Oncoimmunology* 2017;6:e1219825.
30 Nielsen JS, Chang AR, Wick DA, *et al*. Mapping the human T cell repertoire to recurrent driver mutations in MyD88 and EZH2 in lymphoma. *Oncoimmunology* 2017;6:e1321184–10.
31 Sim MJW, Lu J, Spencer M, *et al*. High-Affinity oligoclonal TCRs define effective adoptive T cell therapy targeting mutant KRAS-G12D. *Proc Natl Acad Sci U S A* 2020;117:12826–35.
32 Riemersma SA, Jordanova ES, Schop RF, *et al*. Extensive genetic alterations of the HLA region, including homozygous deletions of HLA class II genes in B-cell lymphomas arising in immune-privileged sites. *Blood* 2000;96:3569–77.
33 Challa-Malladi M, Lieu YK, Califano O, *et al*. Combined genetic inactivation of β2-microglobulin and CD58 reveals frequent escape from immune recognition in diffuse large B cell lymphoma. *Cancer Cell* 2011;20:728–40.
34 Kammertoens T, Friese C, Arina A, *et al*. Tumour ischaemia by interferon-γ resembles physiological blood vessel regression. *Nature* 2017;545:98–102.
35 Brossart P. The role of antigen spreading in the efficacy of immunotherapies. *Clin Cancer Res* 2020;26:4442–7.
36 Reimann M, Schrezenmeier J, Richter-Pechanska P, *et al*. Adaptive T-cell immunity controls senescence-prone MyD88- or CARD11-mutant B-cell lymphomas. *Blood* 2021;137:2785–99.
37 Flümann R, Rehkämper T, Nieper P, *et al*. An autochthonous mouse model of Myd88- and BCL2-Driven diffuse large B-cell lymphoma reveals actionable molecular vulnerabilities. *Blood Cancer Discov* 2021;2:70–91.
38 Stadtmauer EA, Fraietta JA, Davis MM, *et al*. CRISPR-engineered T cells in patients with refractory cancer. *Science* 2020;367. doi:10.1126/science.aba7365. [Epub ahead of print: 28 02 2020].
39 Knittel G, Liedgens P, Korovkina D, *et al*. B-Cell-Specific conditional expression of Myd88p.L252P leads to the development of diffuse large B-cell lymphoma in mice.. *Blood* 2016;127:2732–41.
40 Alexander J, Oseroff C, Sidney J, *et al*. Derivation of HLA-B*0702 transgenic mice: functional CTL repertoire and recognition of human B*0702-restricted CTL epitopes. *Hum Immunol* 2003;64:211–23.
41 Obenaus M, Leitão C, Leisegang M, *et al*. Identification of human T-cell receptors with optimal affinity to cancer antigens using antigen-negative humanized mice. *Nat Biotechnol* 2015;33:402–7.
42 Çakmak-Görür N, Radke J, Rhein S, *et al*. Intracellular expression of FLT3 in Purkinje cells: implications for adoptive T-cell therapies. *Leukemia* 2019;33:1039–43.
43 Karapetyan AR, Chaipan C, Winkelbach K, *et al*. Tcr fingerprinting and off-target peptide identification. *Front Immunol* 2019;10:1–14.

3.3 Publication 3: Long-term in vitro expansion ensures increased yield of central memory T cells as perspective for manufacturing challenges.

Abstract: Adoptive T cell therapy (ATT) has revolutionized the treatment of cancer patients. A sufficient number of functional T cells are indispensable for ATT efficacy; however, several ATT dropouts have been reported due to T cell expansion failure or lack of T cell persistence in vivo. With the aim of providing ATT also to those patients experiencing insufficient T cell manufacturing via standard protocol, we evaluated if minimally manipulative prolongation of in vitro expansion (long-term [LT] >3 weeks with IL-7 and IL-15 cytokines) could result in enhanced T cell yield with preserved T cell functionality. The extended expansion resulted in a 39-fold increase of murine CD8+T central memory cells (Tcm). LT expanded CD8+ and CD4+Tcm cells retained a gene expression profile related to Tcm and T memory stem cells (Tscm). In vivo transfer of LT expanded Tcm revealed persistence and antitumor capacity. We confirmed our in vitro findings on human T cells, on healthy donors and diffuse large B cell lymphoma patients, undergoing salvage therapy. Our study demonstrates the feasibility of an extended T cell expansion as a practicable alternative for patients with insufficient numbers of T cells after the standard manufacturing process thereby increasing ATT accessibility.

International Journal of Cancer (Int. J. Cancer), 2021; volume 148; issue 12; 3097–3110, DOI: 10.1002/ijc.33523

Contribution to the publication

T cell receptor transduced T cells of healthy donors were prepared and expanded in a long-term (LT) culture for the presented study. In vitro experimental set up design of TCR-specific T cell activation was provided, and the manuscript was reviewed.

Received: 16 June 2020 | Revised: 15 January 2021 | Accepted: 27 January 2021

DOI: 10.1002/ijc.33523

TUMOR IMMUNOLOGY AND MICROENVIRONMENT

IJC International Journal of Cancer

Long-term in vitro expansion ensures increased yield of central memory T cells as perspective for manufacturing challenges

Stefanie Herda[1] | Andreas Heimann[1,2] | Benedikt Obermayer[3] | Elisa Ciraolo[1] | Stefanie Althoff[1] | Josefine Ruß[1] | Corinna Grunert[4] | Antonia Busse[5] | Lars Bullinger[5] | Antonio Pezzutto[2,4,5] | Thomas Blankenstein[2,4,6] | Dieter Beule[3] | Il-Kang Na[1,2,5,7]

[1]Experimental and Clinical Research Center, Berlin, Germany

[2]Berlin Institute of Health, Berlin, Germany

[3]Core Unit Bioinformatics – CUBI, Berlin Institute of Health, Berlin, Germany

[4]Max-Delbrück-Center for Molecular Medicine, Berlin, Germany

[5]Department of Hematology, Oncology and Tumor Immunology, Charité-Universitätsmedizin Berlin, corporate member of Freie Universität Berlin, Humboldt-Universität zu Berlin, and Berlin Institute of Health, Berlin, Germany

[6]Institute of Immunology, Charité, Campus Berlin Buch, Berlin, Germany

[7]Berlin Institute of Health Center for Regenerative Therapies, Charité – Universitätsmedizin Berlin, Berlin, Germany

Correspondence
Il-Kang Na, Department of Hematology, Oncology and Tumor Immunology, Charité-Universitätsmedizin, Berlin, Augustenburger Platz 1, 13353 Berlin, Germany.
Email: il-kang.na@charite.de

Funding information
Berlin Institute of Health; Deutsche Forschungsgemeinschaft, Grant/Award Number: TR36; Experimental and Clinical Research Center - ECRC

Abstract

Adoptive T cell therapy (ATT) has revolutionized the treatment of cancer patients. A sufficient number of functional T cells are indispensable for ATT efficacy; however, several ATT dropouts have been reported due to T cell expansion failure or lack of T cell persistence in vivo. With the aim of providing ATT also to those patients experiencing insufficient T cell manufacturing via standard protocol, we evaluated if minimally manipulative prolongation of in vitro expansion (long-term [LT] >3 weeks with IL-7 and IL-15 cytokines) could result in enhanced T cell yield with preserved T cell functionality. The extended expansion resulted in a 39-fold increase of murine $CD8^+$ T central memory cells (Tcm). LT expanded $CD8^+$ and $CD4^+$ Tcm cells retained a gene expression profile related to Tcm and T memory stem cells (Tscm). In vivo transfer of LT expanded Tcm revealed persistence and antitumor capacity. We confirmed our in vitro findings on human T cells, on healthy donors and diffuse large B cell lymphoma patients, undergoing salvage therapy. Our study demonstrates the feasibility of an extended T cell expansion as a practicable alternative for patients with insufficient numbers of T cells after the standard manufacturing process thereby increasing ATT accessibility.

KEYWORDS
adoptive immunotherapy, cytokines, T lymphocytes, translational medical research

Abbreviations: ATT, adoptive T cell therapy; Bcl-2, B cell lymphoma 2; BLI, BioLuminescent imaging; BLITC, BioLuminescent imaging of T cells; CAR, chimeric antigen receptor; DLBCL, diffuse large B cell lymphoma; GO, gene ontology; IFN-γ, interferon-γ; Lag3, lymphocyte activating 3; LT, long-term; MFI, mean fluorescence intensity; NFAT, nuclear factor of activated T cells; Nr4a1, Nuclear Receptor Subfamily 4 Group A Member 1; PCA, principal component analysis; Pdcd1, programmed cell death 1; Rag, recombination-activating gene; Sca1, stem cell antigen 1; ST, short-term; Tcm, central memory T cells; TCR, T-cell receptor; Teff, primarily effector T cells; Tem, effector memory T cells; TIR, T cell inhibitory receptor; TNF-α, tumor necrosis factor-α; Tox, Thymocyte Selection Associated High Mobility Group Box; Tscm, T memory stem cell.

1 | INTRODUCTION

Adoptive T-cell therapy (ATT) using T cells, genetically redirected with tumor-specific T cell receptor (TCR) or chimeric antigen receptors (CARs), has revolutionized the field of cancer immunotherapy. So far, the most notable success resulted from NY-ESO-1 TCR T cells for multiple melanoma[1] and CD19-CAR T cells for B cell-derived malignancies.[2,3] Part of the success of engineered T cells relates to the effective ex vivo expansion of T cells. Under conventional culture conditions with IL-2, T cells differentiate into central memory T cells (Tcm), effector memory T cells (Tem) and primarily effector T cells (Teff). In recent years, it has been shown that T cell cultivation in the presence of IL-7, IL-15 and IL-21[4-10] or low molecular weight compounds such as the glycogen synthase kinase-3β inhibitor TWS119 promotes the generation of valuable Tcm and T memory stem cells (Tscm) improving ATT efficacy.[11-13] Unlike Tem and Teff, Tcm retain their ability to proliferate and survive for long term (LT).[14-16] Clinical T cell manufacturing protocols for ATT include leukapheresis of $CD8^+$ or $CD4^+$ T cells, followed by ex vivo activation, 9 to 14 days expansion and reinfusion of T cells.[17,18] Several recent preclinical studies have attempted to reduce the duration of ex vivo culture to limit T cell differentiation and enhance the efficacy of ATT.[19-21] Although reduction of the manufacturing time could be beneficial for the differentiation state of T cells and their overall quality, this may represent a limitation for those patients experiencing lymphopenia and lymphocyte dysfunctions subsequent to multiple lines of chemotherapy. ATT is a multistep process and some ATT dropouts are caused by failure to obtain sufficient numbers of T cells to reinfuse. Manufacturing of CD19 CAR T cells failed in 6% to 24% of patients, particularly if they were isolated from older or heavily pretreated diffuse large B-cell lymphoma (DLBCL) patients.[8,21,22] In our study, we aim to address whether a simple extension of T cell expansion in the presence of IL-7 and IL-15 may represent an opportunity to prevent or reduce ATT dropouts in a minimally manipulative manner by sticking to the standard cytokine protocol.

What's new

Adoptive T cell therapy (ATT) is a risky procedure involving the isolation, ex-vivo expansion, and reinfusion of tumor-specific T cells. T cell manufacturing in ATT represents a bottleneck that can limit access to therapy for those patients that experience lymphopenia or lymphocyte dysfunctions. Here, the authors evaluated if minimally manipulative prolongation of in vitro expansion (>3 weeks with IL-7 and IL-15 cytokines) could result in enhanced T cell yields with preserved T cell functionality. The results demonstrate the feasibility of extended T cell expansion as an alternative for patients with insufficient numbers of T cells after the standard manufacturing procedure.

2 | MATERIALS AND METHODS

2.1 | Mice

See Supplemental Table 1. All mice were kept under specific pathogen-free conditions following institutional guidelines.

2.2 | Murine T-cell preparation and culture

T cells were harvested from spleens, using a $CD4^+$ or $CD8^+$ isolation kit (Miltenyi Biotec, Bergisch Gladbach, Germany). T cells were cultured in T cell medium (TCM) consisting of RPMI and 10% fetal bovine serum (FBS; both from Life Technologies, Carlsbad, CA, United States) supplemented with 100 U/mL penicillin, 100 mg/mL streptomycin, 1 mmol/L sodium pyruvate, 1x nonessential amino acids, 50 mmol/L β-mercaptoethanol and 2 mmol/L L-glutamine (all from Sigma-Aldrich, Merck KGaA, Darmstadt, Germany). For activation, T cells were stimulated in vitro for 72 hours (polyclonal T cells from albino B6 mice) in TCM plus 1 ng/mL recombinant human IL-2 (PeproTech, Cranbury, NJ, United States) in culture plates coated with 3 μg/mL anti-CD3 (clone 145-2C11) and 2 μg/mL anti-CD28 (clone 37.51; both BD Biosciences, San Jose, CA, United States). Transgenic T cells from Marilyn BioLuminescent imaging of T cells (BLITC) were activated only for 24 hours, since previous results revealed a significant activation-induced cell death after 72 hours (Supplemental Figure 1).

Afterward, T cells were expanded using TCM containing 50 ng/mL recombinant human IL-15 and 10 ng/mL recombinant human IL-7 (both Peprotech, Cranbury, NJ, United States) for further 4 days (short-term culture, ST) or 18 days ($CD4^+$) and 25 days ($CD8^+$) (Long-term culture, LT). Medium was refreshed every third or fourth day.

2.3 | Human T-cell culture

PBMC were isolated by density gradient centrifugation (Ficoll-Hypaque; GE Healthcare, Chicago, IL, United States) from fresh heparinized blood samples from nine healthy donors and from six patients with relapsed/refractory DLBCL which were candidates for high-dose chemotherapy with stem cell support. PBMC were stimulated in vitro for 72 hours in TCM plus 1 ng/mL recombinant human IL-2 (PeproTech, Cranbury, NJ, United States) in culture plates coated with 3 mg/mL anti-CD3 (clone OKT3) and anti-CD28 (clone 15E8, both Miltenyi Biotec, Bergisch Gladbach, Germany). Afterward, human T cells were expanded as murine T cells.

2.4 | Flow cytometry

Surface staining was performed in the presence of Fc-blocking antibodies (#101320, BioLegend, San Diego, CA, United States) according

to standard staining protocols. Intracellular staining for B-cell lymphoma 2 (Bcl-2), interferon-γ (IFN-γ), IL-2, IL-10 and tumor necrosis factor-α (TNF-α) was done with fixation/permeabilization buffer (#420801, #421002, BioLegend, San Diego, CA, United States), according to the manufacturer's instructions. Antibodies are listed in Supplemental Table 2. Samples were acquired on a FACS Canto II (BD Biosciences, San Jose, CA, United States) and CytoFLEX LX (Beckman Coulter, Krefeld, Deutschland), and all analyses were performed using the FlowJo software (FlowJo, LLC, Ashland, OR, United States).

2.5 | In vitro stimulation assay

5 x 10^5 cells/mL expanded T cells were plated into flat 24-well plates coated with anti-CD3/CD28 at 37°C. After 4 hours, granzyme B concentration was determined in the supernatant using the granzyme B Mouse Uncoated ELISA Kit (#88-8022-88, Thermo Fisher Scientific, Waltham, MA, United States), according to the manufacturer's protocol. Expanded T cells were also restimulated in the presence of 10 μg/mL Brefeldin A (Sigma-Aldrich, Merck KGaA, Darmstadt, Germany) and analyzed by standard flow cytometry staining protocols (see section "Flow cytometry").

2.6 | In vitro proliferation assay

Expanded T cells from albino B6 mice were adjusted to 10^7/mL and labeled with 10 μM CFSE (Sigma-Aldrich, Merck KGaA, Darmstadt, Germany) for 10 minutes at room temperature. Cells were washed with FBS and twice with TCM. To analyze in vitro proliferation, CFSE-labeled T cells were plated (10^5 cells/well) for 24 hours into flat 96-well plates coated with anti-CD3/CD28, respectively, 3 and 2 μg/mL, and then transferred into TCM for 3 days with IL-7/15. CFSE signal was then measured by flow cytometry at 24 hours after labeling and at day 4.

2.7 | Cell preparation for RNA sequencing and transcriptome analysis

$CD8^+$ or $CD4^+$ T cells were sorted for $CD44^+CD62L^+$ (>97%) using a FACS Aria II or Aria III (BD Biosciences). Afterward, RNA was isolated with the RNeasy Mini Kit (QIAGEN, Germantown, MR, United States). The RNA library was generated by using the NEBNext Ultra II Directional RNA Library Prep Kit for Illumina (NEB, Ipswich, MA, United States). Illumina sequencing was performed with NextSeq 500/550 High Output Kit v2 (Illumina, San Diego, CA, United States). RNA-seq expression data were normalized and log-transformed as log2(1 + TPM) (TPM: transcripts per million) for our own data and GSE80306.[23] The sequencing coverage and quality statistics for each sample are summarized in Supplemental Table 5. Microarray data were downloaded from GEO using the R package GEOquery (v2.46.15) for GSE92381,[23] GSE61697,[24] GSE23321,[11] GSE93211[12] and GSE80306[23] or directly extracted from cel files using the packages affy (v1.56), affydata (v1.26) and limma (v.3.34.9) for GSE41909[4] and GSE68003,[13] with rma background correction, quantile normalization and avgdiff summarization. Datasets were summarized over gene names, mapping mouse and human gene names onto each other using orthologues from MGI (HOM_MouseHumanSequence.rpt), and then combined after removing the bottom 5% of expressed genes, quantile normalization and batch correction with respect to assay using ComBat (package sva, v3.26.0). Clustering and principal component analysis (PCA) was performed using row z-scores for the gene set of Gattinoni et al.[11] Differential expression analysis was performed using DESeq2[25] using experimental batch as covariate and GO term analysis with topGO (v2.30.1).

2.8 | In vivo engraftment and persistence assay

Expanded T cells from BLITC mice were sorted for $CD44^+CD62L^+$ (>97%) using a FACS Aria II or Aria III (BD Biosciences, San Jose, CA, United States) and transferred into female albino recombination-activating gene, knock out (RagKO) mice via intravenous injection. Renilla luciferase signals of transferred T cells were measured monthly by BioLuminescent imaging (BLI). Mice were sacrificed after 1 month (engraftment) or 6 months (persistence) to quantify T cell numbers in secondary lymphoid organs using flow cytometry.

2.9 | SV40 TAg tumor model

The cell line TC200.09 was kindly provided by the Thomas Blankenstein's research group and all details are already described in Reference 26. Albino-RagKO mice were challenged with 5×10^6 TAg^+ 200ΔLuc cells, a gastric carcinoma cell line, which was genetically modified from the TC200.09 cell line[26] as described in Reference 27 and was grown in RPMI/FBS plus Dox (0.5 μg/mL). The retroviral packaging cell line PlatE (RRID:CVCL_B488) was grown in DMEM/FBS. All experiments were performed with mycoplasma-free cells. Tumors were grown for 45 days before ATT. $CD8^+$ T cells were transduced with SV40 Tag-specific TCR-I as described in Reference 27. Briefly, $CD8^+$ T cells from BLITC mice were sorted, in vitro activated and transduced with a retroviral vector expressing the alpha- and beta-chain of TCR-I (pMP71-TCR-I).[28] After in vitro expansion for 1 week (ST) or 4 weeks (LT), V_β7-positive $CD8^+$ T cells expressing TCR-I were sorted using a FACS Aria II or Aria III (BD Biosciences) and injected intravenously into tumor-bearing mice (10^5 T cells/mouse). Mean tumor diameter was determined every 2 days by caliper measurement and tumor size was calculated as length × width × weight/2. Mice were sacrificed if tumor volume became 1000 mm^3.

2.10 | H-Y tumor model

The male-derived urothelial carcinoma cell line MB49 (RRID:CVCL_7076) was kindly provided by the Thomas Blankenstein's research group. Cells

were grown in RPMI/FBS[29] and were adjusted to 2×10^5 cells/mL in PBS, mixed 1:1 with matrigel (BD Biosciences, San Jose, CA, United States) and kept on ice until subcutaneous injection of 100 µL (10^4 cells/mouse) into the hind flank of female age-matched albino RagKO mice. Thirteen days later, ST or LT expanded T cells from Marilyn BLITC mice[27] were sorted for $CD44^+$ and $CD62L^+$ (>97%) using a FACS Aria II or Aria III (BD Biosciences) and injected intravenously into tumor-bearing mice (5×10^5 T cells/mouse). Mean tumor diameter was determined every 2 days by caliper measurement and tumor size was calculated as length × width × weight/2. Mice were sacrificed if tumor volume became 1000 mm^3. All experiments were performed with mycoplasma-free cells.

2.11 | BioLuminescent imaging (BLI)

In vivo BLI was performed using a Xenogen IVIS 200 (PerkinElmer, Waltham, MA, United States) after mice were anesthetized with isoflurane (Baxter, Deerfield, IL, United States) in an XGI-8 anesthesia system (PerkinElmer, Waltham, MA, United States). In order to analyze Renilla luciferase signals (T cell engraftment, migration and persistence), mice were imaged 3 minutes after intravenous injection of freshly prepared coelenterazine (Biosynth Ltd, Newbury, United Kingdom) dissolved in 30% DMSO (Sigma-Aldrich, Merck KGaA, Darmstadt, Germany) and diluted in 70% PBS (#K813-500 mL, VWR) (100 µg/100 µL per mouse). To analyze nuclear factor of activated T cells (NFAT) dependent click-beetle luciferase signals (T cell activation), mice received intraperitoneally D-Luciferin (Biosynth Ltd, Newbury, United Kingdom) (300 µg/g body weight) prepared in PBS and were imaged 10 minutes later. Images were acquired for 5 minutes using small binning. All data were analyzed using Living Image analysis software (PerkinElmer, Waltham, MA, United States). The signal strength was quantified by photon/s/cm^2/steradian after digital setting of equal regions of interest.

2.12 | Generation of genetic modified $CD3^+$ T cells

Isolated human peripheral blood lymphocytes (PBL), isolated from healthy donors, were transduced with a specific tyrosinase-specific TCR-T58 as previously.[30] Briefly, 1×10^6 cells peripheral blood lymphocytes (PBL) were isolated from healthy donors, and seeded in

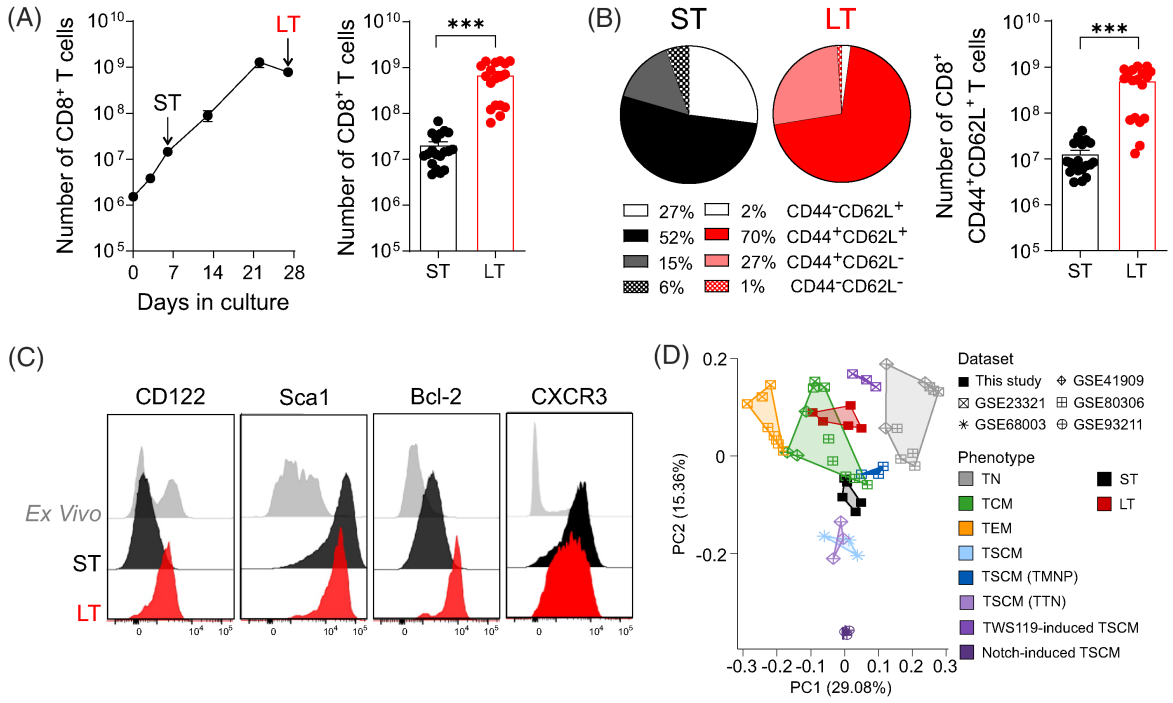

FIGURE 1 Extended expansion of murine T cells leads to increased numbers of $CD8^+$ T cells with Tcm/Tscm phenotype and preserved in vitro functional properties. Polyclonal $CD8^+$ T cells were isolated from C57BL/6 mice, activated via anti-CD3/CD28 and IL-2 for 72 hours and further cultured with IL-7/IL-15 for 4 (ST) or >21 (LT) days. The quantification and phenotypical analysis was done by flow cytometry. A, Growth kinetic of $CD8^+$ T cells is displayed by line diagram as mean values ± SEM. The bar shows mean ± SEM of total $CD8^+$ T cell numbers. B, Distributions of $CD8^+$ T cell subpopulations, defined by CD44 and CD62L, are illustrated in pies. The bar shows mean ± SEM of total $CD8^+CD44^+CD62L^+$ T cell numbers. Data were generated in 5 to 7 independent experiments with n = 5-9 mice. ***$P < .001$, paired t test. C, The $CD8^+CD44^+CD62L^+$ T cell subset resulting from the T cell culture was further characterized by CD122, Sca-1, Bcl-2 and CXCR3 and compared to ex vivo $CD8^+CD44^+CD62L^+$ T cells. Shown are representative histograms from three independent experiments with n = 3 mice. D, Principal component analysis (PCA) of ST and LT Tcm, IL-7/IL-15-generated Tscm cells (TTN,[4] GSE41909), naturally occurring $CD8^+$ T cell subsets (Tnaive/TN, Tem/TEM, Tcm/TCM, Tscm/TSCM,[11,20,34,53] GSE23321), TWS119-enriched Tscm (TSCM,[13] GSE68003) and Notch-induced Tscm (iTSCM,[12] GSE93211), memory T cells with naive phenotype (TMNP,[23] GSE80306) based on 852 genes described by Gattinoni et al from which 427 genes were expressed in all datasets [Color figure can be viewed at wileyonlinelibrary.com]

1 mL T cell medium containing 100 IU/mL IL-2 and on an anti-hCD3/hCD28-coated 24 well plates. Packaging cell line HEK-293T (RRID: CVCL_0063), stably transduced with MLV gag/pol and GALVenv, was transfected with retroviral vector MP71-encoding for tyrosinase-specific TCR-T58. PBLs were transduced by spinoculation with the infected HEK-293T supernatant and containing the virus particles and incubated 48 and 72 hours after activation, on retronectin coated plates in the presence of proteamin sulfate (4 μg/mL) and IL-2. Transduction efficiency was analyzed by flow cytometry by staining for CD8 (APC-H7), mTCRß-constant (PE) and DAPI. Cells were further cultured with IL-7 and IL-15 (each 5 ng/mL). Subsequent specific activation experiments were performed by seeding T cells on a peptid-coated (TCR-tyrosinase$^{369\text{-}377}$: YMDGTMSQV) plate. All experiments were performed with mycoplasma-free cells.

2.13 | Statistics

Statistical analysis was performed using the two-tailed paired *t* test, using GraphPad Prism 7.0 software (GraphPad Software). *P* values <.05 were considered statistically significant.

3 | RESULTS

3.1 | Extended expansion of murine T cells leads to increased numbers of CD8$^+$ T cells with Tcm and Tscm phenotype and preserved in vitro functional properties

In order to evaluate the ability of T cells to expand in a LT culture setting, we used a combined approach of previous published protocols with activation of murine T cells via anti-CD3/CD28 antibodies and consecutive expansion culture in the presence of IL-2 or IL-7/IL-15.[4,11,31] After 2 weeks of expansion, murine T cells exhibited a strong increase in the number of CD8$^+$ T cells. At around week 3 of culture, the CD8$^+$ T cell expansion reached a plateau phase. When we compared CD8$^+$ cell numbers between ST (7 days) and LT (>21 days) expansion, we found a 39-fold increase of CD8$^+$ LT T cells with respect to ST (Figure 1A). The majority of expanded CD8$^+$ T cells were CD44$^+$CD62L$^+$, a phenotype associated with Tcm subpopulation[4,32,33] (Figure 1B). Distribution analyses of subpopulations after 2 and 3 weeks of expansion showed that the increase in Tcm was accompanied by a decrease in naive T cells (data not shown), suggesting

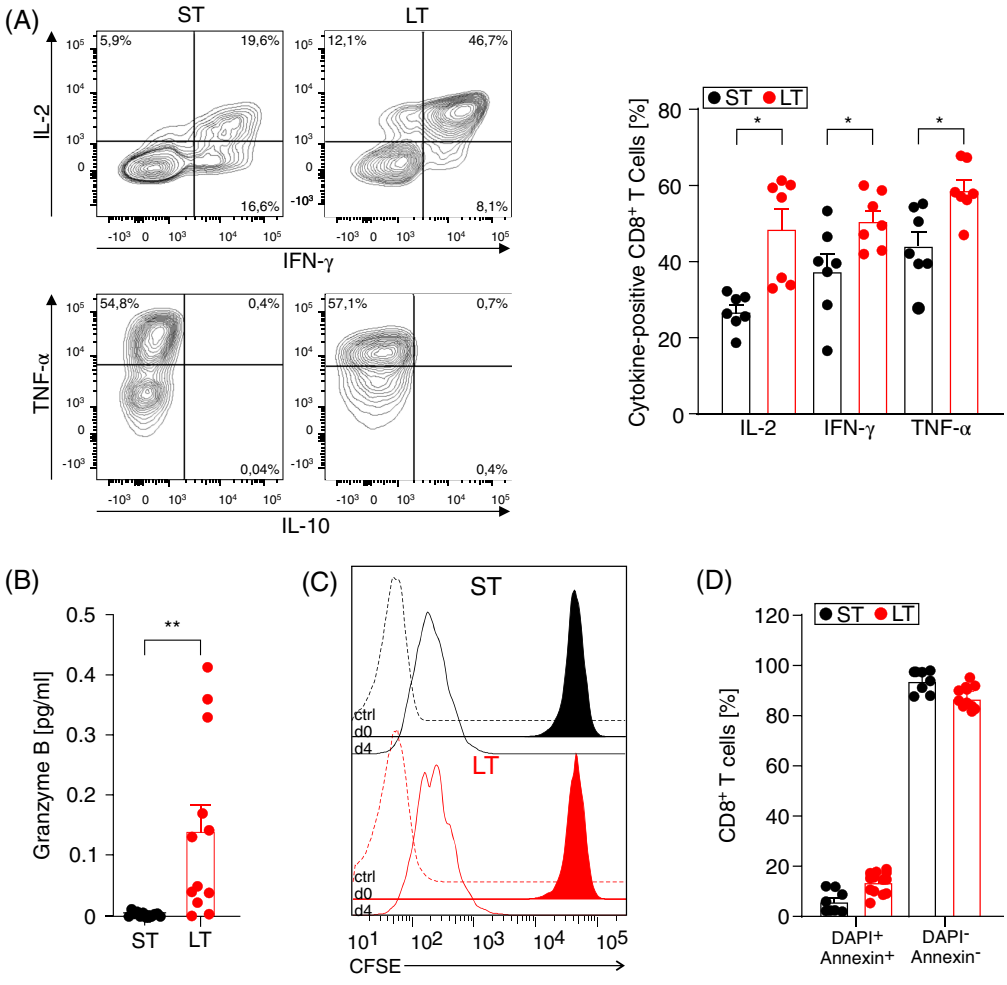

FIGURE 2 LT CD8$^+$ T cells have an increased cytokine expression after in vitro restimulation. ST and LT CD8$^+$ T cells were restimulated with anti-CD3/CD28 for 4 hours (A,B,D) or 24 hours (C). A, Left: Representative counter plots illustrate frequencies of cytokine-expressing CD8$^+$ T cells. Right: The bars show mean values ± SEM. *P < .05, nonparametric paired *t* test. B, The granzyme B concentration in supernatants of restimulated cells was analyzed in triplicates via ELISA. The bars show mean values ± SEM. **P < .01, nonparametric paired *t* test. C, Representative intensity histograms of restimulated CFSE-labeled ST and LT CD8$^+$ T cells. MFI values ± SD: ST-d4 = 233,8 ± 38,8; LT-d4 = 358,5 ± 166,3. D, Representative counter plots illustrate frequencies of apoptotic and/or dead cells (Annexin V referred to as Annexin$^+$ and/or DAPI$^+$) and living cells (Annexin$^-$ DAPI$^-$). The bars show mean values ± SEM. All data were obtained from two independent experiments with n > 2 mice [Color figure can be viewed at wileyonlinelibrary.com]

a conversion of naive to Tcm. The CD44$^+$CD62L$^+$ subset was further characterized for Tscm markers by flow cytometry. ST and LT Tcm revealed an overall increase of stem cell antigen 1 (Sca1), Bcl-2 and CXCR3 expression in culture settings and an even higher expression level of CD122 and Bcl-2 in LT CD8$^+$CD44$^+$CD62L$^+$ T cells (Figure 1C).[12,34]

In order to position LT murine CD8$^+$CD44$^+$CD62L$^+$ T cells into the established hierarchy of T cell subpopulations, we compared their transcriptome profile with published expression data from naturally occurring CD8$^+$ T cell subsets and differently induced Tscm.[4,11,13,23] Unsupervised hierarchical clustering and PCA using the gene set of Gattinoni et al[11] revealed that both ST and LT CD8$^+$CD44$^+$CD62L$^+$ T cells were closely related to previously published CD8$^+$ Tcm/Tscm transcriptomic signatures, whereas the LT signature tended to overlap more with the previously published Tcm datasets (Figure 1D; Supplemental Figure 2).

Afterward, we defined whether LT CD8$^+$ T cell functionality was maintained with respect to ST culture. Upon activation with anti-CD3/CD28 antibodies, LT CD8$^+$ T cells expressed higher amounts of intracellular IL-2, IFN-γ and TNF-α compared to ST CD8$^+$ T cells (Figure 2A). Granzyme B was also significantly higher expressed by LT CD8$^+$ T cells (Figure 2B). On the contrary, IL-10 was not detectable at any time point. We did not observe any significant difference in proliferation capability (Figure 2C, mean fluorescence intensity (MFI) ± SD for ST-d4 = 233,8 ± 38,8 and LT-d4 = 358,5 ± 166,3) and apoptosis susceptibility between the two groups (Figure 2D). Taken together, these data suggested that higher numbers of murine CD8$^+$ T cells with characteristic features related to Tcm and Tscm and preserved functionality could be achieved by LT expansion with IL-7/IL-15.

3.2 | LT CD8$^+$ T cells displayed preserved engraftment, persistence and antitumor capacity in vivo

We also studied the engraftment and persistence capacity of LT expanded T cells under homeostatic conditions in vivo. For this purpose, we isolated T cells from our published bioluminescent dual-luciferase reporter mouse, called BLITC mouse.[27] BLITC cells constitutively express Renilla luciferase and an additional Click Beetle luciferase under the control of the NFAT-responsive promoter, thus allowing to simultaneously analyze T cell migration, expansion and activation in mouse models. ST and LT CD8$^+$CD44$^+$CD62L$^+$ BLITC cells were transferred into Rag1 KO (RagKO) deficient mice, where small lymphoid organs do not contain mature B and T lymphocytes, and we monitored in vivo engraftment and persistence of adoptively transferred T cells over 1 and 6 months, respectively, via BLI analysis (Figure 3A,B). After 1 month, we observed Renilla luciferase signals in cervical and inguinal lymph nodes and quantified the signal intensity by digitally setting regions of interest and computing total flux values. The signal intensities were comparable in both ST and LT groups, suggesting no difference in the engraftment capability of LT T cells (Supplemental Figure 3A). Additionally, we quantified infiltrated CD8$^+$ T cells in peripheral lymph nodes and spleen using flow cytometry underlining the BLI data with comparable absolute numbers of ST and LT CD8$^+$ T cells (Supplemental Figure 3B). In a 6-months follow-up study, comparable Renilla luciferase signals and CD8$^+$ T cell numbers were detectable, hence suggesting similar persistence of transferred ST and LT CD8$^+$ T cells (Figure 3C,D; Supplemental Figure 3C). Since for ATT efficacy, it is essential that transferred T cells maintain or even increase antitumor activity, we tested

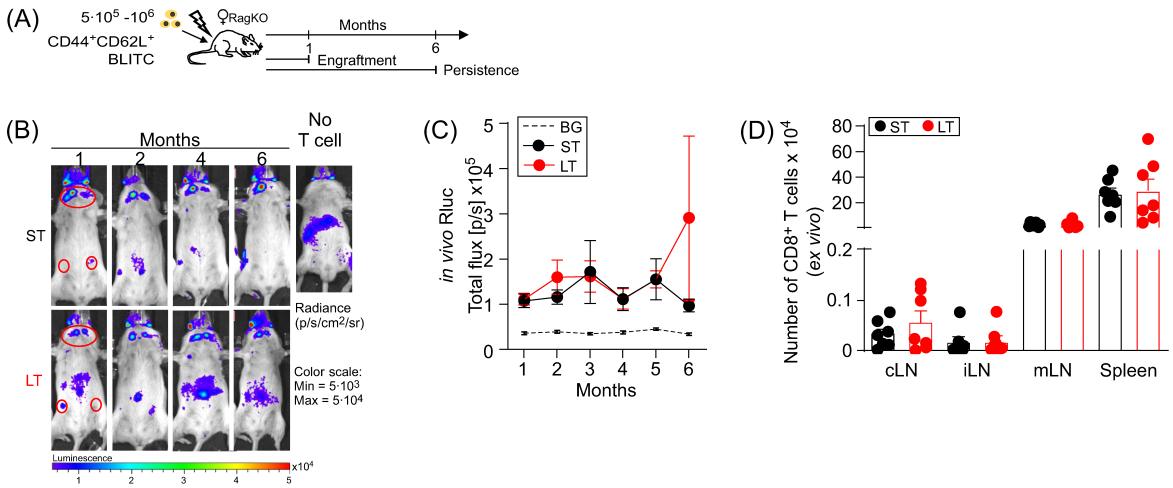

FIGURE 3 Preserved engraftment, persistence and antitumor capacity of LT CD8$^+$ T cells. A, Scheme for T cell transfer into female RagKO mice in order to analyze in vivo engraftment and persistence. B, Representative Renilla luciferase signals of ST or LT CD8$^+$CD44$^+$CD62L$^+$ T cells 1 to 6 months after transfer into female RagKO mice. C, The diagram shows mean ± SEM of Renilla luciferase flux values in the cervical (cLN) 6 months after transfer. BG indicates the background. D, Mice were sacrificed after 1 or 6 months and CD8$^+$ T cells were quantified in different organs via flow cytometry. The bar diagram shows mean data ± SEM of total T cell numbers. All data were generated in two independent experiments with n = 6-8 mice per group [Color figure can be viewed at wileyonlinelibrary.com]

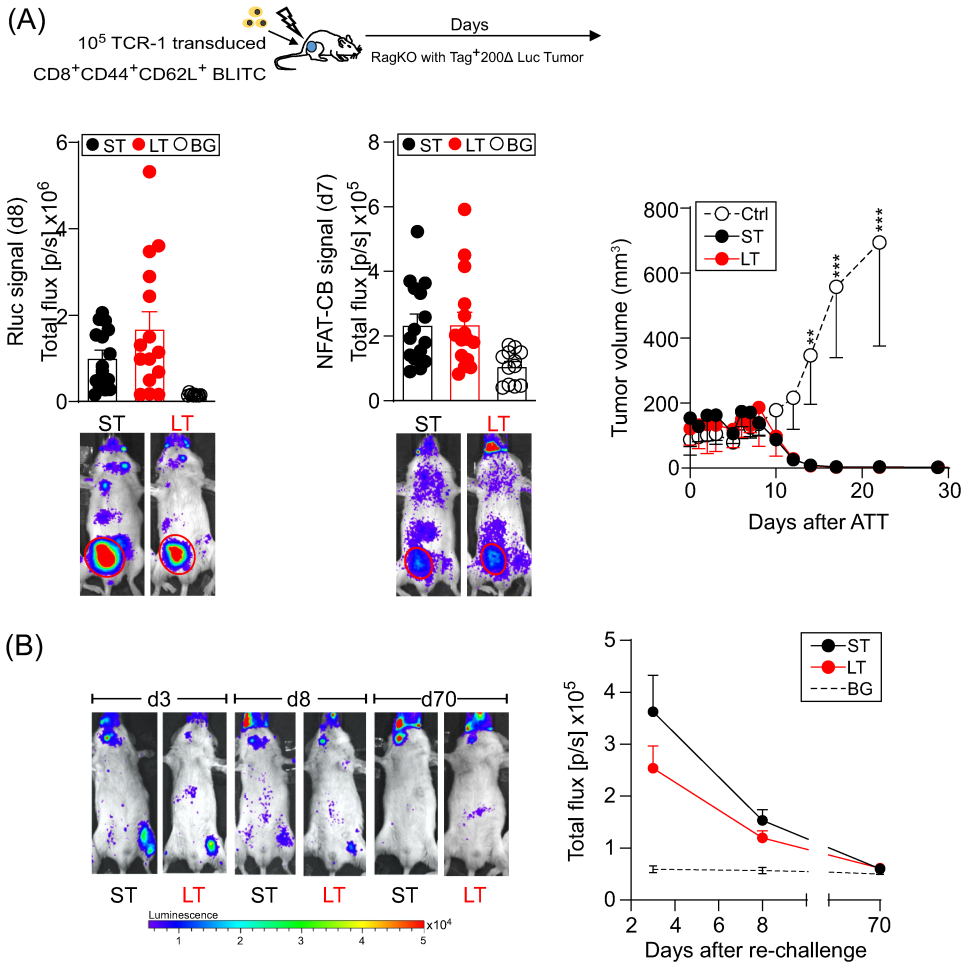

FIGURE 4 Effect of LT CD8$^+$ T cells engraftment on tumor growth. A, Scheme for T cell transfer into Tag$^+$200ΔLuc-tumor bearing female RagKO mice. Shown are representative Renilla and NFAT-click beetle luciferase signals of ST and LT CD44$^+$CD62L$^+$ TCR-1 transduced T cells 7 (NFAT-CB) and 8 (Renilla) days after transfer into Tag$^+$200ΔLuc-tumor bearing mice. Bar diagrams show mean ± SEM of luciferase flux values in the tumor region. Tumor growth kinetics are displayed by line diagram, mean ± SEM. $^{**}P < .01$, $^{***}P < .001$, two-way ANOVA test. All data were generated in two independent experiments with n = 15 mice per group. B, Tag$^+$200ΔLuc-tumor free mice from panel A were rechallenged with 5×10^6 freshly cultured Tag$^+$200ΔLuc tumor cells on the left flank
(note: tumor site of the first challenge was the right flank). Shown are representative Renilla luciferase signals of ST and LT CD44$^+$CD62L$^+$ TCR-1 transduced T cells 3, 8 and 70 days after tumor rechallenge into Tag$^+$200ΔLuc-tumor free mice. The line diagram shows mean ± SEM of luciferase flux values in the tumor region over 70 days. Tumor growth kinetics are not displayed due to missing growth. All data were generated in two independent experiments with n = 12 mice per group [Color figure can be viewed at wileyonlinelibrary.com]

ST and LT CD8$^+$ T cells using the SV40 large T antigen (Tag) tumor model.[26,35] CD8$^+$ BLITC cells were retroviral transduced with TCR-I, a TCR specific for epitope I of Tag protein, then expanded for 7 (ST) to 28 (LT) days and transferred into RagKO mice bearing Tag-positive 200ΔLuc tumors.[27] TCR-I transduced ST and LT CD8$^+$ BLITC cells infiltrated rapidly into the tumor, got activated by the tumor cells and induced a complete tumor rejection within 20 days (Figure 4A). In contrast, in control mice that received no T cells, tumors underwent progressive growth until mice were sacrificed at day 21. In order to test the in vivo persistence of TCR-I CD8$^+$ LT T cells, animals with eradicated tumors from the previous experiments were rechallenged with tumor cells after at least 2 months from ATT. As displayed in Figure 4B, after 3 days from rechallenge, ATT recipients triggered a strong T cell BLI signal at the tumor site and tumor growth was detected, thus demonstrating the persistence of a strong tumor-specific T cell reactivity. In naive-challenged RagKO mice, injected Tag-positive 200ΔLuc tumor cells develop a tumor that shows a constant tumor growth over the time with a tumor volume enriching between 300 and 500 mm^3 after 40 days (data not shown). In summary, these data showed that LT CD8$^+$ T cells retain anti-tumor function and their prolonged expansion does not negatively affect their therapeutic efficacy.

3.3 | LT CD4$^+$ T cells possess central memory/memory stem cell-like phenotype and in vitro functional properties

As for the CD8$^+$ T cell subpopulation, we investigated the feasibility of a prolonged cell culture for CD4$^+$ T cells, by using the same expansion protocol. Although the number of CD4$^+$ T cells was sustained

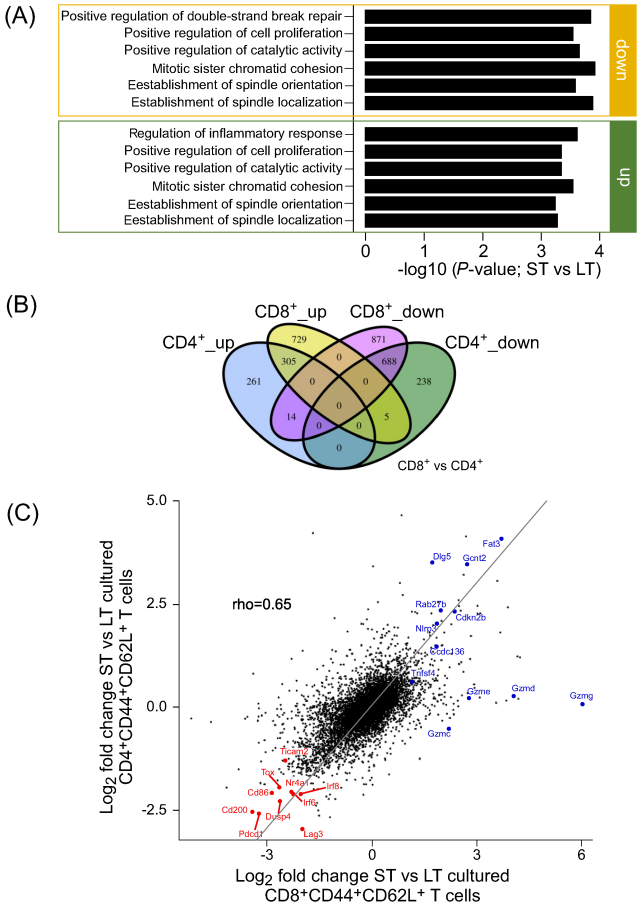

FIGURE 5 Molecular profiles of LT CD8$^+$ and CD4$^+$ T cells identify transcriptional regulators and markers for proliferation, apoptosis and activation. RNA sequencing of polyclonal CD8$^+$CD44$^+$CD62L$^+$ and CD4$^+$CD44$^+$CD62L$^+$ T cells generated via ST or LT expansion with IL-7/IL-15. A, Gene list with GO terms. B, Venn diagram with numbers of differentially regulated genes compared between ST and LT CD8$^+$CD44$^+$CD62L$^+$ and CD4$^+$CD44$^+$CD62L$^+$ T cells. C, Scatter plot with log2 fold changes between ST and LT CD8$^+$CD44$^+$CD62L$^+$ vs CD4$^+$CD44$^+$CD62L$^+$ T cells. Selected genes were highlighted [Color figure can be viewed at wileyonlinelibrary.com]

over time, the overall increase of CD4$^+$ T cells was weaker and maintained from day 7 to day 21 in a sort of stationary state (Supplemental Figure 4A). Moreover, the expansion yield for CD4$^+$ T cells as well as for the CD4$^+$CD44$^+$CD62L$^+$ subpopulation was nearly comparable between ST and LT CD4$^+$ T cells (Supplemental Figure 4B). As shown for CD8$^+$ T cells, also LT CD4$^+$ T cells exhibited phenotypical features of Tcm and Tscm (Supplemental Figure 4C), and CD122, Sca1, Bcl-2 and CXCR3 markers appeared increased in both ST and LT, thus indicating a stable phenotype over time.

We further compared the transcriptome profile of expanded CD4$^+$ cells with published expression data from mouse[12] or human.[24] Consistently, ST and LT CD4$^+$CD44$^+$CD62L$^+$ T cells grouped closely with CD4$^+$ Tcm, and with naturally or Notch-induced CD4$^+$ Tscm subsets (Supplemental Figures 4D and 5). Notably, the grouping is similar for both murine[12] and human[24] T cells.

We also tested the in vitro and in vivo properties of ST and LT CD4$^+$ T cells. After activation via anti-CD3/CD28, LT CD4$^+$ T cells expressed intracellular IL-2 and IFN-γ at higher level than ST, while TNF-α expression remained comparable (Supplemental Figure 4E). The in vitro proliferation and apoptotic rate after restimulation was also comparable between the two groups (Supplemental Figure 4F,G). Furthermore, we investigated the antitumor activity of ST and LT CD4$^+$CD44$^+$CD62L$^+$ H-Y TCR transgenic T cells isolated from Marilyn-BLITC mice (Marilyn-BLITC Tcm).[27] ST and LT Marilyn-BLITC Tcm were transferred into female RagKO mice bearing H-Y positive MB49 tumors. In contrast to the antitumor activity mediated by CD8$^+$ T cells, we recorded only a delay in tumor progression for CD4$^+$ comparably for ST and LT T cells (Supplemental Figure 4H).

3.4 | Longitudinal transcriptional alterations during T-cell expansion with IL-7/IL-15

We compared the transcriptome of ST and LT murine CD8$^+$CD44$^+$CD62L$^+$ and CD4$^+$CD44$^+$CD62L$^+$ T cells for differently expressed genes, in order to identify longitudinal transcriptional alterations. For this, we performed differential gene expression analysis using DESeq2.[25] Comparing ST and LT Tcm, we found 2612 altered genes for CD8$^+$ and 1511 altered genes for CD4$^+$ T cells (adjusted $P < .05$ and fold change >.5). The majority of these genes showed moderate but significant expression alterations with absolute log2 fold change between 1.5 and 2.0. To identify gene expression patterns that elucidate biological functions or pathways affected in LT CD8$^+$ and CD4$^+$ T cells, gene ontology (GO) term enrichment analysis was performed for both, in order to assign the differently expressed genes to biologically meaningful GO categories (Figure 5A). Top significant genes for each GO term are listed in Supplemental Table 3. Genes encoding key regulators of proliferation were downregulated in both T cell subsets, whereas regulators of cellular responses and signaling were upregulated over time. Furthermore, we compared the overlap of altered genes in CD8$^+$ and CD4$^+$ T cell expansion and found 688 of 931 (74%) downregulated genes in LT CD4$^+$ T cells similarly downregulated in CD8$^+$ T cells. Three hundred five of 580 (53%) upregulated genes in LT CD4$^+$ T cells were also upregulated in LT CD8$^+$ T cells (Supplemental Table 4). This relatively high correlation is illustrated by the Venn diagram and a scatter plot with selected genes highlighted (Figure 5B,C).

3.5 | An extended expansion of human T cells from healthy donors and DLBCL patients results in increased numbers of CD8$^+$ and CD4$^+$ Tcm cells with preserved in vitro function

As the clinical application of ATT has markedly increased and the number of infused T cells is critical to the outcome, our final aim was to transfer our findings on T cell LT expansion to the human setting.

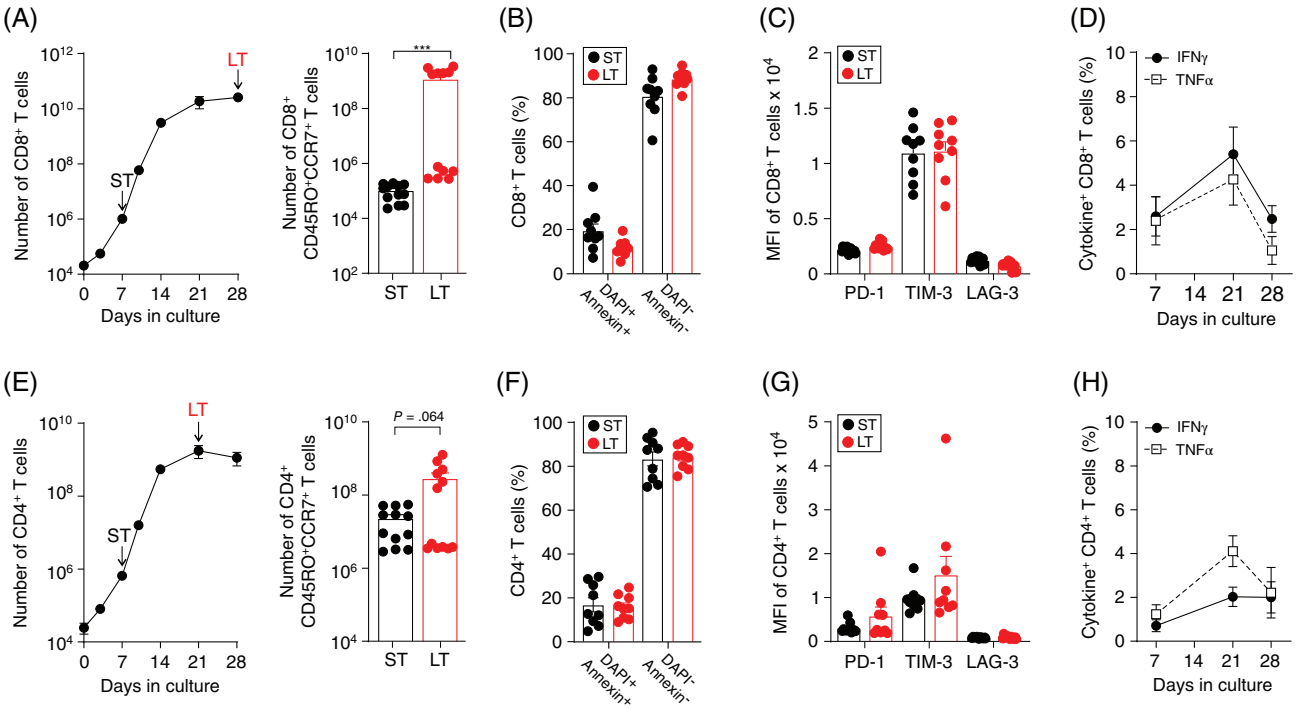

FIGURE 6 Extended T cell culture results in increased numbers of $CD8^+$ and $CD4^+$ T cells from healthy donors with preserved in vitro function. T cells from healthy donors were enriched using a Ficoll density gradient, activated via anti-CD3/CD28 and IL-2 for 72 hours and further cultured with IL-7/IL-15 for 4 (ST) or 25 (LT) days. The quantification and phenotypical analysis was done by flow cytometry. A, Growth kinetic of $CD8^+$ T cells is displayed by line diagram as mean values ± SEM. Before-after diagram shows mean ± SEM of total $CD8^+CD45RO^+CCR7^+$ T cell numbers. ***$P < .001$, nonparametric paired *t* test. B, ST and LT $CD8^+$ T cells were restimulated for 4 hours using anti-CD3/CD28. The bars show mean values ± SEM of frequencies of apoptotic and/or dead cells (Annexin V referred as $Annexin^+$ and/or $DAPI^+$) and living ($Annexin^-DAPI^-$) $CD8^+$ T cells. C, The bars show mean values ± SEM of inhibitory T cell receptor expression on $CD8^+$ T cells after restimulation for 10 days. D, Expanded $CD8^+$ T cells were restimulated at the indicated time points as described in B. The line diagram shows mean values ± SEM of IFN-γ and TNF-α expressing $CD8^+$ T cells over time. E, Growth kinetic of $CD4^+$ T cells is displayed by line diagram as mean values ± SEM. Before-after diagram shows mean ± SEM of total $CD4^+CD45RO^+CCR7^+$ T cell numbers. $P = .064$, nonparametric paired *t* test. F, ST and LT $CD4^+$ T cells were treated as described in B. The bars show mean values ± SEM of frequencies of apoptotic and/or dead cells ($Annexin^+$ and/or $DAPI^+$) and living ($Annexin^-DAPI^-$) $CD4^+$ T cells. G, The bars show mean values of the mean fluorescence intensity (MFI) ± SEM of inhibitory T cell receptor expression on $CD4^+$ T cells after restimulation for 10 days. H, The line diagram shows mean values ± SEM of IFN-γ and TNF-α expressing $CD4^+$ T cells upon restimulation. Growth kinetics were generated in two independent experiments with n = 4 healthy donors. Residual data were generated in three independent experiments with n = 9 healthy donors [Color figure can be viewed at wileyonlinelibrary.com]

We firstly analyzed the expansion and in vitro properties of T cells from healthy donors. T cells were enriched by density gradient centrifugation, activated and cultured as described for murine T cells. In line with our murine data, we observed a marked increase in human $CD8^+$ T cell numbers during the first 3 weeks and, subsequently the $CD8^+$ T cell expansion kinetic slowed down, reaching a plateau phase (Figure 6A, left graph). We also analyzed the phenotype of cultured $CD8^+$ T cells regarding the expression of CD45RO and CCR7 via flow cytometry. The LT expansion resulted in a 10^4-fold increase of human $CD8^+CD45RO^+CCR7^+$ Tcm cells (Figure 6A, right graph; Supplemental Figure 6). We then tested possible differences in $CD8^+$ T cell functionality after ST and LT expansion by restimulating them with anti-CD3/CD28 antibodies for either 4 hours or 10 days, in order to and analyze cell death/apoptosis and cytokine production as well as the expression of exhaustion markers (T cell inhibitory receptors, TIRs), respectively. The apoptosis and expression levels of TIRs were comparable between ST and LT $CD8^+$ T cells (Figure 6B,C). $CD8^+$ T cells expressed comparable amounts of IFN-γ and TNF-α after 1 and 4 weeks of expansion with a clear peak of production after 3 weeks (Figure 6D). Interestingly, human $CD4^+$ T cell expanded much stronger and longer than murine $CD4^+$ T cells in LT cultures, thus resulting in 50-fold increase of human $CD4^+CD45RO^+CCR7^+$ T cells after 3 weeks (Figure 6E; Supplemental Figure 6). Similarly to human $CD8^+$ T cells, the extent of apoptosis and TIRs expression upon in vitro restimulation were comparable between both groups (Figure 6F,G), and at the same time, ST and LT $CD4^+$ T cells expressed comparable amounts of IFN-γ and TNF-α cytokines with a peak for IFN-γ at week 3 (Figure 6H). Noteworthy, IL-2 was also measured but hardly detectable at any time point for $CD4^+$ and $CD8^+$ (data not shown).

In order to estimate the impact of genetic modification on LT T cell culture, we transduced human peripheral lymphocytes isolated from a healthy donor with tyrosinase-specific TCR-T58. Transduced $CD8^+$ T cells exhibited increased growth over time

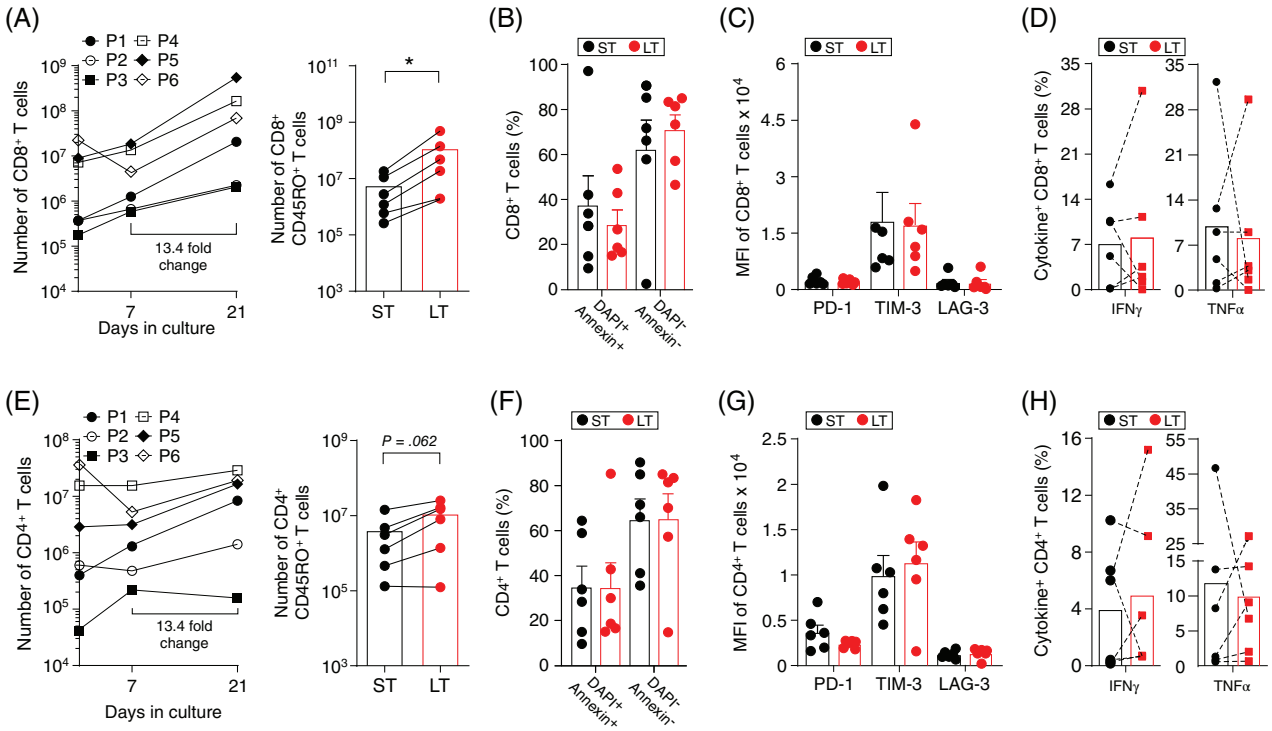

FIGURE 7 Extended T cell culture results in increased numbers of $CD8^+$ and $CD4^+$ T cells from DLBCL patients with individual in vitro function. T cells from DLBCL patients were enriched using a Ficoll density gradient, activated via anti-CD3/CD28 and IL-2 for 72 hours and further cultured with IL-7/IL-15 for 18 days. The quantification and phenotypical analysis were done by flow cytometry. A + E, Growth kinetics of $CD8^+$ and $CD4^+$ T cells are displayed by line diagrams for each patient. Before-after diagram shows the mean + individual values of total $CD8^+CD45RO^+$ and $CD4^+CD45RO^+$ T cell numbers. *$P < .05$, nonparametric paired *t* test. B + F, ST and LT $CD8^+$ and $CD4^+$ T cells were restimulated for 4 hours using anti-CD3/CD28 to analyze cell death and cytokine expression. The bars show mean values ± SEM of frequencies of apoptotic and/or dead cells (Annexin V referred as $Annexin^+$ and/or $DAPI^+$) and living ($Annexin^-DAPI^-$) $CD8^+$ T cells. C + G, ST and LT $CD8^+$ and $CD4^+$ T cells were restimulated for 10 days using low-dose anti-CD3/CD28 to analyze the expression of inhibitory T cell receptors. The bars show mean values ± SEM of the mean fluorescence intensity (MFI) ± SEM of inhibitory T cell receptor expression on $CD8^+$ and $CD4^+$ T cells after restimulation for 10 days. D + H, Expanded $CD8^+$ and $CD4^+$ T cells were restimulated at the indicated time points as described in B + F. The before-after diagram shows mean values and individual values of IFN-γ and TNF-α expressing $CD8^+$ and $CD4^+$ T cells over time [Color figure can be viewed at wileyonlinelibrary.com]

while $CD4^+$ to a lesser extent (Supplemental Figure 7A). In addition, transduction did not affect proliferation of $CD45RO^+CCR7^+$ $CD8^+$ and $CD4^+$ T cells (Supplemental Figure 7B). After 28 days, T cell numbers increased by more than 10-fold and about 10-fold, respectively. TIR expressions by transduced T cells were also comparable to nontransduced human T cells shown in Figure 6C,G (Supplemental Figure 7C). We also defined the ability of LT transduced $CD8^+$ and $CD4^+$ T cells to be activated. As for T cells in Figure 6D,H, transduction did not affect the ability of $CD8^+$ and $CD4^+$ to produce the proinflammatory cytokines TNFα and IFNγ after activation with anti CD3/CD28 antibodies when comparing ST and LT T cells (Supplemental Figure 7D). Transduced $CD8^+$ T cells were also able to respond to TCR-tyrosinase (T58) specific activation (Supplemental Figure 7D, black line). As last, we tested the ability of permanent stimulation to evoke exhaustion and TIR expression in transduced $CD8^+$ and $CD4^+$ T cells. After 11 days of stimulation with anti CD3/CD28 antibodies only lymphocyte activating 3 (Lag3) expression increased respect day 0, while the other TIRs were unaffected (Supplemental Figure 7E). At the same time, no significant increase of tumor death was identified after 11 days of anti CD3/CD28 stimulation (Supplemental Figure 7F) in LT cultured $CD4^+$ and $CD8^+$.

Since in clinical practice treatment of relapsed/refractory lymphoma patients with CAR T cells is hampered in some cases by the failure to generate sufficient numbers of T cells,[8,21,22] we next evaluated T cell expansion in DLBCL patients undergoing salvage therapy as potential candidates for CAR T-cell therapy. We obtained samples from six patients, enriched T cells from peripheral blood mononuclear cells (PBMCs) and cultured them following the same procedure as described for the healthy donors. We determined the main representative T cell phenotype thorough flow cytometric analysis of CD45RO and CCR7 cell membrane markers, and in four of the six patients we found a significant reduced numbers of early lineage T cells, naive T cell (Tn) ($CD8^+/CD4^+$ $CD45RO^+$ $CCR7^-$) and Tcm ($CD8^+/CD4^+$ $CD45RO^+$ $CCR7^+$) (Supplemental Figure 8). After in vitro expansion, five patients exhibited a comparable initial T cell proliferation with an averaged 2.3-fold T cell expansion within the first week, while for one patient (patient number 6), the absolute number of T cells dropped to about 17%. However,

after further expansion, an averaged 13.4-fold and 3.4-fold increase for $CD8^+$ and $CD4^+$ T cells, respectively, was achieved (Figure 7A,E). The number of $CD45RO^+$ $CD8^+$ and $CD4^+$ T cells has also expanded over time (Figure 7B, F). In order to test T cell exhaustion after prolonged culture condition, we measured TIRs in ST and LT T cells. TIR expressions were comparably expressed and their expression did not increase over time for both $CD4^+$ and $CD8^+$ T cells (Figure 7C,G). On the other hand, the stable expression of exhaustion markers did not correlate with the functionality of T cells, which instead expressed IFN-γ and TNF-α with high variability upon activation and over time (Figure 7D,H).

4 | DISCUSSION

ATT has developed into an important new tool in the treatment of malignancies, particularly hematologic malignancies, with CAR-T cell therapies possibly revolutionizing treatment of relapsed/refractory lymphoma and multiple myeloma. In solid tumors, CAR-T cells are only beginning to be used, most likely TCRs addressing tumor associated antigens will play a major role in the future in these entities. Despite the impressive results in the early outcome of ATT patients, the clinical success is far from being achieved in all patients. Beside escape mechanisms involving downregulation of targeted antigens and engraftment failure, ATT has further encountered several limitations during the manufacturing process due to insufficient T cell collection, generation and/or expansion. This is particularly evident in older and in heavily pretreated patients.[8,21,22] In our study, we investigated whether a limited number of T cells after manufacturing procedure could be circumvented by simply extending the time of current protocols with the aim of achieving an adequate T cell graft to avoid ATT dropout while being minimally manipulative. Certainly, this would only be a viable option if the Tcm/Tscm properties could be maintained despite extended expansion, which is why we also tested for potential loss of T cell function. We firstly provided the proof of concept of a LT IL-7/IL-15 expansion protocol and preserved T cell functionality for murine T cells in an ATT tumor model. Several studies have shown that IL-7 and IL-15 offer better growth support than IL-2[10] and promote a Tcm/Tscm phenotype,[4,32,33,36] thus ultimately improving ATT efficacy.[37] In all these studies, T cells were cultured for 1 or 2 weeks, while only Cieri et al[4] investigated T cell expansion over 4 weeks in order to test the expansion potential of individual T cell subsets, however longitudinal changes in T cell function and transcriptome were not addressed. Therefore, we not only investigated the extent of T cell expansion, but simultaneously examined whether T cell functionality could be maintained despite an extended expansion culture protocol. Murine $CD8^+$ T cells steadily expanded up to 4 weeks when cultured with IL-7/IL-15, while murine $CD4^+$ T cells expanded to a lesser extent without significant differences between ST and LT culture. To date, a comprehensive analysis of the gene expression profile of LT expanded murine Tcm remains missing. As few murine datasets of $CD4^+$ and $CD8^+$ are available we included in our study some selected human data set, and the analysis was performed using batch correction to remove systematic differences between datasets of different origin, and caused by the species differences. Unsupervised hierarchical clustering and PCA of RNA sequencing of data derived from murine $CD8^+$ and $CD4^+$ Tcm after ST and LT expansion and published signatures T cell subtypes revealed that after LT expansion, $CD8^+$ Tcm were closely related to a typical $CD8^+$ Tcm and Wnt-induced Tscm expression signature thus demonstrating the maintenance of a Tcm phenotype in LT condition. At the same time similarly to the ST $CD4^+$ Tcm, LT $CD4^+$ Tcm cells positioned most closely to $CD4^+$ or Notch-induced $CD4^+$ Tscm cells, thus indicating a stable profile over time. The (GO) term enrichment analysis between ST and LT culture of murine T cells revealed that among the 2612 and 1511 altered genes identified in $CD8^+$ and $CD4^+$, respectively, over half of the gene overlap between $CD8^+$ and $CD4^+$, thus suggesting the existence of a specific cluster of genes that are similarly regulated by IL-7/IL-15 over time. On the other hand, the downregulation of a set of genes encoding for key regulators of cell cycle and proliferation may be explained with a possible enrichment of a plateau-phase in LT culture. This is in line with previous findings showing a similar cell cycle arrest with the induction of a resting phase in IL-15-induced memory-like $CD8^+$ T cells.[32] In addition, LT Tcm cells downregulated genes associated with immune checkpoint inhibition (*Cd200*, *Pdcd1*, *Lag3*)[38,39] and T cell dysfunction (*Dusp4*, *Tox* and *Nr4a1*)[40-43] thus suggesting that a prolonged in vitro expansion with IL-7/IL-15 does not induce T cell exhaustion with consequent loss of T cell functions.

All data derived from the longitudinal phenotypical and molecular analyses revealed that an extended expansion using IL-7/IL-15 is feasible and increases T cell numbers with favorable Tcm/Tscm phenotype and largely preserved transcriptional activity.

Regarding the in vitro functionality, proliferative capacity, apoptosis susceptibility and upregulation of TIRs upon polyclonal stimulation with anti-CD3/CD28 have been shown to be comparable between ST and LT culture. Upon restimulation, LT $CD8^+$ and $CD4^+$ T cells could even produce larger amounts of IL-2, IFN-γ and granzyme B than after ST culture. The higher granzyme B expression is noteworthy, since the proportion of Tcm/Tscm is predominant. Here, it must be mentioned that no isolated Tcm were stimulated, so that it can be assumed that the smaller fraction of Teff also contributes to the measured granzyme B production. Interestingly, Chattopadhyay et al have shown granzyme B expression by Tcm, but only by those, which are CD27 negative and CD57 bright.[44]

In respect to in vivo functionality, multiple studies have shown a correlation between engraftment and persistence of adoptively transferred T cells and clinical outcome.[45-47] We clearly show here that T cell function is preserved when T cells are expanded for a longer period in the presence of IL-7/IL-15, and that such LT T cells are able to engraft, expand, persist and develop antitumor activity. This has been demonstrated differently for IL-2,[19,48,49] where shortly IL-2 expanded T cells could outperform the longer cultured T cells in expansion, survival capacity and in vivo antitumor activity. These data underline the clinical relevance of our findings.

In order to evaluate whether such minimally manipulative good manufacturing practice-feasible procedure might be an option for patients with hampered T cell proliferation, we assessed the effect of

IL-7/IL-15 LT expansion on T cells derived from healthy donors as well as from DLBCL patients. As for murine T cells, we observed a long-lasting expansion of human $CD8^+$ T cells over 4 weeks. Differently from murine $CD4^+$ T cells, human $CD4^+$ T cells from healthy donors significantly increased over time. Such differences are in line with previous findings about the diverse priming and differentiation between murine and human $CD4^+$ T cells.[34] The ability of human $CD4^+$ T cells to expand is critical for medical treatment since the impact of $CD4^+$ T cells for the antitumor immunity as either supporting partner or as effector cells has been increasingly acknowledged.[50-52] In our experimental settings, LT expansion of human T cells provided less differentiated $CD45RO^+CCR7^+$ $CD8^+$ and $CD4^+$ T cells, respectively. Functional assays displayed that ST and LT human T cells possess similar apoptosis susceptibility and upregulation of TIRs upon polyclonal stimulation with anti-CD3/CD28. Activation and cytokine expression of ST and LT T cells were comparable. Interestingly, IFNγ and TNFα expression level peaked after 3 weeks of expansion and declined shortly after. When the LT expansion protocol was applied to T cells derived from DLBCL patients, improved numbers of T cells could also be achieved, albeit the expansion was not as vigorous as seen for the healthy donors, possibly due to the heavy pretreatment of DLBCL patients. In addition, over the stimulation period, T cells from DLBCL patients behave inconsistently, with large variations in the pattern of response to stimulation between patients. This likely reflects different functional capability of T cells, possibly reflecting the influence of different therapies, age, comorbidity and disease status on T cell function. DLBCL patients can lack T cells with early lineage phenotype (Tnaive or Tcm), and dropouts in clinical trials can occur due to failure of CAR T cell expansion[8,21,22] underlying the need for strategies to improve the proliferative and functional properties of T cells from heavily pretreated and/or older patients. However, LT culture induced an averaged increase of $CD45RO^+$ $CD8^+$ and $CD4^+$ in DLBCL patients of our study, which may represent a perspective for those patients who experience manufacturing failure. At the same time, cytokine expression by LT T cells was overall preserved although with great variability in the production of IFNγ and TNFα for the individual patients.

In conclusion, we provide data showing that the T cell yield can be significantly increased and in addition to that, we demonstrate that a prolonged expansion may be a feasible treatment option since T cell functionality is preserved. T cell manufacturing is indisputably a resource consuming and cost-intensive process and certainly, we are aware that prolonged time until ATT entails the risk of disease progression. However, dropout in T cell manufacturing still represent an unmet medical need for some patients, and an extended manufacturing protocol may signify a therapeutic opportunity to circumvent otherwise ATT dropout. Further investigations are required to identify possible markers or clinical conditions that could help to identify those patients who might be in need of a prolonged T-cell expansion.

ACKNOWLEDGMENTS

The authors thank R. Manteufel, I. Hoeft, K. Pawletta and B. Frenzel for taking excellent care of experimental mice as well as T. Daberkow-Nitzsche and S. Jeuthe for assistance with rules and regulations. They are also grateful to O. Lantz for providing MataHari the mice. This work was supported by the Deutsche Forschungsgemeinschaft through the "Sonderforschungsbereich" TR36, the Experimental and Clinical Research Center and the Berlin Institute of Health.

CONFLICT OF INTEREST

Lars Bullinger declares being on the advisory committees of Abbvie, Amgen, Bristol-Myers Squibb, Celgene, Daiichi Sankyo, Gilead, Hexal, Janssen, Jazz Pharmaceuticals, Menarini, Novartis, Pfizer, Sanofi, Seattle Genetics. The other authors declared no potential conflicts of interest.

ETHICS STATEMENTS

All mice experiments were conducted in compliance with the institutional guidelines of the Max Delbrück Center for Molecular Medicine (Berlin, Germany) and approved by the Landesamt für Gesundheit und Soziales Berlin, Germany (G0048/14, G0005/15, G0307/15). Human samples were obtained from healthy donors referred to our Hematology, Oncology and Tumorimmunology Unit (Charité-Berlin) after signed an informed consent. The study was approved by the Charité-Berlin local ethics committee (no. EA1/070/17).

CONSENT FOR PUBLICATION

The risk of identification of the healthy donors/patients is minimized by anonymization to prevent the identity of the healthy donors/patients.

DATA AVAILABILITY STATEMENT

The sequencing data generated are available in Gene Expression Omnibus under the accession GSE140250. The other datasets used and/or analyzed during the current study are available from the corresponding author on reasonable request.

ORCID

Elisa Ciraolo https://orcid.org/0000-0002-5601-1695
Il-Kang Na https://orcid.org/0000-0001-9902-5424

REFERENCES

1. Rapoport AP, Stadtmauer EA, Binder-Scholl GK, et al. NY-ESO-1-specific TCR-engineered T cells mediate sustained antigen-specific antitumor effects in myeloma. *Nat Med*. 2015;21:914-921.
2. Chavez JC, Bachmeier C. Kharfan-Dabaja MA. CAR T-cell therapy for B-cell lymphomas: clinical trial results of available products. *Ther Adv Hematol*. 2019;10:2040620719841581.
3. Sermer D, Brentjens R. CAR T-cell therapy: full speed ahead. *Hematol Oncol*. 2019;37(Suppl 1):95-100.
4. Cieri N, Camisa B, Cocchiarella F, et al. IL-7 and IL-15 instruct the generation of human memory stem T cells from naive precursors. *Blood*. 2013;121:573-584.
5. Gong W, Hoffmann JM, Stock S, et al. Comparison of IL-2 vs IL-7/IL-15 for the generation of NY-ESO-1-specific T cells. *Cancer Immunol Immunother*. 2019;68:1195-1209.
6. Hoffmann JM, Schubert ML, Wang L, et al. Differences in expansion potential of naive chimeric antigen receptor T cells from healthy donors and untreated chronic lymphocytic leukemia patients. *Front Immunol*. 2017;8:1956.

7. Klebanoff CA, Gattinoni L, Palmer DC, et al. Determinants of successful CD8+ T-cell adoptive immunotherapy for large established tumors in mice. *Clin Cancer Res*. 2011;17:5343-5352.
8. Singh N, Perazzelli J, Grupp SA, Barrett DM. Early memory phenotypes drive T cell proliferation in patients with pediatric malignancies. *Sci Transl Med*. 2016;8:320ra3.
9. Zeng R, Spolski R, Finkelstein SE, et al. Synergy of IL-21 and IL-15 in regulating CD8+ T cell expansion and function. *J Exp Med*. 2005;201:139-148.
10. Zoon CK, Seitelman E, Keller S, et al. Expansion of melanoma-specific lymphocytes in alternate gamma chain cytokines: gene expression variances between T cells and T-cell subsets exposed to IL-2 versus IL-7/15. *Cancer Gene Ther*. 2014;21:441-447.
11. Gattinoni L, Lugli E, Ji Y, et al. A human memory T cell subset with stem cell-like properties. *Nat Med*. 2011;17:1290-1297.
12. Kondo T, Morita R, Okuzono Y, et al. Notch-mediated conversion of activated T cells into stem cell memory-like T cells for adoptive immunotherapy. *Nat Commun*. 2017;8:15338.
13. Sabatino M, Hu J, Sommariva M, et al. Generation of clinical-grade CD19-specific CAR-modified CD8+ memory stem cells for the treatment of human B-cell malignancies. *Blood*. 2016;128:519-528.
14. Buchholz VR, Flossdorf M, Hensel I, et al. Disparate individual fates compose robust CD8+ T cell immunity. *Science*. 2013;340:630-635.
15. Gerlach C, Rohr JC, Perie L, et al. Heterogeneous differentiation patterns of individual CD8+ T cells. *Science*. 2013;340:635-639.
16. Restifo NP, Gattinoni L. Lineage relationship of effector and memory T cells. *Curr Opin Immunol*. 2013;25:556-563.
17. Levine BL, Miskin J, Wonnacott K, Keir C. Global manufacturing of CAR T cell therapy. *Mol Ther Methods Clin Dev*. 2017;4:92-101.
18. Rohaan MW, Wilgenhof S, Haanen J. Adoptive cellular therapies: the current landscape. *Virchows Arch*. 2019;474:449-461.
19. Ghassemi S, Nunez-Cruz S, O'Connor RS, et al. Reducing ex vivo culture improves the antileukemic activity of chimeric antigen receptor (CAR) T cells. *Cancer Immunol Res*. 2018;6:1100-1109.
20. Gattinoni L, Klebanoff CA, Palmer DC, et al. Acquisition of full effector function in vitro paradoxically impairs the in vivo antitumor efficacy of adoptively transferred CD8+ T cells. *J Clin Invest*. 2005;115:1616-1626.
21. Schuster SJ, Bishop MR, Tam C, et al. Global pivotal phase 2 trial of the CD19-targeted therapy CTL019 in adult patients with relapsed or refractory (R/R) diffuse large B-cell lymphoma (DLBCL) - an interim analysis. *Hematol Oncol*. 2017;35:27.
22. Petersen CT, Hassan M, Morris AB, et al. Improving T-cell expansion and function for adoptive T-cell therapy using ex vivo treatment with PI3Kdelta inhibitors and VIP antagonists. *Blood Adv*. 2018;2:210-223.
23. Pulko V, Davies JS, Martinez C, et al. Human memory T cells with a naive phenotype accumulate with aging and respond to persistent viruses. *Nat Immunol*. 2016;17:966-975.
24. Takeshita M, Suzuki K, Kassai Y, et al. Polarization diversity of human CD4+ stem cell memory T cells. *Clin Immunol*. 2015;159:107-117.
25. Love MI, Huber W, Anders S. Moderated estimation of fold change and dispersion for RNA-seq data with DESeq2. *Genome Biol*. 2014;15:550.
26. Anders K, Buschow C, Herrmann A, et al. Oncogene-targeting T cells reject large tumors while oncogene inactivation selects escape variants in mouse models of cancer. *Cancer Cell*. 2011;20:755-767.
27. Szyska M, Herda S, Althoff S, et al. A transgenic dual-luciferase reporter mouse for longitudinal and functional monitoring of T cells in vivo. *Cancer Immunol Res*. 2018;6:110-120.
28. Textor A, Schmidt K, Kloetzel PM, et al. Preventing tumor escape by targeting a post-proteasomal trimming independent epitope. *J Exp Med*. 2016;213:2333-2348.
29. Lattime EC, Gomella LG, McCue PA. Murine bladder carcinoma cells present antigen to BCG-specific CD4+ T-cells. *Cancer Res*. 1992;52:4286-4290.
30. Wilde S, Sommermeyer D, Frankenberger B, et al. Dendritic cells pulsed with RNA encoding allogeneic MHC and antigen induce T cells with superior antitumor activity and higher TCR functional avidity. *Blood*. 2009;114:2131-2139.
31. Herda S, Raczkowski F, Mittrucker HW, et al. The sorting receptor Sortilin exhibits a dual function in exocytic trafficking of interferon-gamma and granzyme a in T cells. *Immunity*. 2012;37:854-866.
32. Carrio R, Bathe OF, Malek TR. Initial antigen encounter programs CD8+ T cells competent to develop into memory cells that are activated in an antigen-free, IL-7- and IL-15-rich environment. *J Immunol*. 2004;172:7315-7323.
33. Gargett T, Brown MP. Different cytokine and stimulation conditions influence the expansion and immune phenotype of third-generation chimeric antigen receptor T cells specific for tumor antigen GD2. *Cytotherapy*. 2015;17:487-495.
34. Gattinoni L, Zhong XS, Palmer DC, et al. Wnt signaling arrests effector T cell differentiation and generates CD8+ memory stem cells. *Nat Med*. 2009;15:808-813.
35. Staveley-O'Carroll K, Schell TD, Jimenez M, et al. In vivo ligation of CD40 enhances priming against the endogenous tumor antigen and promotes CD8+ T cell effector function in SV40 T antigen transgenic mice. *J Immunol*. 2003;171:697-707.
36. Gomez-Eerland R, Nuijen B, Heemskerk B, et al. Manufacture of gene-modified human T-cells with a memory stem/central memory phenotype. *Hum Gene Ther Methods*. 2014;25:277-287.
37. Xu Y, Zhang M, Ramos CA, et al. Closely related T-memory stem cells correlate with in vivo expansion of CAR.CD19-T cells and are preserved by IL-7 and IL-15. *Blood*. 2014;123:3750-3759.
38. Thommen DS, Schumacher TN. T cell dysfunction in cancer. *Cancer Cell*. 2018;33:547-562.
39. Wherry EJ, Kurachi M. Molecular and cellular insights into T cell exhaustion. *Nat Rev Immunol*. 2015;15:486-499.
40. Bignon A, Regent A, Klipfel L, et al. DUSP4-mediated accelerated T-cell senescence in idiopathic CD4 lymphopenia. *Blood*. 2015;125:2507-2518.
41. Khan O, Giles JR, McDonald S, et al. TOX transcriptionally and epigenetically programs CD8(+) T cell exhaustion. *Nature*. 2019;571:211-218.
42. Liu X, Wang Y, Lu H, et al. Genome-wide analysis identifies NR4A1 as a key mediator of T cell dysfunction. *Nature*. 2019;567:525-529.
43. Nowyhed HN, Huynh TR, Thomas GD, Blatchley A, Hedrick CC. Cutting edge: the orphan nuclear receptor Nr4a1 regulates CD8+ T cell expansion and effector function through direct repression of Irf4. *J Immunol*. 2015;195:3515-3519.
44. Chattopadhyay PK, Betts MR, Price DA, et al. The cytolytic enzymes granyzme A, granzyme B, and perforin: expression patterns, cell distribution, and their relationship to cell maturity and bright CD57 expression. *J Leukoc Biol*. 2009;85:88-97.
45. Huang J, Khong HT, Dudley ME, et al. Survival, persistence, and progressive differentiation of adoptively transferred tumor-reactive T cells associated with tumor regression. *J Immunother*. 2005;28:258-267.
46. Robbins PF, Dudley ME, Wunderlich J, et al. Cutting edge: persistence of transferred lymphocyte clonotypes correlates with cancer regression in patients receiving cell transfer therapy. *J Immunol*. 2004;173:7125-7130.
47. Louis CU, Savoldo B, Dotti G, et al. Antitumor activity and long-term fate of chimeric antigen receptor-positive T cells in patients with neuroblastoma. *Blood*. 2011;118:6050-6056.
48. Zhang X, Lv X, Song Y. Short-term culture with IL-2 is beneficial for potent memory chimeric antigen receptor T cell production. *Biochem Biophys Res Commun*. 2018;495:1833-1838.
49. Tran KQ, Zhou J, Durflinger KH, et al. Minimally cultured tumor-infiltrating lymphocytes display optimal characteristics for adoptive cell therapy. *J Immunother*. 2008;31:742-751.

50. Spitzer MH, Carmi Y, Reticker-Flynn NE, et al. Systemic immunity is required for effective cancer immunotherapy. *Cell*. 2017;168:487-502. e15.
51. Linnemann C, van Buuren MM, Bies L, et al. High-throughput epitope discovery reveals frequent recognition of neo-antigens by CD4+ T cells in human melanoma. *Nat Med*. 2015;21:81-85.
52. Perez-Diez A, Joncker NT, Choi K, et al. CD4 cells can be more efficient at tumor rejection than CD8 cells. *Blood*. 2007;109:5346-5354.
53. Gattinoni L, Finkelstein SE, Klebanoff CA, et al. Removal of homeostatic cytokine sinks by lymphodepletion enhances the efficacy of adoptively transferred tumor-specific CD8+ T cells. *J Exp Med*. 2005;202:907-912.

SUPPORTING INFORMATION

Additional supporting information may be found online in the Supporting Information section at the end of this article.

How to cite this article: Herda S, Heimann A, Obermayer B, et al. Long-term in vitro expansion ensures increased yield of central memory T cells as perspective for manufacturing challenges. *Int. J. Cancer*. 2021;148:3097–3110. https://doi.org/10.1002/ijc.33523

4 Discussion

4.1 Neoantigens as targets for hematological and solid neoplasms

An early and major hurdle in effective TCR-T cell therapy is the identification of target antigens. Different antigen characteristics are evaluated for predicting suitable and potent neoantigens. These characteristics include the processing of the particular antigen in the target cell and its presentation on the cell surface, as well as the immunogenicity of the antigen itself. Additionally, a highly preferable feature is tumor specificity, which is given with neoantigens, or expression of the antigens must not be on relevant healthy tissue to prevent severe toxicity when targeting TAAs. In an ideal situation, the antigen is derived from a recurrent driver mutation making antigen loss unlikely, expression is present across a wide range of tumor entities and distributed homogeneously on the tumor cell surface. A higher mutational burden is often correlated with higher objective response rates and treatment with immune checkpoint blockage augments effective T cell responses[108–111]. Studies using neoantigen vaccines indicate the potential of targeting neoantigens for personalized therapies, and vaccinations might contribute to an increased neoantigen-specific T cell repertoire or even convert immunologically `cold' tumors with low mutational burden into potentially targetable tumors[112–115]. In hematological cancers, tumor mutational burden is lower compared to several other solid tumors. However, some recurrent mutations or gene-fusion products are prevalent in a number of patient subgroups.[116–118] Clonal and recurrent neoantigens are being investigated as targets for TCR-T cell therapy with great interest, especially if they are present in founder clones. Targeting recurrent driver mutations minimizes the risk of immune evasion by tumor cells and they hold the potential to become targets for off-the-shelf TCR-T cell therapy. Several targets are under investigation for solid tumors and include for instance KRAS, TP53 and PIK3CA[105,119–123]. One potential neoepitope target in a subgroup of Non-Hodgkin Lymphoma (NHL) patients is the recurrent mutation MyD88 L265P[124,125]. The mutated peptide RPIPIKYKAM is presented on HLA-B*07:02 and is therefore targetable by TCR-T cell therapy. Publication 2 describes the priming, identification, and characterization of a MyD88 L265P mutation-specific TCR isolated from healthy donor lymphocytes[126], showing that this mutations indeed elicited antigen-

specific T cell expansion and suggests to be a suitable target for TCR-T cell therapy. Targeting this mutation with a high-affinity TCR could present an off-the-shelf ATT approach for HLA-B*07:02 positive patients carrying the L265P point mutation.

4.2 Challenges of neoepitope identification

Clinical studies showed the potential of immune checkpoint blockade and helped to understand the capabilities of the underlying neoantigen-specific T cell responses[127–129]. Efforts are made to identify putative neoantigens, especially the ones derived from recurrent and driver mutations. While whole genome and RNA-sequencing methods reliably identify non-synonymous mutations in tumors, downstream workflows often rely on computational models and algorithms trained on binding data sets with prediction-based output for putative neoantigens[52,59,130,131]. Predictions of peptide processing and presentation on HLA complexes remain difficult, especially for HLA alleles which are less common in the population and therefore less represented in datasets used to train computational models. The success of eliciting an immune response by any target peptide depends on several factors such as the binding affinity of the peptide to its MHC molecule, but also the peptide sequence itself, and the spatial structure of the peptide in the MHC groove, the latter influencing the availability of amino acid residues for TCR recognition. Post-translational modifications and proteasomal processing may affect the overall availability of the epitope, or lead may even to its destruction. Advancements in MS procedures and detection sensitivity are allowing better detection of naturally presented HLA ligands. Mass-spectrometry is an unbiased process that enables the direct identification of extracted neoantigens.[59,132] In general, the incidence of processed, naturally presented and immunogenic neoepitopes among predicted candidates is very low[133,134]. This notion is confirmed in Publication 1, in which only one of the predicted candidates was shown to be naturally processed and presented, although four predicted candidates led to the isolation of high-affinity TCRs when stimulated with exogenously peptide-loaded target cells[135]. Posttranslational modifications, such as phosphorylation, may have also resulted in the absence of epitope-specific TCRs after priming of lymphocytes with unmodified peptide or minimal-tandem genes. Nevertheless, after proving the processing and presentation of a putative neoepitope and identifying a specific high-affinity TCR, only experiments in preclinical

animal models will validate that a neoepitope can indeed serve as a true rejection antigen.

4.3 Immunogenicity of the target antigen

Successful isolation of tumor-specific T cells depends not only on MHC binding affinity and the method used for isolation, but also on whether the presented epitope is immunogenic and specific T cells can be found in the donor repertoire in sufficiently high frequencies. Numerous cumulative effects ultimately determine which peptides function as immunogenic epitopes. Factors that determine whether a presented peptide is recognized by T cells include antigen processing and presentation, the amount and quality of peptides presented on the target cell surface, as well as characteristics inherent to the peptide and the donor to be able to induce an immune response.[136–140]

Although recognition of pMHC ligands by the TCR is highly peptide-specific, some TCRs can also recognize sequence-related and -unrelated ('mimicry') epitopes presented by homologous or heterologous MHC molecules[141,142]. Some data suggest that sequence homology between a neoantigen and microbial peptides at least partially contributes to the immunogenicity of the neoantigen[142–144]. Neoantigens with high homology to self-peptides are assumed to be less immunogenic when homology occurs among TCR contacting amino acid residues, while neoantigens with high homology to foreign pathogens in the sense of molecular mimicry should rather be highly immunogenic. Calis et al. proposed that the ‘hole in the TCR repertoire’ to recognize non-self-peptides arises from the disability to distinguish too similar peptide sequences when amino acid residues of the non-self peptide which are available for TCR interaction are identical to self-peptides. They estimated that about one-third of the non-self pMHC were too similar to self-peptides and therefore T cells should be tolerant towards these peptides.[145]

4.4 Choice of the donor T cell repertoire for isolation of neoantigen-specific T cells

The here presented research, together with works from other groups have shown that it is possible to identify and expand neoantigen-specific T cells from healthy donors and from patients. The identification of a specific TCR, preferably a high-affinity TCR, be achieved by isolating antigen-specific T cells from TILs or patient peripheral blood. They

can also be generated by de novo priming of healthy donor T cells. Results presented in publication 1 and 2 highlight that the choice of a T cell repertoire influences the success of priming and isolation efforts for antigen-reactive TCRs for specific putative neoantigens. In a side-by-side comparison between different donor TCR repertories, including patients, partially HLA-matched allogeneic healthy human repertoires and TCR repertoires of transgenic mice, the same predicted neoantigen elicited different responses depending on the T cell repertoire after peptide priming or immunization. For some neoepitope candidates, it was possible to isolate specific TCRs from multiple donors and from humanized mouse models. This indicates that some peptides bear inherent properties which renders them more immunogenic. An advantage of using allogeneic donor repertoires, or a mouse repertoire, for the generation of T cells directed against a selection of predicted neoepitopes can be assumed in a setting when only limited patient material is available. Furthermore, the individual donor repertoire has a significant impact on the successful isolation of neoepitope-specific TCRs as it was evident by the numbers of donors which had to be primed and tested to isolate a high-affinity TCR against individual neoepitopes as well as against the recurrent MyD88 L256P mutation.

In 2017, it was shown that the peptide RPIPIKYKAM from the mutant region of MyD88 L265P can potentially bind to HLA-B*07:02 and induce peptide-specific CD8+ T cells. Antigen recognition was demonstrated only by co-culture of peptide-loaded (artificial) antigen-presenting cells and CD8+ enriched T cells from MyD88 mutation-positive patients and healthy human PBMCs. Generated CTLs were also cocultured with exogenously loaded peptide, however, recognition of endogenously processed and presented epitopes was not presented.[124] Publication 2 describes the isolation of a high-affinity TCR specific for the described HLA-B*07:02-restricted epitope from peripheral blood of an HLA-B*07:02-positive donor. Notably, it was necessary to test 24 donors and 13 TCR sequences were isolated. From these sequences, seven high-affinity TCRs were identified from five donors. Ultimately, only one TCR was able to recognize tumor cells which endogenously express the mutation.[126] For the isolation of TCRs directed against potential individual neoepitopes from patients with solid tumors, as described in publication 1, we tested fewer human donors for reactivity against multiple potential

neoepitopes from two patients. In addition to the isolated six TCRs from the human repertoire one TCR was identified from the transgenic mouse repertoire. Endogenous processing of the tested epitopes could only be confirmed for one epitope by recognition via the TCRs isolated from both, the healthy human and the transgenic mouse repertoire. Taking into consideration that only a few healthy donor repertoires were used, it is possible that investigating the repertoire of more donors would have led to the identification of more specific TCRs.

While the effects of aging and chronic viral infections generally negatively affect the TCR repertoire, increased HLA-I polymorphism has been shown not only to result in a broader immunopeptidome but also to increase the diversity of the TCR repertoire[146,147]. Consequently, the individual composition of donor HLA haplotypes may also influence the success of isolation of neoepitope-specific TCRs. In the presented publication 1 and 2, all stimulated donors were matched only for HLA-A*02:01 or HLA -B*07:02, respectively. However, the influence of the donor HLA-I polymorphisms on the success of isolating specific high-avidity TCRs should be the subject of prospective studies, in addition to potential epitope immunogenicity.

4.5 Advantages of targeting the lymphoma-specific driver mutation MyD88 by TCR-T cells compared to approved CD19-CAR T cells

The lymphoma-specific driver mutation MyD88 L265P is not only the hallmark mutation in Waldenström macroglobulinemia[148], but also frequently found in aggressive B-cell lymphomas, for instance, in 30 % of activated B cell-like (ABC) DLBCL and 45-60 % of primary central nervous CNS lymphoma (PCNSL). These are diseases with a pressing need for novel specific and well-tolerated therapies.[125,149–151] The MyD88 L265P is not expressed in healthy tissue, and therefore T cells should be able to distinguish between non-mutated healthy cells and the mutated non-self peptide presented on the individual's HLA-B*07:02 molecule. The high-avidity TCR specific for the mutated RPIPIKYKAM peptide of MyD88 L265P described in publication 2 was further characterized to exclude off-target toxicity and alloreactivity in in vitro assays and therapeutic efficacy of this novel precision immunotherapy was proven in vivo in two different xenograft models.[126]

Compared to the approved CD19 CAR T cell products, precision immunotherapy with a TCR directed against the point-mutated MyD88 L265P epitope offers unique opportunities. General advantages are that surface expression of an antigen, or the modulation thereof, is not a limitation for TCR-T cell therapy and T cells can recognize their target independently of the targets original cellular localization, i.e. intracellular or surface proteins.[152] Furthermore, the L265P-specific TCR targets a recurrent driver mutation and therefore, antigen-loss variants are less likely to occur, in contrast to anti-CD19 therapy where CD19-loss variants have been reported as a relapse mechanism.[100–104] Another advantage is the absolute tumor specificity where unwanted (off-tumor) on-target toxicity is not anticipated.[153,154] In contrast, on-target toxicity of CARs directed against B lineage antigens, such as CD19, causes prolonged B cell aplasia, resulting in a substantial increase in morbidity and additional treatment efforts, including immunoglobulin substitution and treatment of infectious complications, and thus negatively affecting quality of life. Furthermore, adverse events associated with CD19-CAR-T therapies such as cytokine release syndrome (CRS) is linked to high systematic cytokine levels during target/CAR-T cell engagement and CAR-T cell expansion caused by the overactivation of CAR-T cells. Due to a more physiological level of cellular signaling in TCR-T cells a lower risk for CRS and neurotoxicity is expected.[152,155,156] This would additionally lower the need of intervention and decrease further add-on costs for health care systems. Less severe acute toxicities may enable an outpatient setting in the future and reduce hospitalization costs. Finally, in contrast to high-dose chemotherapy and autologous or allogenic hematopoietic stem cell transplantation (HSCT), for TCR-T cell therapy the patients' age is not a limiting factor and only low-dose conditioning chemotherapy, and supportive care is required.

4.6 Optimizing TCR-T cell manufacturing processes for clinical application

Adoptive T cell therapy encounters various restrictions. Apart from escape mechanisms such as downregulation of the target antigen for CAR-T or HLA-loss for TCR-T cell approaches, the manufacturing process poses additional hurdles. Some of these include insufficient numbers of lymphocytes at collection, suboptimal expansion and generation of transduced T cells, or expansion of T cells with an unfavorable phenotype and functional ability. This is especially true in elderly and severely pre-treated patients.[157–

[159] Various T cell production protocols are being applied and protocol deviations include for instance culture medium composition, cell seeding densities, or distinct phenotypic properties of starting populations[160–162]. It is clear, that not only the number of lymphocytes but also their functional properties can vary greatly in the various patient cohorts. These functional properties are evident in the ability of T cells to be activated and expanded during the production process. This has also been observed in the presented study (publication 3)[158].

From analysis in various mouse models[161,163–168] and also data from clinical trials of CAR-T cells for neuroblastoma[169] and B cell malignancies[170,171], as well as TILs for melanoma[172,173] demonstrate that (stem cell) memory T cell subgroups show superior expansion, persistence, and antitumor efficacy after in vivo transfer. These T cell subgroups are classified by their phenotype, but also proliferation potential and telomere length have been correlated with better therapeutic efficacy[158,174].

At least for CAR-T cells it is now generally accepted that an optimal therapeutic effect is achieved when ex vivo expanded T cells show the phenotype of early memory differentiation (Tscm or Tcm)[175]. T cells with an early lineage phenotype, naïve (Tn) or Tcm, are particularly suitable as starting cell material, but they occur at a much lower frequency in tumor patients such as DLBCL patients compared to healthy donors.[158,159,161] Thus, strategies to improve the proliferative and functional properties of T cells from heavily pretreated and/or older patients are urgently needed. Established clinical protocols for the production of T cells for ATT include collection of leukapheresis from the patient and the selection of desired lymphocytes, either CD8+ and/or CD4+ T cells, for activation by their endogenous TCR-CD3 complex. Activated cells are genetically modified and afterwards expanded. In current protocols ex vivo expansion of cells occurs for up to 14 days before cells are re-infused into the patient.[158,170,176] Recent attempts have been made to investigate strategies to reduce the duration of ex vivo culture to limit T cell differentiation.[177–179] Shorter culture duration might therefore improve ATT in terms of differentiation state and functionality of T cells, however, this may be a limitation for patients with lymphopenia and lymphocyte dysfunction due to heavy pre-treatment with chemotherapy. For these patients, a longer expansion time might be necessary to obtain sufficient cell numbers for treatment. The here presented study

showed that a prolonged T cell expansion protocol seems to be a practicable alternative for patients with insufficient numbers of T cells. The extension of the in vitro culture for more than three weeks with cytokines interleukin-7 and -15 (IL-7 and IL-15) resulted in higher T cell yields and preserved T cell functionality, persistence, and antitumor capacity. This would reduce manufacturing failure for patients with insufficient T cell numbers after the standard manufacturing process, and thereby increasing ATT accessibility for these patients.[162] However, the long-term expansion protocol could pose a challenge for patients with rapidly progressing disease or heavy pre-treatment with no further treatment options since the vein-to-vein time is significantly extended.

The clinical outcome of patients treated with ATT might rather depend on their ability to proliferate and persist in vivo, than on the bulk number of infused cells[180]. Different transcriptional, phenotypical, and functional features define T cell function as well as dysfunction, and contain several cellular states including terminal differentiation, exhaustion, senescence, and apoptosis. Thus, a careful design of ex vivo culture conditions during manufacturing processes may promote the acquisition of a favorable functional status of the cell product. Current protocols for generating TCR-T and CAR-T cells involve CD3/CD28 stimulation for efficient retro-viral gene transfer[51,181]. However, this TCR activation leads to cellular differentiation[182,183] and the substantial in vitro expansion can cause shortening of telomeres[72,174,184]. Rapid replication induced oxidative stress can further accelerate telomere shortening and replicative senescence[185,186], factors which limit the effectiveness against tumors. To address this issue, several strategies have been developed to limit cellular differentiation, including the use of a specific cytokine cocktail for the expansion of T cells. Cytokines IL-7 and IL-15, which support the generation of human Tscm from naïve precursors are frequently used in manufacturing protocols.[165,187] The addition of IL-21 can further improve the number of T cells with phenotypic and functional characteristics associated with long-lived memory T cells. IL-21 not only prevents apoptosis and limits terminal differentiation of antigen-specific T cells but may also enable effector cells to reacquire central memory features after adoptive transfer in vivo.[188] This provides a rationale to further optimize TCR-T or CAR-T cells to inducibly or constitutively secrete active cytokines such as IL-21 or IL-18, creating so called “armored gene modified T cells”[188–191].

In addition to cytokines, it has been shown that small molecules, which alter cell signaling, metabolic modulation, and epigenetic modification, can be added during the ex vivo priming and expansion phase and may foster features of Tcm and Tscm. Examples of such molecules include the histone deacetylase inhibitor (HDACi), AKT inhibitors, N-acetylcysteine, and the glycogen synthase kinase-3β inhibitor TWS119, a pharmacologic agonist of the canonical Wnt/β-catenin pathway.[192]

A by far simpler approach to limit differentiation is to use lentiviral transduction to stably express a CAR in non-activated T cells. This eliminates the need for long-term ex vivo cultures of T cells, thereby reducing the costs for cultivation and minimizing the vein-to-vein time.[177,193] However, the optimal T cell subpopulation for transduction of non-activated T cells is not yet defined.

5 Conclusion

Various challenges must be overcome in the development and clinical transfer of adoptive TCR-T cell therapies, including the identification of epitopes presented by the tumor, the isolation of high-affinity TCRs, and the expansion of patient TCR-T cells in sufficient quantities, with the preferred phenotype.

The experience gathered with mutation-specific epitopes suggests that, despite possible disadvantages in terms of safety, the generation of TCRs from allogeneic and partially matched healthy donors, or from humanized transgenic mice might be a viable strategy for the development of mutation-specific ATT. TCRs identified by this approach offer an ATT treatment option for patients with relapsed or refractory disease after revalidation of the presence of the identified neoepitope – ideally on the patient´s tumor tissue.

To follow the three R principle, isolation from the human repertoire is the preferred method. However, in contrast to TSA, the isolation of high-affinity TCRs directed against TAAs, such as cancer-testis antigens, from the human repertoire is still a challenge. In general, it is not possible to isolate a high-affinity TCR from the HLA-compatible repertoire without subsequent affinity maturation, which poses a significant safety risk. A topic of current evaluation is whether it is possible to isolate a high-affinity TCR directed against an HLA-A*02:01-restricted cancer germline antigen from the HLA-A*02:01 negative repertoire. As for the transgenic mice, high-affinity TCR can be isolated since their repertoire has not been trained on HLA-A*02:01 epitopes. However, setting up a pipeline for the identification of the alloreactive TCRs, e.g., from HLA-A*02:01 mismatched repertoires, is necessary for further investigations.

Regarding the manufacturing of TCR-T cells from patients for clinical application, it was demonstrated that an extended T cell expansion is a feasible and practicable alternative for patients with insufficient numbers of T cells after the standard TCR-T cell production process thereby increasing ATT accessibility. However, the results need to be confirmed on a GMP-compliant manufacturing platform that is compatible with this prolonged culture period. Sufficient T cell numbers in the apheresis product may still pose a bottleneck for the production of T cell products. It remains to be evaluated whether in vivo transduction protocols can overcome this challenge.

6 Abbreviation

ABC	Activated B cell like
APC	Antigen presenting cell
ATT	Adoptive T cell therapy
CAR	Chimeric antigen receptor
CD	Cluster of differentiation
CDR	Complementary determining region
CRS	Cytokine release syndrome
CTL	Cytotoxic T lymphocyte
DN	Double negative
DLBCL	Diffuse large B cell lymphoma
DP	Double positive
ER	Endoplasmic Reticulum
HDACi	histone deacetylase inhibitor
HLA	Human leukocyte antigen
IL	Interleukin
IFNy	Interferon y
ITAM	Immunoreceptor-based tyrosine activation motifs
LT	Long-term
MHC	Major histocompatibility complex
MS	Mass spectrometry
MyD88	Myeloid differentiation primary response 88
NHL	Non-Hodgkin lymphoma
PCNSL	Primary central nervous system lymphoma
pMHC	Peptide MHC
scFv	Single chain variable fragment
SNV	Single nucleotide variation
TAA	Tumor-associated antigen
TAP	Transporter associated with antigen processing
Tcm	Central memory T cells
TCR	T cell receptor

Abbreviation

TIL	Tumor infiltrating lymphocyte
Tn	Naïve T cells
TSA	Tumor-specific antigen
Tscm	Stem memory T cells
V(D)J	Variable (Diversity) Joining

7 References

1. Davis, M. M. & Bjorkman, P. J. T-cell antigen receptor genes and T-cell recongition. *Nature* **334**, 395–402 (1988).
2. Yoshikai, Y. *et al.* Organization and sequences of the variable, joining and constant region genes of the human T-cell receptor alpha-chain. *Nature* **316**, 837–840 (1985).
3. Lewis, S. M. The Mechanism of V(D)J Joining: Lessons from Molecular, Immunological, and Comparative Analyses. *Adv. Immunol.* **56**, 27–150 (1994).
4. Nikolich-Žugich, J., Slifka, M. K. & Messaoudi, I. The many important facets of T-cell repertoire diversity. *Nat. Rev. Immunol.* **4**, 123–132 (2004).
5. Arstila, T. P. *et al.* A direct estimate of the human αβ T cell receptor diversity. *Science* . **286**, 958–961 (1999).
6. Qi, Q. *et al.* Diversity and clonal selection in the human T-cell repertoire. *Proc. Natl. Acad. Sci. U. S. A.* **111**, 13139–13144 (2014).
7. Robins, H. S. *et al.* Comprehensive assessment of T-cell receptor beta-chain diversity in alphabeta T cells. *Blood* **114**, 4099–4107 (2009).
8. Lustgarten, J., Waks, T. & Eshhar, Z. CD4 and CD8 accessory molecules function through interactions with major histocompatibility complex molecules which are not directly associated with the T cell receptor-antigen complex. *Eur. J. Immunol.* **21**, 2507–2515 (1991).
9. Spits, H. Development of aß T cells in the human thymus. *Nat. Rev. Immunol.* **2**, 760–772 (2002).
10. Janeway, C. J., Travers, P. & Walport, M. *Janeway's Immunobiology*. (Garland Science, 2012).
11. Janeway, C. J., Travers, P. & Walport, M. The major histocompatibility complex and its functions. in *mmunobiology: The Immune System in Health and Disease.* (Garland Science, 2001).
12. Freeman, G. J. *et al.* Cloning of B7-2: a CTLA-4 counter-receptor that costimulates human T cell proliferation. *Science* **262**, 909–911 (1993).
13. Bour-Jordan, H. & Bluestone, J. A. CD28 Function: A Balance of Costimulatory and Regulatory Signals. *J Clin Immunol.* **22**, 1–7 (2001).
14. Curtsinger, J. M. & Mescher, M. F. Inflammatory cytokines as a third signal for T cell activation. *Curr. Opin. Immunol.* **22**, 333–340 (2010).

15. Howard Grey, B. M. *et al.* The Small Subunit of HLA-Antigens is ß2-Microglobulin. *J. Exp. Med.* **138**, 1608–1612 (1073).
16. Beck, S. *et al.* Complete sequence and gene map of a human major histocompatibility complex. *Nature* **401**, 921–923 (1999).
17. van den Elsen, P. J. & van der Vlag, J. Expression regulation of major histocompatibility complex class I and class II encoding genes. *Front. Immunol.* **2**, 1–34 (2011).
18. Rammensee, H.-G., Friede, T. & Stevanovic, S. MHC ligands and peptide motifs: first listing. *Immunogenetics* **41**, 178–228 (1995).
19. Akiyama, K. *et al.* Replacement of proteasome subunits X and Y by LMP7 and LMP2 induced by interferon-gamma for acquirement of the functional diversity responsible for antigen processing. *FEBS Lett.* **343**, 85–88 (1994).
20. Aki, M. *et al.* Interferon-γ Induces Different Subunit Organizations and Functional Diversity of Proteasomes. *J. Biochem.* **115**, 257–269 (1994).
21. Strehl, B. *et al.* Antitopes Define Preferential Proteasomal Cleavage Site Usage. *J. Biol. Chem.* **283**, 17891–17897 (2008).
22. Cresswell, P., Ackerman, A. L., Giodini, A., Peaper, D. R. & Wearsch, P. A. Mechanisms of MHC class I-restricted antigen processing and cross-presentation. *Immunol. Rev.* **207**, 145–157 (2005).
23. Kloetzel, P. M. Antigen Processing by the Proteasome. *Nat. Rev.* **2**, 179–187 (2001).
24. Baldwin, R. X. Immunity to Methylcholanthrene-induced tumours in inbred rats following atrophy and regression, of the implanted tumours. *Br. J. Cancer* **9**, 652–657 (1955).
25. Gross, L. Intradermal Immunization of C3H Mice against a Sarcoma That Originated in an Animal of the Same Line. *Cancer Res.* **3**, 326–333 (1943).
26. Klein,Hansolofsjã-Gren, G. Demonstration of Host Resistance against Isotransplantation of Lymphomas Induced by the Gross Agent. *Cancer Res.* **22**, 955–961 (1962).
27. Sjögren, H. O., Hellström, I. & Klein, G. Resistance of polyoma virus immunized mice to transplantation of established polyoma tumors. *Exp. Cell Res.* **23**, 204–208 (1961).
28. Klein, E. & Sjögren, H. O. Humoral and cellular factors in homograft and isograft immunity against sarcoma cells. *Cancer Res.* 452–61 (1960).

29. G C Perri, B. D., Faulk, M., Shapiro, E., Mellors, J. & L Money, D. W. Function of the thymus and growth of tumor homograft. *Biochem. Biophys. Res. Comm* **33**, 654 (1959).

30. Burnet, F. M. The Concept of Immunological Surveillance. *Prog. Exp. tumor Res. Fortschritte der Exp. Tumorforschung. Prog. la Rech. Exp. des tumeurs* **13**, 1–27 (1970).

31. Schreiber, R. D., Old, L. J. & Smyth, M. J. Cancer immunoediting: Integrating immunity's roles in cancer suppression and promotion. *Science.* **331**, 1565–1570 (2011).

32. Willimsky, G. & Blankenstein, T. Sporadic immunogenic tumours avoid destruction by inducing T-cell tolerance. *Nature* **437**, 141–146 (2005).

33. Ciampricotti, M. *et al.* Development of metastatic HER2 + breast cancer is independent of the adaptive immune system. *J. Pathol. J Pathol* **224**, 56–66 (2011).

34. Shresta, S., Pham, C. T., Thomas, D. A., Graubert, T. A. & Ley, T. J. How do cytotoxic lymphocytes kill their targets? *Curr. Opin. Immunol.* **10**, 581–587 (1998).

35. Barth, R. J., Mule, J. J., Spiess, P. J. & Rosenberg, S. A. Interferon gamma and tumor necrosis factor have a role in tumor regressions mediated by murine CD8+ tumor-infiltrating lymphocytes. *J. Exp. Med.* **173**, 647–658 (1991).

36. Luckheeram, R. V., Zhou, R., Verma, A. D. & Xia, B. CD4+T Cells: Differentiation and Functions. *Clin. Dev. Immunol.* **2012**, 12 (2012).

37. Van Der Bruggen, P. *et al.* A Gene Encoding an Antigen Recognized by Cytolytic T Lymphocytes on a Human Melanoma. *Science.* **254**, 1643–1647 (1991).

38. Dauer, M. *et al.* FastDC derived from human monocytes within 48 h effectively prime tumor antigen-specific cytotoxic T cells. *J. Immunol. Methods* **302**, 145–155 (2005).

39. De Plaen, E. *et al.* Structure, chromosomal localization, and expression of 12 genes of the MAGE family. *Immunogenetics* **40**, 360–369 (1994).

40. Chen, Y. T. *et al.* A testicular antigen aberrantly expressed in human cancers detected by autologous antibody screening. *Proc. Natl. Acad. Sci. U. S. A.* **94**, 1914 (1997).

41. Schumacher, T. N. & Schreiber, R. D. Neoantigens in cancer immunotherapy. *Science.* **348**, 69- (2015).

42. Kawakami, Y. *et al.* Identification of the immunodominant peptides of the MART-1 human melanoma antigen recognized by the majority of HLA-A2-restricted tumor

infiltrating lymphocytes. *J. Exp. Med.* **180**, 347 (1994).

43. Brichard, V. *et al.* The Tyrosinase Gene Codes for an Antigen Recognized by Autologous Cytolytic T Lymphocytes on HLA-A2 Melanomas. *J. Exp. Med.* **178**, 489–495 (1993).
44. Chang, K., Pastan, I. & Willingham, M. C. Isolation and characterization of a monoclonal antibody, K1, reactive with ovarian cancers and normal mesothelium. *Int. J. cancer* **50**, 373–381 (1992).
45. Bernhard, H. *et al.* Adoptive transfer of autologous, HER2-speciWc, cytotoxic T lymphocytes for the treatment of HER2-overexpressing breast cancer. *Cancer Immunol Immunother* **57**, 271–280 (2008).
46. Cheever, M. A. *et al.* The prioritization of cancer antigens: a national cancer institute pilot project for the acceleration of translational research. *Clin. Cancer Res.* **15**, 5323–5337 (2009).
47. Leisegang, M. *et al.* MHC-restricted fratricide of human lymphocytes expressing survivin-specific transgenic T cell receptors. *J. Clin. Invest.* **120**, 3869–3877 (2010).
48. Morgan, R. A. *et al.* Cancer regression and neurologic toxicity following anti-MAGE-A3 TCR gene therapy. *J. Immunother.* **36**, 133 (2013).
49. Morgan, R. A. *et al.* Case Report of a Serious Adverse Event Following the Administration of T Cells Transduced With a Chimeric Antigen Receptor Recognizing ERBB2. *Mol. Immunol.* **18**, 843–851 (2010).
50. Johnson, L. A. *et al.* Gene therapy with human and mouse T-cell receptors mediates cancer regression and targets normal tissues expressing cognate antigen. *Blood* **114**, 535–546 (2009).
51. Rohaan, M. W. *et al.* MART-1 TCR gene-modified peripheral blood T cells for the treatment of metastatic melanoma: a phase I/IIa clinical trial. *Immuno-Oncology Technol.* **15**, 1–14 (2022).
52. Bjerregaard, A. *et al.* MuPeXI: prediction of neo-epitopes from tumor sequencing data. *Cancer Immunol. Immunother.* **66**, 1123–1130 (2001).
53. Andreatta, M. & Nielsen, M. Gapped sequence alignment using artificial neural networks: application to the MHC class I system. *Bioinformatics* **32**, 511–517 (2016).
54. Kuttler, C. *et al.* An algorithm for the prediction of proteasomal cleavages. *J. Mol. Biol.* **298**, 417–429 (2000).

55. Hundal, J. *et al.* pVAC-Seq: A genome-guided in silico approach to identifying tumor neoantigens. *Genome Med.* **8**, 1–11 (2016).

56. McGranahan, N. & Swanton, C. Neoantigen quality, not quantity. *Sci. Transl. Med.* **11**, (2019).

57. Balachandran, V. P. *et al.* Identification of unique neoantigen qualities in long-term survivors of pancreatic cancer. *Nature* **551**, S12–S16 (2017).

58. Lang, F., Schrörs, B., Löwer, M., Türeci, Ö. & Sahin, U. Identification of neoantigens for individualized therapeutic cancer vaccines. *Nat. Rev. Drug Discov.* **21**, 261–282 (2022).

59. Schrader, M., Fricker, L. & Bassani-Sternberg, M. Mass Spectrometry Based Immunopeptidomics for the Discovery of Cancer Neoantigens. in *Methods in Molecular Biology* vol. 1719 209–221 (2019).

60. Newey, A. *et al.* Immunopeptidomics of colorectal cancer organoids reveals a sparse HLA class i neoantigen landscape and no increase in neoantigens with interferon or MEK-inhibitor treatment. *J. Immunother. Cancer* **7**, (2019).

61. Rie Dutoit, V. *et al.* Exploiting the glioblastoma peptidome to discover novel tumour-associated antigens for immunotherapy. *BRAIN - A J. Neurol.* **135**, 1042–1054 (2012).

62. Migliorini, D. *et al.* Phase I/II trial testing safety and immunogenicity of the multipeptide IMA950/poly-ICLC vaccine in newly diagnosed adult malignant astrocytoma patients. *Neuro. Oncol.* **21**, 923–933 (2019).

63. Srivastava, A. K., Guadagnin, G., Cappello, P. & Novelli, F. Post-Translational Modifications in Tumor-Associated Antigens as a Platform for Novel Immuno-Oncology Therapies. *Cancers (Basel).* **15**, 1–17 (2022).

64. Creech, A. L. *et al.* The role of Mass Spectrometry and Proteogenomics in the Advancement of HLA Epitope Prediction. *Proteomics* **18**, (2018).

65. Chai, S. *et al.* NeoSplice: a bioinformatics method for prediction of splice variant neoantigens. *Bioinforma. Adv.* 1–10 (2022) doi:10.1093/bioadv/vbac032.

66. Rosenberg, S. A. *et al.* Use of tumor-infiltrating lymphocytes and interleukin-2 in the immunotherapy of patients with metastatic melanoma. A preliminary report. *N. Engl. J. Med.* **319**, 1676–1680 (1988).

67. Rosenberg, S. A. *et al.* Treatment of patients with metastatic melanoma with autologous tumor-infiltrating lymphocytes and interleukin 2. *J. Natl. Cancer Inst.* **86**,

1159–1166 (1994).

68. van den Berg, J. H. *et al.* Tumor infiltrating lymphocytes (TIL) therapy in metastatic melanoma: boosting of neoantigen-specific T cell reactivity and long-term follow-up. *J. Immunother. Cancer* **8**, (2020).
69. Dudley, M. E. *et al.* CD8+ enriched 'Young' tumor infiltrating lymphocytes can mediate regression of metastatic melanoma. *Clin. Cancer Res.* **16**, 6122–6131 (2010).
70. Dudley, M. E. *et al.* Randomized Selection Design Trial Evaluating CD8-Enriched Versus Unselected Tumor-Infiltrating Lymphocytes for Adoptive Cell Therapy for Patients With Melanoma. *J. Clin. Oncol.* **31**, 2152–2159 (2013).
71. Friedman, K. M., Devillier, L. E., Feldman, S. A., Rosenberg, S. A. & Dudley, M. E. Augmented lymphocyte expansion from solid tumors with engineered cells for costimulatory enhancement. *J Immunother* **34**, 651–661 (2011).
72. Tran, K. Q. *et al.* Minimally cultured tumor-infiltrating lymphocytes display optimal characteristics for adoptive cell therapy. *J. Immunother.* **31**, 742–751 (2009).
73. Creelan, B. C., Wang, C., Haura, E. B. & Antonia, S. J. Tumor-infiltrating lymphocyte treatment for anti-PD-1-resistant metastatic lung cancer: a phase 1 trial. *Nat. Med.* **27**, 1410–1418 (2021).
74. Stevanovic, S. *et al.* Complete Regression of Metastatic Cervical Cancer After Treatment With Human Papillomavirus-Targeted Tumor-Infiltrating T Cells. *J. Clin. Oncol.* **33**, 1543–1550 (2015).
75. Kluger, H. M. Tumor mutational burden (TMB) in immune checkpoint inhibitor (ICI)-naïve and -experienced patients with metastatic melanoma treated with lifileucel, a tumor-infiltrating lymphocyte (TIL) cell therapy. in *ASCO Annual Meeting* (2022).
76. David O'Malley. Phase 2 efficacy and safety of autologous tumor-infiltrating lymphocyte (TIL) cell therapy in combination with pembrolizumab in immune checkpoint inhibitor-naïve patients with advanced cancers. in *SITC Annual Meeting* (2001).
77. Stromnes, I. M. *et al.* T Cells Engineered against a Native Antigen Can Surmount Immunologic and Physical Barriers to Treat Pancreatic Ductal Adenocarcinoma. *Cancer Cell* **28**, 638–652 (2015).
78. Stromnes, I. M., Schmitt, T. M., Chapuis, A. G., Hingorani, S. R. & Greenberg, P. D. Re-adapting T cells for cancer therapy: From mouse models to clinical trials. *Immunol.*

Rev. **257**, 145–164 (2014).

79. Kunert, A. *et al.* TCR-engineered T cells meet new challenges to treat solid tumors: choice of antigen, T cell fitness, and sensitization of tumor milieu. *Front. Immunol.* **4**, (2013).
80. Ikeda, H. T-cell adoptive immunotherapy using tumor-infiltrating T cells and genetically engineered TCR-T cells. *Int. Immunol.* **28**, 349–353 (2016).
81. Stone, J. D., Aggen, D. H., Schietinger, A., Schreiber, H. & Kranz, D. M. A sensitivity scale for targeting T cells with chimeric antigen receptors (CARs) and bispecific T-cell Engagers (BiTEs). *Oncoimmunology* **1**, 863 (2012).
82. Schmitt, T. M., Stromnes, I. M., Chapuis, A. G. & Greenberg, P. D. New strategies in engineering T-cell receptor gene-modified T cells to more effectively target malignancies. *Clin. Cancer Res.* **21**, 5191–5197 (2015).
83. Kochenderfer, J. N. & Rosenberg, S. A. Treating B-cell cancer with T cells expressing anti-CD19 chimeric antigen receptors. *Nat. Rev. Clin. Oncol.* **10**, 267 (2013).
84. Turtle, C. J., Riddell, S. R. & Maloney, D. G. CD19-Targeted Chimeric Antigen Receptor-Modified T-Cell Immunotherapy for B-Cell Malignancies. *Clin. Pharmocol Ther* **100**, 252–258 (2016).
85. European Medicines Agency - Medicines Catalogue. https://www.ema.europa.eu/en/medicines.
86. ClinicalTrial.gov. NCT05239143 : P-MUC1C-ALLO1 Allogeneic CAR-T Cells in the Treatment of Subjects With Advanced or Metastatic Solid Tumors.
87. Bamdad, C. C. *et al.* Phase I/II first-in-human CAR T–targeting MUC1 transmembrane cleavage product (MUC1*) in patients with metastatic breast cancer. *Journal of Clinical Oncology* vol. 40 TPS1130–TPS1130 (2022).
88. Matsuzaki, J., Lele, S., Odunsi, K. & Tsuji, T. Identification of Claudin 6-specific HLA class I- and HLA class II-restricted T cell receptors for cellular immunotherapy in ovarian cancer. *Oncoimmunology* **11**, (2022).
89. Romain, G. *et al.* Multidimensional single-cell analysis identifies a role for CD2-CD58 interactions in clinical antitumor T cell responses. *J. Clin. Invest.* **132**, (2022).
90. Subklewe, M., Von Bergwelt-Baildon, M. & Humpe, A. Chimeric Antigen Receptor T Cells: A Race to Revolutionize Cancer Therapy. *Transfus. Med. Hemotherapy* **46**, 15–24 (2019).

91. Sterner, R. C. & Sterner, R. M. CAR-T cell therapy: current limitations and potential strategies. *Sterner Sterner Blood Cancer J.* **11**, 69 (2021).
92. Schuster, S. J. *et al.* Tisagenlecleucel in Adult Relapsed or Refractory Diffuse Large B-Cell Lymphoma. *N. Engl. J. Med.* **380**, 45–56 (2019).
93. Brentjens, R. *et al.* CD19-targeted T cells rapidly induce molecular remissions in adults with chemotherapy-refractory acute lymphoblastic leukemia. *Sci Transl Med* **5**, 177–215 (2013).
94. Maude, S. L. *et al.* Tisagenlecleucel in Children and Young Adults with B-Cell Lymphoblastic Leukemia. *N Engl J Med* **378**, 439–448 (2018).
95. Maude, S. L. *et al.* Chimeric Antigen Receptor T Cells for Sustained Remissions in Leukemia. *N. Engl. J. Med.* **371**, 1507–1517 (2014).
96. Wittibschlager, V. *et al.* CAR T-Cell Persistence Correlates with Improved Outcome in Patients with B-Cell Lymphoma. *Int. J. Mol. Sci.* **24**, 5688 (2023).
97. Joseph Melenhorst, J. *et al.* Decade-long leukaemia remissions with persistence of CD4 + CAR T cells. *Nature* **602**, 503 (2022).
98. Carrington, M. *et al.* HLA and HIV-1: Heterozygote advantage and B*35-Cw*04 disadvantage. *Science.* **283**, 1748–1752 (1999).
99. Cappell, K. M. *et al.* Long-Term Follow-Up of Anti-CD19 Chimeric Antigen Receptor T-Cell Therapy. *J. Clin. Oncol.* **38**, 3805–3815 (2020).
100. Ghorashian, S. *et al.* Enhanced CAR T cell expansion and prolonged persistence in pediatric patients with ALL treated with a low-affinity CD19 CAR. *Nat. Med. 2019 259* **25**, 1408–1414 (2019).
101. Campillo-Davo, D., Flumens, D. & Lion, E. The Quest for the Best: How TCR Affinity, Avidity, and Functional Avidity Affect TCR-Engineered T-Cell Antitumor Responses. *cells* **9**, 1–18 (2020).
102. Dourthe, M.-E. *et al.* Determinants of CD19-positive vs CD19-negative relapse after tisagenlecleucel for B-cell acute lymphoblastic leukemia. *Leukemia* **35**, 3383–3393 (2021).
103. Plaks, V. *et al.* CD19 target evasion as a mechanism of relapse in large B-cell lymphoma treated with axicabtagene ciloleucel. *Blood* **138**, 1081–1085 (2021).
104. Park, J. H. *et al.* Long-Term Follow-up of CD19 CAR Therapy in Acute Lymphoblastic Leukemia. *N. Engl. J. Med.* **378**, 449–459 (2018).

105. Tran, E. *et al.* T-Cell Transfer Therapy Targeting Mutant KRAS in Cancer. *N. Engl. J. Med.* **375**, 2255–2262 (2016).

106. Dhatchinamoorthy, K., Colbert, J. D. & Rock, K. L. Cancer Immune Evasion Through Loss of MHC Class I Antigen Presentation. *Front. Immunol.* **12**, 1–27 (2021).

107. Taylor, B. C. & Balko, J. M. Mechanisms of MHC-I Downregulation and Role in Immunotherapy Response. *Front. Immunol.* **13**, 1–6 (2022).

108. Hellmann, M. D. *et al.* Nivolumab plus Ipilimumab in Lung Cancer with a High Tumor Mutational Burden. *N. Engl. J. Med.* **378**, 2093–2104 (2018).

109. Anagnostou, V. *et al.* Evolution of neoantigen landscape during immune checkpoint blockade in non-small cell lung cancer. *Cancer Discov.* **7**, 264 (2017).

110. Rizvi, N. A. *et al.* Mutational landscape determines sensitivity to PD-1 blockade in non–small cell lung cancer. *Science* **348**, 124 (2015).

111. Mcgranahan, N. *et al.* Clonal neoantigens elicit T cell immunoreactivity and sensitivity to immune checkpoint blockade HHS Public Access. *Sci. March* **25**, 1463–1469 (2016).

112. Ott, P. A. *et al.* An immunogenic personal neoantigen vaccine for patients with melanoma. *Nature* **547**, 217–221 (2017).

113. Sahin, U. *et al.* Personalized RNA mutanome vaccines mobilize poly-specific therapeutic immunity against cancer. *Nat. Lett.* **547**, 222–226 (2017).

114. Carreno, B. M. *et al.* A dendritic cell vaccine increases the breadth and diversity of melanoma neoantigen-specific T cells. *Science* **348**, 803 (2015).

115. Keskin, D. B. *et al.* Neoantigen vaccine generates intratumoral T cell responses in phase Ib glioblastoma trial. *Nat. 2018 5657738* **565**, 234–239 (2018).

116. Cancer Genome Atlas Research Network. Genomic and Epigenomic Landscapes of Adult De Novo Acute Myeloid Leukemia. *N. Engl. J. Med.* **368**, 2059–2074 (2013).

117. Schischlik, F. *et al.* Mutational landscape of the transcriptome offers putative targets for immunotherapy of myeloproliferative neoplasms. *Blood* **134**, 199–210 (2019).

118. Spaapen, R., Li, Y., Berneman, Z., Biernacki, M. A. & Bleakley, M. Neoantigens in Hematologic Malignancies. *Front. Immunol.* **11**, 121 (2020).

119. Yossef, R. *et al.* Enhanced detection of neoantigen-reactive T cells targeting unique and shared oncogenes for personalized cancer immunotherapy. *JCI insight* **3**, (2018).

120. Wang, Q. J. *et al.* Identification of T-cell Receptors Targeting KRAS-mutated Human Tumors. *Cancer Immunol. Res.* **4**, 204 (2016).

121. Baleeiro, R. B. *et al.* Optimized Anchor-Modified Peptides Targeting Mutated RAS Are Promising Candidates for Immunotherapy. *Front. Immunol.* **13**, 1–13 (2022).

122. Chandran, S. S. *et al.* Immunogenicity and therapeutic targeting of a public neoantigen derived from mutated PIK3CA. *Nat. Med.* **28**, 946–957 (2022).

123. Levin, N. *et al.* Identification and validation of T-cell receptors targeting RAS hotspot mutations in human cancers for use in cell-based immunotherapy. *Clin. Cancer Res.* **27**, (2021).

124. Nelde, A. *et al.* HLA class I-restricted MYD88 L265P-derived peptides as specific targets for lymphoma immunotherapy. (2017) doi:10.1080/2162402X.2016.1219825.

125. Ngo, V. N. *et al.* Oncogenically active MYD88 mutations in human lymphoma. *Nature* **470**, 115 (2011).

126. Çınar, Ö. *et al.* High-affinity T-cell receptor specific for MyD88 L265P-mutation for adoptive T-cell therapy of B-cell malignancies. *J Immunother Cancer* **9**, 2410 (2021).

127. Abbas, H. A. *et al.* Single cell T cell landscape and T cell receptor repertoire profiling of AML in context of PD-1 blockade therapy. *Nat. Commun.* **12**, (2021).

128. Carretero-González, A. *et al.* Analysis of response rate with ANTI PD1/PD-L1 monoclonal antibodies in advanced solid tumors: a meta-analysis of randomized clinical trials. *Oncotarget* **9**, 8706–8715 (2018).

129. Valpione, S. *et al.* The T cell receptor repertoire of tumor infiltrating T cells is predictive and prognostic for cancer survival. *Nat. Commun. 2021 121* **12**, 1–8 (2021).

130. Liu, S. *et al.* Efficient identification of neoantigen-specific T-cell responses in advanced human ovarian cancer. *J. Immunother. Cancer* **7**, 1–17 (2019).

131. Vormehr, M. *et al.* Mutanome directed cancer immunotherapy. *Curr. Opin. Immunol.* **39**, 14–22 (2016).

132. Freudenmann, L. K., Marcu, A. & Stevanović, S. Mapping the tumour human leukocyte antigen (HLA) ligandome by mass spectrometry. *Immunology* **154**, 331–345 (2018).

133. Popović, J. *et al.* The only proposed T-cell epitope derived from the TEL-AML1 translocation is not naturally processed. *Blood* **118**, 946–954 (2011).

134. Darbyshire, M., Du Toit, Z., Rogers, M. F., Gaunt, T. R. & Campbell, C. Estimating the

frequency of Single point Driver Mutations across common Solid tumours. *Nat. Sci. Reports* **9**, (2019).

135. Grunert, C. *et al.* Isolation of Neoantigen-Specific Human T Cell Receptors from Different Human and Murine Repertoires. *Cancers (Basel).* **14**, (2022).
136. Tenzer, S. *et al.* Antigen processing influences HIV-specific cytotoxic T lymphocyte immunodominance. *Nat. Immunol.* **10**, 636–646 (2009).
137. Sette, A. *et al.* The relationship between class I binding affinity and immunogenicity of potential cytotoxic T cell epitopes. *J Immunol* **153**, 5586–92 (1994).
138. Riley, T. P. *et al.* Structure Based Prediction of Neoantigen Immunogenicity. *Front. Immunol. | www.frontiersin.org* **10**, 1–14 (2019).
139. Fritsch, E. F. *et al.* HLA-Binding Properties of Tumor Neoepitopes in Humans. *Cancer Immunol. Res.* **2**, 522–529 (2014).
140. Wei, J. *et al.* Ribosomal Proteins Regulate MHC Class I Peptide Generation for Immunosurveillance. *Mol. Cell* **73**, 1162-1173.e5 (2019).
141. Leng, Q., Tarbe, M., Long, Q. & Wang, F. Pre-existing heterologous T-cell immunity and neoantigen immunogenicity. *Clin. Transl. Immunol.* **9**, (2020).
142. Wucherpfennig, K. W. & Strominger, J. L. Molecular mimicry in T cell-mediated autoimmunity: Viral peptides activate human T cell clones specific for myelin basic protein. *Cell* **80**, 695–705 (1995).
143. Pro, S. C. *et al.* Microbiota epitope similarity either dampens or enhances the immunogenicity of disease-associated antigenic epitopes. *PLoS One* **13**, 1–23 (2018).
144. Zugel, U. *et al.* Crossrecognition by CD8 T cell receptor ap cytotoxic T lymphocytes of peptides in the self and the mycobacterial hsp60 which share intermediate sequence homology. *Eur. J. Immunol* **25**, 451–458 (1995).
145. Calis, J. J. A., De Boer, R. J. & Kesmir, C. Degenerate T-cell Recognition of Peptides on MHC Molecules Creates Large Holes in the T-cell Repertoire. *PLoS Comput Biol* **8**, 1–11 (2012).
146. Krishna, C., Chowell, D., Gönen, M., Elhanati, Y. & Chan, T. A. Genetic and environmental determinants of human TCR repertoire diversity. *Immun. Ageing* **17**, 1–7 (2020).
147. Chowell, D. *et al.* Evolutionary divergence of HLA class I genotype impacts efficacy of cancer immunotherapy. *Nat. Med.* **25**, 1715–1720 (2019).

148. de Groen, R. A. L., Schrader, A. M. R., Kersten, M. J., Pals, S. T. & Vermaat, J. S. P. MYD88 in the driver's seat of B-cell lymphomagenesis: from molecular mechanisms to clinical implications. *Haematologica* **104**, 2337–2348 (2019).

149. Vermaat, J. S. *et al.* MYD88 mutations identify a molecular subgroup of diffuse large B-cell lymphoma with an unfavorable prognosis. *Haematologica* **105**, 424–434 (2020).

150. Rovira, J. *et al.* MYD88 L265P mutations, but no other variants, identify a subpopulation of DLBCL patients of activated B-cell origin, extranodal involvement, and poor outcome. *Clin. Cancer Res.* **22**, 2755–2764 (2016).

151. Yu, X. *et al.* MYD88 L265P mutation in lymphoid malignancies. *Cancer Res.* **78**, 2457–2462 (2018).

152. Harris, D. T. & Kranz, D. M. Adoptive T Cell Therapies: A Comparison of T Cell Receptors and Chimeric Antigen Receptors. *Trends Pharmacol. Sci.* **37**, 220–230 (2016).

153. Drandi, D. *et al.* Highly sensitive MYD88L265P mutation detection by droplet digital polymerase chain reaction in Waldenström macroglobulinemia. *Haematologica* **103**, 1029–1037 (2018).

154. Staiger, A. M. *et al.* Allele-specific PCR is a powerful tool for the detection of the MYD88 L265P mutation in diffuse large B cell lymphoma and decalcified bone marrow samples. *Br. J. Haematol.* **171**, 145–148 (2015).

155. Xiao, X. *et al.* Mechanisms of cytokine release syndrome and neurotoxicity of CAR T-cell therapy and associated prevention and management strategies. *J. Exp. Clin. Cancer Res. 2021 401* **40**, 1–23 (2021).

156. Lee, D. W. *et al.* ASTCT Consensus Grading for Cytokine Release Syndrome and Neurologic Toxicity Associated with Immune Effector Cells. *Biol. Blood Marrow Transplant.* **25**, 625–638 (2019).

157. Stroncek, D. F. *et al.* Elutriated lymphocytes for manufacturing chimeric antigen receptor T cells. *J. Transl. Med.* **15**, 59 (2017).

158. Singh, N., Perazzelli, J., Grupp, S. A. & Barrett, D. M. Early memory phenotypes drive T cell proliferation in patients with pediatric malignancies. *Sci. Transl. Med.* **8**, 1–10 (2016).

159. Petersen, C. T. *et al.* Improving T-cell expansion and function for adoptive T-cell

therapy using ex vivo treatment with PI3Kd inhibitors and VIP antagonists. *Blood Adv.* **2**, 210–223 (2018).

160. Joedicke, J. J. *et al.* Accelerating clinical-scale production of BCMA CAR T cells with defined maturation stages. *Mol. Ther. - Methods Clin. Dev.* **24**, 181–198 (2022).
161. Sommermeyer, D. *et al.* Chimeric antigen receptor-modified T cells derived from defined CD8+ and CD4+ subsets confer superior antitumor reactivity in vivo. *Leukemia* **30**, 492–600 (2016).
162. Herda, S. *et al.* Long-term in vitro expansion ensures increased yield of central memory T cells as perspective for manufacturing challenges. *Int. J. Cancer* **148**, 3097–3110 (2021).
163. Gerlach, C. *et al.* Heterogeneous differentiation patterns of individual CD8+ T cells. *Science* vol. 340 (2013).
164. Graef, P. *et al.* Serial Transfer of Single-Cell-Derived Immunocompetence Reveals Stemness of CD8+ Central Memory T Cells. *Immunity* **41**, 116–126 (2014).
165. Cieri, N. *et al.* IL-7 and IL-15 instruct the generation of human memory stem T cells from naive precursors. *Blood* **121**, 573–584 (2013).
166. Gattinoni, L. *et al.* A human memory T cell subset with stem cell–like properties. *Nat. Med. 2011 1710* **17**, 1290–1297 (2011).
167. Klebanoff, C. A. *et al.* Determinants of successful CD8 + T-cell adoptive immunotherapy for large established tumors in mice. *Clin. Cancer Res.* **17**, 5343–5352 (2011).
168. Klebanoff, C. A. *et al.* Central memory self/tumor-reactive CD8+ T cells confer superior antitumor immunity compared with effector memory T cells. *Proc. Natl. Acad. Sci. U. S. A.* **102**, 9571 (2005).
169. Louis, C. U. *et al.* Antitumor activity and long-term fate of chimeric antigen receptor-positive T cells in patients with neuroblastoma. *Blood* **118**, 6050–6056 (2011).
170. Arcangeli, S. *et al.* Next-Generation Manufacturing Protocols Enriching TSCM CAR T Cells Can Overcome Disease-Specific T Cell Defects in Cancer Patients. *Front. Immunol.* **11**, 1217 (2020).
171. Turtle, C. J. *et al.* CD19 CAR-T cells of defined CD4+:CD8+ composition in adult B cell ALL patients. *J. Clin. Invest.* **126**, 2123–2138 (2016).
172. Rosenberg, S. A. *et al.* Durable complete responses in heavily pretreated patients

with metastatic melanoma using T-cell transfer immunotherapy. *Clin. Cancer Res.* **17**, 4550–4557 (2011).

173. Zhou, J., Nagarkatti, P., Zhong, Y. & Nagarkatti, M. Characterization of T-Cell Memory Phenotype after In Vitro Expansion of Tumor-infiltrating Lymphocytes from Melanoma Patients. *Anticancer Res* **31**, 4099–4109 (2011).
174. Zhou, J. *et al.* Telomere length of transferred lymphocytes correlates with in vivo persistence and tumor regression in melanoma patients receiving cell transfer therapy. *J. Immunol.* **175**, 7046 (2005).
175. Meyran, D. *et al.* Early-phenotype CAR-T cells for the treatment of pediatric cancers. *Ann. Oncol.* **32**, 1366–1380 (2021).
176. Brentjens, R. J. *et al.* Safety and persistence of adoptively transferred autologous CD19-targeted T cells in patients with relapsed or chemotherapy refractory B-cell leukemias. *Blood* **118**, 4817–4828 (2011).
177. Ghassemi, S. *et al.* Rapid manufacturing of non-activated potent CAR T cells. *Nat. Biomed. Eng. 2022 62* **6**, 118–128 (2022).
178. Engels, B. *et al.* Retroviral Vectors for High-Level Transgene Expression in T Lymphocytes. *Hum. Gene Ther.* **14**, 1155–1168 (2003).
179. Pallarès-Masmitjà, M. *et al.* Find and cut-and-transfer (FiCAT) mammalian genome engineering. *Nat. Commun.* **12**, 1–9 (2021).
180. Mueller, K. T. *et al.* Cellular kinetics of CTL019 in relapsed/refractory B-cell acute lymphoblastic leukemia and chronic lymphocytic leukemia. *Blood* **130**, 2317–2325 (2017).
181. Schuster, S. *et al.* Global pivotal phase 2 trial of the Cd19-targeted therapy Ctl019 in adult patients with relapsed or refractory (R/R) diffuse large B-cell lymphoma (Dlbcl)-an interim analysis. Hematol Oncol. 2017;35:27. in *AACR-ICML JOINT SESSION - Cancer Immunotherapy* (2017).
182. Hwang, J. R., Byeon, Y., Kim, D. & Park, S. G. Recent insights of T cell receptor-mediated signaling pathways for T cell activation and development. *Exp. Mol. Med. 2020 525* **52**, 750–761 (2020).
183. Huang, W. & August, A. The signaling symphony: T cell receptor tunes cytokine-mediated T cell differentiation. *J. Leukoc. Biol.* **97**, 477–485 (2015).
184. Hodes, R. J., Hathcock, K. S. & Weng, N. P. Telomeres in T and B cells. *Nat. Rev.*

Immunol. 2002 29 **2**, 699–706 (2002).

185. Campisi, J. The biology of replicative senescence. *Eur. J. Cancer* **33**, 703–709 (1997).
186. Rottenberg, M., Wang, R., Gnanaprakasam, J. N. R. & Wu, R. Metabolic Reprogramming in Modulating T Cell Reactive Oxygen Species Generation and Antioxidant Capacity. *Front. Immunol.* **9**, 1 (2018).
187. Xu, Y. *et al.* Closely related T-memory stem cells correlate with in vivo expansion of CAR.CD19-T cells and are preserved by IL-7 and IL-15. *Blood* **123**, 3750–3759 (2014).
188. Štach, M. *et al.* Inducible secretion of IL-21 augments anti-tumor activity of piggyBac-manufactured chimeric antigen receptor T cells. *Cytotherapy* **22**, 744–754 (2020).
189. Pegram, H. J. *et al.* Tumor-targeted T cells modified to secrete IL-12 eradicate systemic tumors without need for prior conditioning. *Blood* **119**, 4133 (2012).
190. Hu, B. *et al.* Augmentation of Antitumor Immunity by Human and Mouse CAR T Cells Secreting IL-18. *Cell Rep.* **20**, 3025–3033 (2017).
191. Kueberuwa, G., Kalaitsidou, M., Cheadle, E., Hawkins, R. E. & Gilham, D. E. CD19 CAR T Cells Expressing IL-12 Eradicate Lymphoma in Fully Lymphoreplete Mice through Induction of Host Immunity. *Mol. Ther. Oncolytics* **8**, 41–51 (2017).
192. Marro, B. S. *et al.* Discovery of Small Molecules for the Reversal of T Cell Exhaustion. *Cell Rep.* **29**, 3293-3302.e3 (2019).
193. Wang, S. Y., Moore, T. V., Dalheim, A. V., Scurti, G. M. & Nishimura, M. I. Melanoma reactive TCR-modified T cells generated without activation retain a less differentiated phenotype and mediate a superior in vivo response. *Sci. Rep.* **11**, 13327 (2021).

8 List of Publications

Activated SUMOylation restricts MHC class I antigen presentation to confer immune evasion in cancer; Uta M. Demel; Marlitt Böger; Schayan Yousefian; Corinna Grunert; Le Zhang; Paul W. Hotz; Adrian Gottschlich; Hazal Köse; Konstandina Isaakidis; Dominik Vonficht et al.; Journal of Clinical Investigation, 2022-05-02; DOI: 10.1172/JCI152383

Isolation of Neoantigen-Specific Human T Cell Receptors from Different Human and Murine Repertoires; Corinna Grunert, Gerald Willimsky, Caroline Anna Peuker, Simone Rhein, Leo Hansmann, Thomas Blankenstein, Eric Blanc, Dieter Beule, Ulrich Keller, Antonio Pezzutto and Antonia Busse; Cancers; 2022; 14(7); DOI: 10.3390/cancers14071842

Treatment with ribociclib shows favourable immunomodulatory effects in patients with hormone receptor-positive breast cancer—findings from the RIBECCA trial; Caroline A. Peuker, Sarvenaz Yaghobramzi, Corinna Grunert, Luisa Keilholz, Enio Gjerga, Steffen Hennig, Sigrid Schaper, Il-Kang Na, Ulrich Kelle, Sara Brucker, Thomas Decker, Peter Fasching, Tanja Fehm, Wolfgang Janni, Sherko Kümmel, Andreas Schneeweiss, Martin Schuler, Diana Lüftner, Antonia Busse; European Journal of Cancer; 2022; 162; DOI: 10.1016/j.ejca.2021.11.025

High-affinity T-cell receptor specific for MyD88 L265P mutation for adoptive T-cell therapy of B-cell malignancies; Özcan Çınar, Bernadette Brzezicha, Corinna Grunert, Peter Michael Kloetzel, Christin Beier, Caroline Anna Peuker, Ulrich Keller, Antonio Pezzutto, Antonia Busse; Journal for ImmunoTherapy of Cancer; 2021; 9(e002410); DOI: 10.1136/jitc-2021-002410

Long-term in vitro expansion ensures increased yield of central memory T cells as perspective for manufacturing challenges; Stefanie Herda, Andreas Heimann, Benedikt Obermayer, Elisa Ciraolo, Stefanie Althoff, Josefine Ruß, Corinna Grunert, Antonia Busse, Lars Bullinger, Antonio Pezzutto, Thomas Blankenstein, Dieter Beule, Il-Kang Na; Int. J. Cancer; 2021; 148; DOI: 10.1002/ijc.33523

9 Supplementary materials

Isolation of Neoantigen-Specific Human T Cell Receptors from Different Human and Murine Repertoires

Supplementary Figures

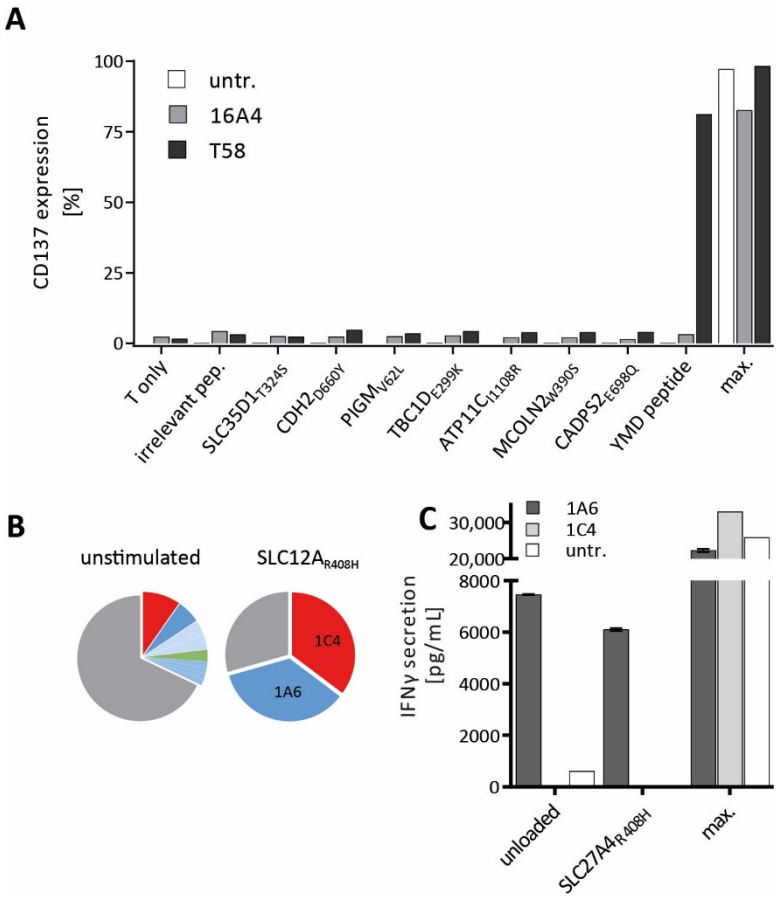

Figure S1. Test of patient derived TCRs from single-cell sorting from patients BIH146 and BIH56. (**A**) Peptide recognition assay of peptide-loaded target cells by TCR 16A4-transduced (16A4-td) PBLs identified for patient BIH146. Peptide reactivity was measured by surface expression of activation marker CD137 on 16A4-td PBLs after a 20h co-culture with peptide-loaded target cells. Activation marker expression from one donor is shown. Alive, single cells were gated on CD8+, mTCRß+. (**B**) Single-cell sequencing of peptide-stimulated PBMCs of patient BIH56. Pie charts show frequencies of detected TCR clones of unstimulated and neoepitope candidate SLC12A$_{R408H}$ stimulated T cells. TCRs of 1C4 and 1A6 were identified, grey segments represent all TCRα/β rearrangements which were detected only once per sample. (**C**) TCR 1C4 and 1A6 were expressed on PBLs and tested for reactivity in a co-culture with peptide-loaded target cells. IFNγ-release was measured after an overnight co-culture in duplicates, error bars show standard deviation. Untr.: untransduced; T58: control TCR specific for Tyrosinase peptide (YMD: YMDGTMSQV); max.: PMA/Ionomycin for maximal; unspecific activation.

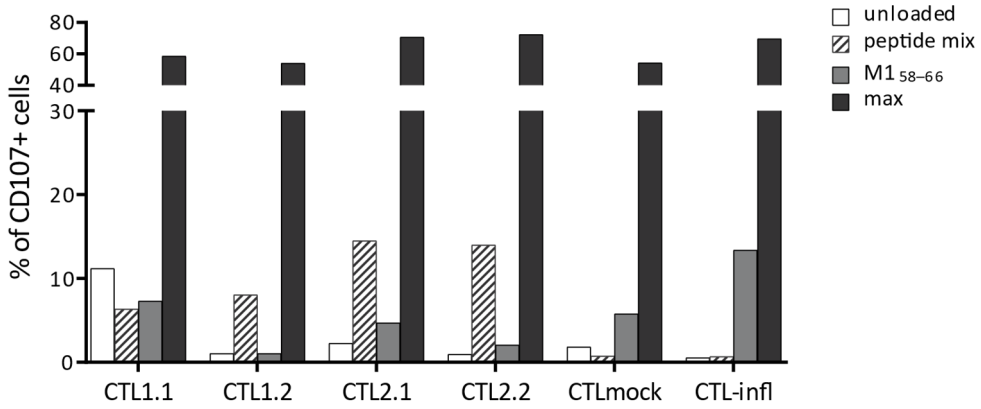

Figure S2. Degranulation assay of cytotoxic T cell lines (CTLs). CTLs were generated by stimulation of bulk CD8+ T cells from healthy donor A with a peptide pool of three candidate neoantigen peptides ($CDH2_{D660Y}$, $SLC35D1_{T324S}$ and $PIGM_{V62L}$). Peptide reactivity was assessed by measuring expression of degranulation marker CD107 after incubation with peptide-loaded target cells by flow cytometry. The surface expression of CD107 on CTLs is shown for 4 generated CTL lines from donor A. CTLs generated against influenza peptide $M1_{58-66}$ were used as an assay control. CTL were gated on single, viable, CD8+ cells.

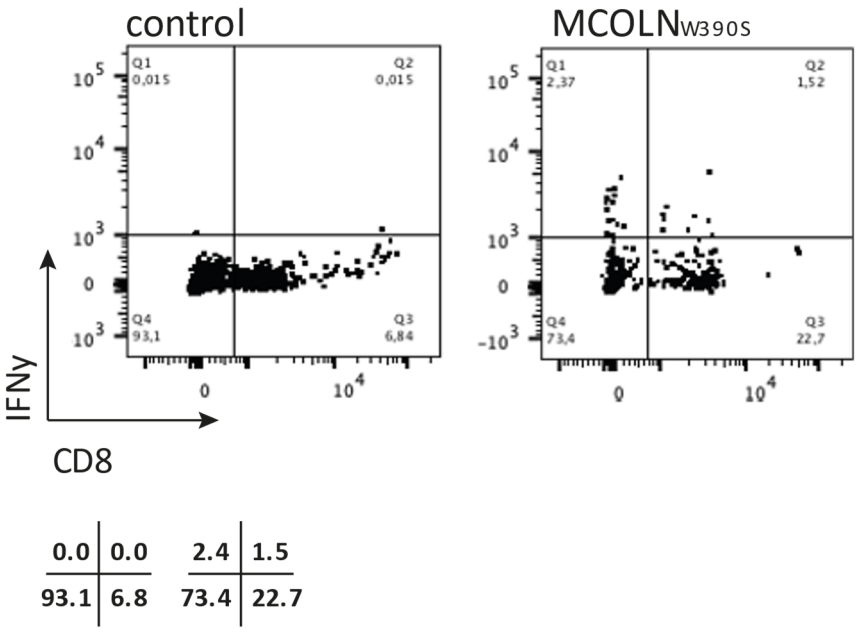

Figure S3. Generation of neoepitope candidate specific TCRs in ABabDII mice for patient BIH146. Splenocytes of immunized ABabDII mice were cultured to expand peptide reactive CD8+ cells. Expanded cells were sorted after an IFNγ capture assay and IFNγ+ cells were sorted. Cells were gated on CD3+CD8+IFNγ+ cells. Cells cultured without peptide served as a negative control. Plots are shown for peptide $SLC12A_{R408H}$ stimulated splenocytes, from which TCR m875 was identified.

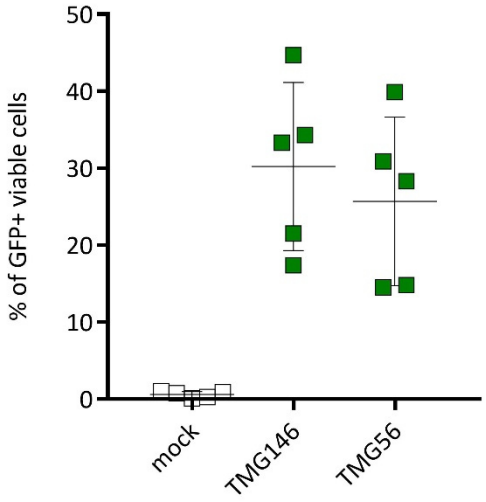

Figure S4: Nucleofection of multiple myeloma cell line U266 with TMG-constructs. U266 cells were nucleofected with neoepitope-encoding Tandem Minigenes (TMG). Nucleofection efficiency was determined 16-20 h post nucleofection by detection of eGFP expression via flow-cytometry of viable cells (n=5). Mock cells were nucleofected with PBS. Cells were immediately used as target cells in co-culture experiments. TMG146 – TMG encoding for predicted neoepitope candidates for patient BIH146; TMG56 - TMG encoding for predicted neoepitope candidates for patient BIH56.

High-affinity T-cell receptor specific for MyD88 *L265P mutation for adoptive T-cell therapy of B-cell malignancies*

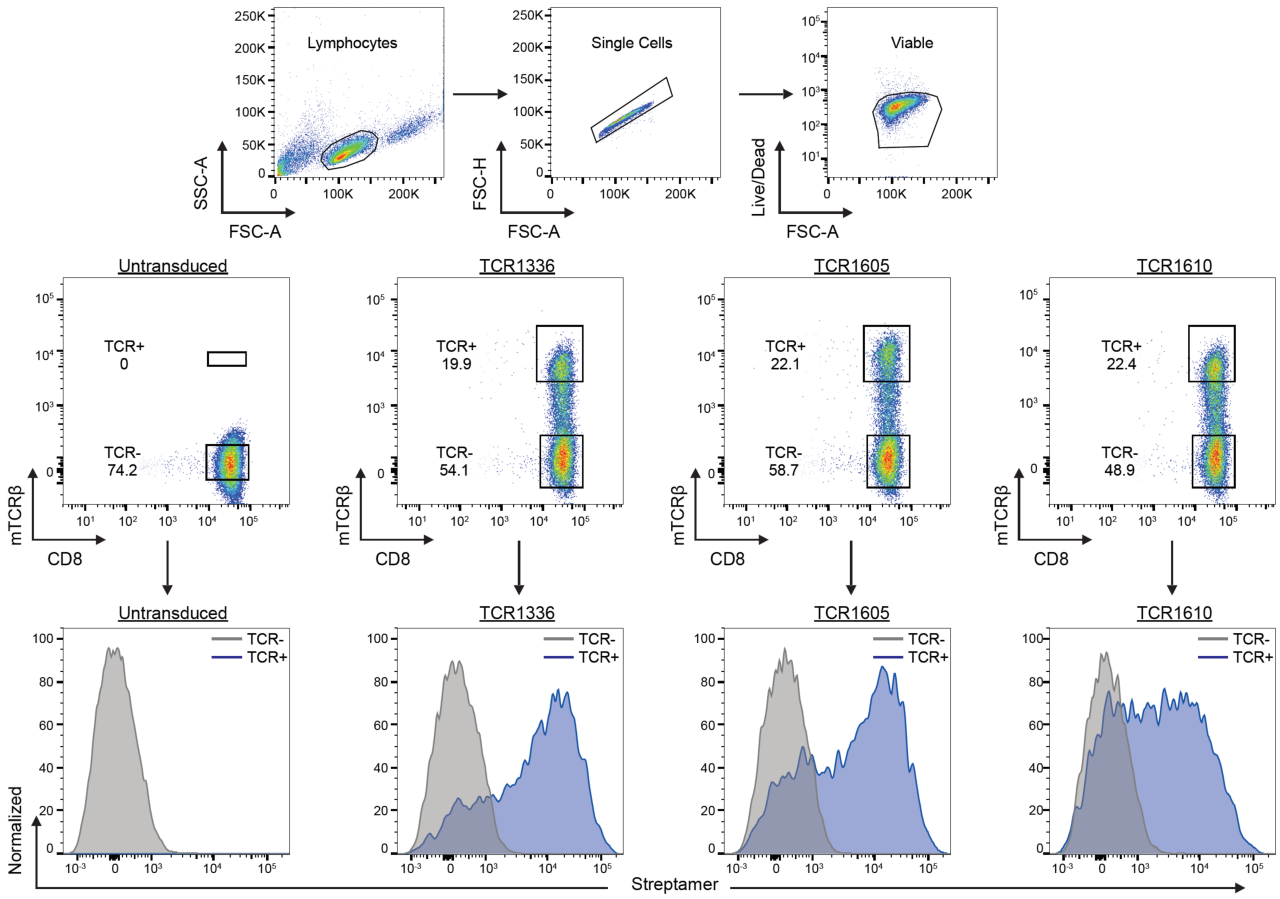

Supplementary Figure 1: Representative streptamer staining of TCR-transduced T cells

CD8+ T cells isolated from healthy donors transduced with the mutation-specific TCRs were stained with anti-mouse TCR β constant domain antibody and streptamer to test the surface expression the TCRs, and functionality of the alpha-beta TCR pairings from the sequencing results.

A

Peptide	HLA type	Sequence	Affinity (nM)	% Rank	Length
9mer	HLA-B07:02	**RPIPIKYKA**	613	1.30 (WB)	9mer
Mut	HLA-B07:02	**RPIPIKYKAM**	12	0.06 (SB)	10mer
Pre-1	HLA-B07:02	**KRPIPIKYKAM**	156	0.60 (SB)	11mer
Pre-2	HLA-B07:02	**QKRPIPIKYKAM**	219	0.70 (SB)	12mer

B

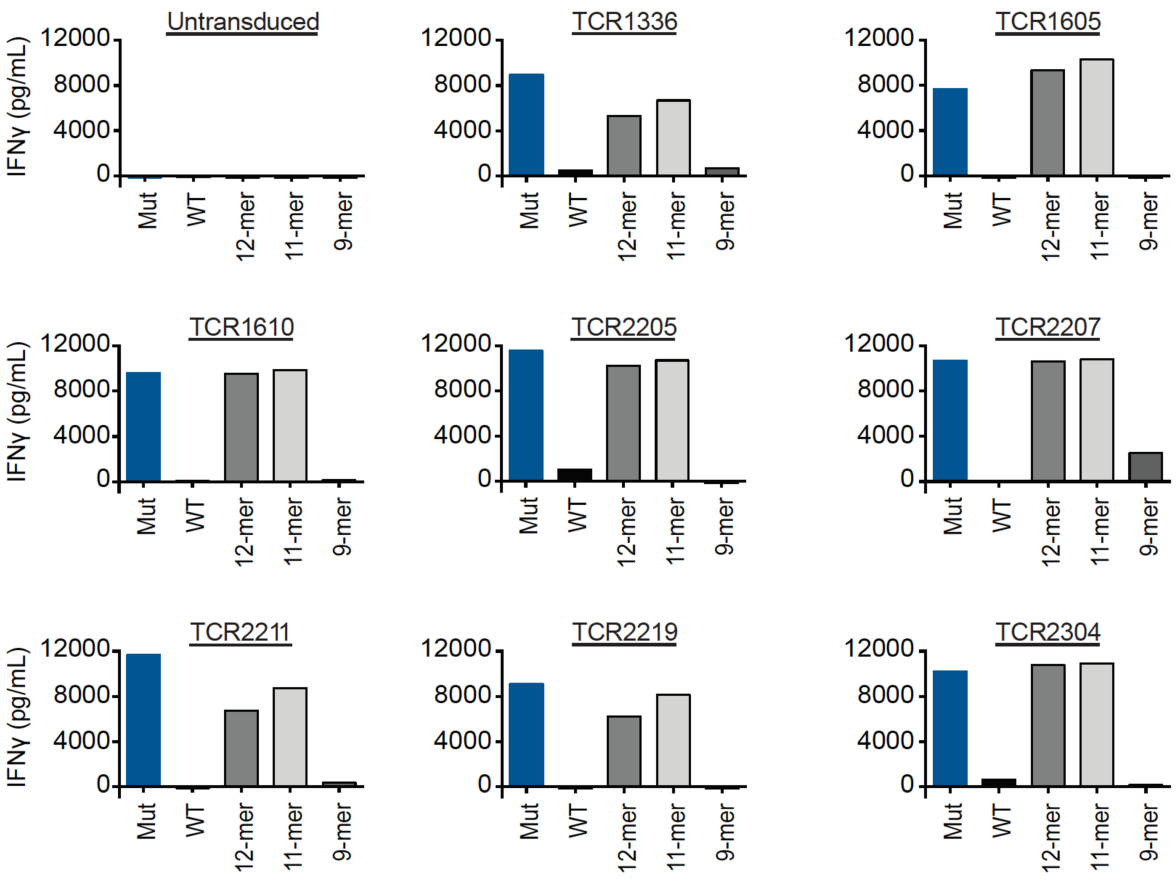

Supplementary Figure 2: Precursor peptides and epitope recognition

A. HLA binding prediction for 9-12mer peptides detected in the mass-spectrometric analysis of the mutant epitope (NetMHC 4.0). *B.* HLA-B*07:02 expressing K562 cells were loaded with peptides and co-cultured with TCR-T cells for 16 hours. IFNγ response was measured by ELISA. Mutation-specific TCRs recognized precursor peptides similarly to the 10mer epitope.

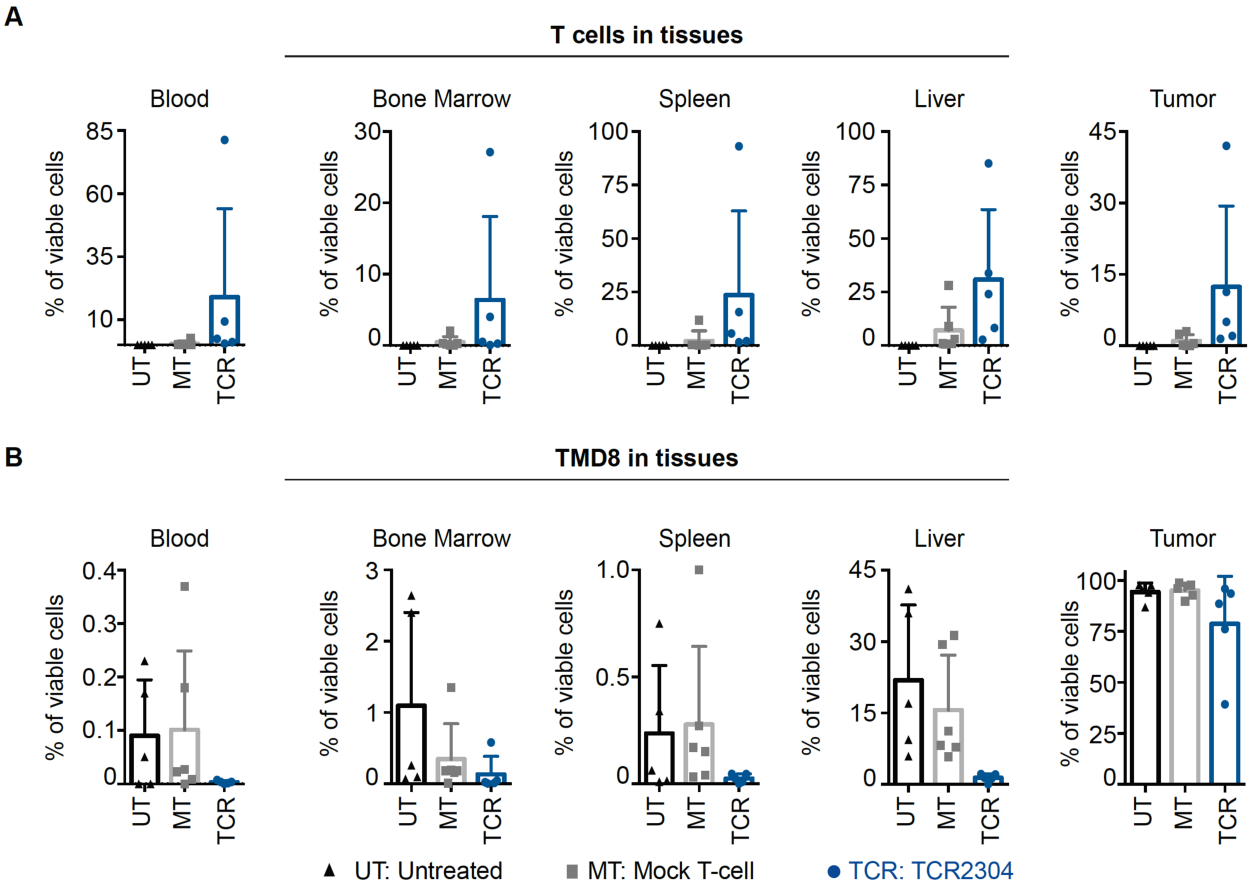

Supplementary Figure 3: Flow cytometric analysis of systemic dissemination of TMD8 cells

NOG mice were s.c. injected with 5x10^6 HLA-B*07:02 positive luciferase expressing TMD8 cells. *A.* Proportion of T cells in tissues of tumor bearing NOG mice. *B.* Proportion of TMD8 cells in tissues of tumor bearing NOG mice. Analysis from single, viable cells. Each symbol represents an individual mouse.

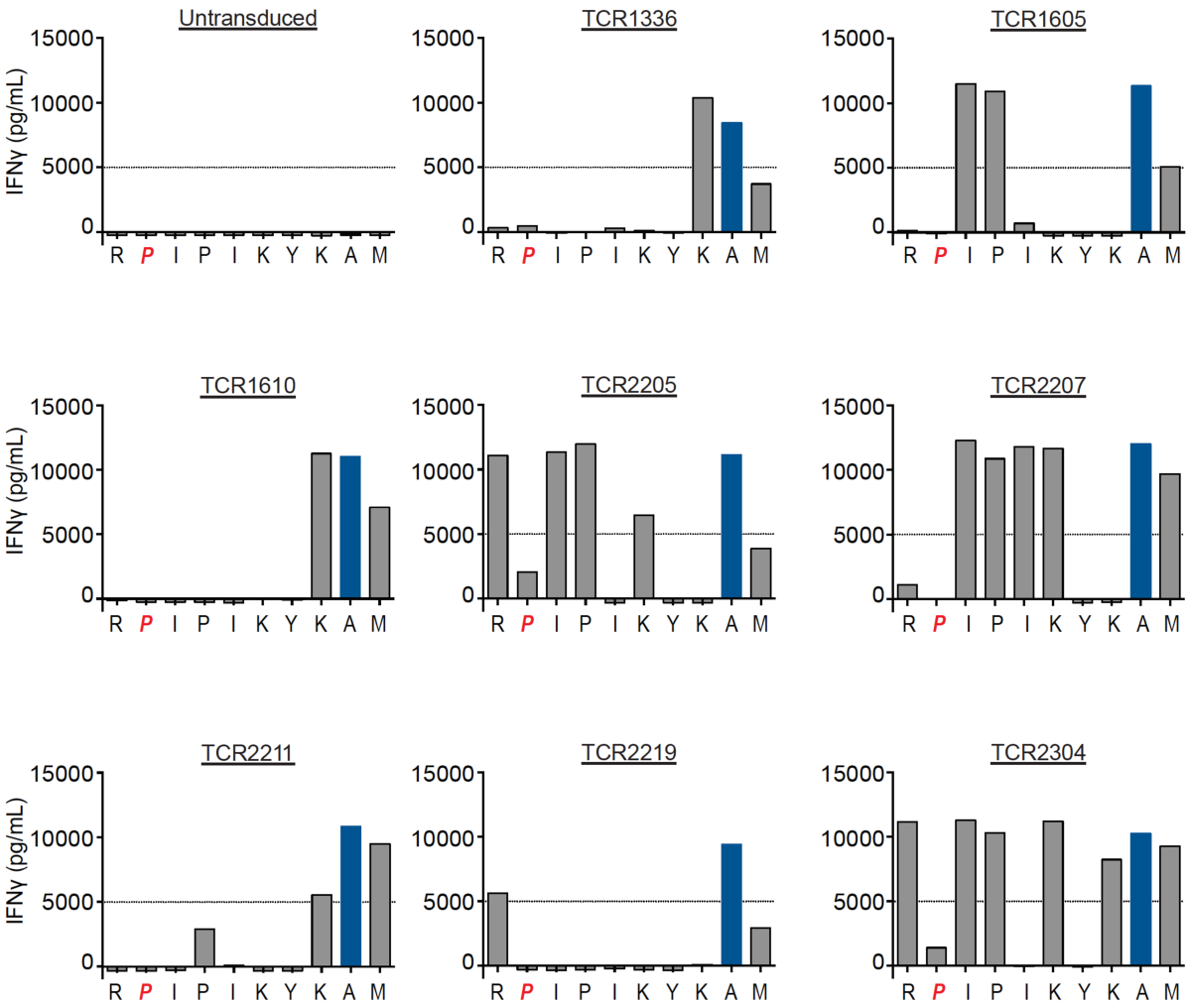

Supplementary Figure 4: Unique alanine scan results of mutation-specific TCRs

HLA-B*07:02 positive K562 cells were loaded either with 10mer mutant epitope or one of the 9 alanine scan peptides in high concentration (10 µg/ml) –to determine the most crucial amino acid positions for recognition, and co-cultured with TCR-T cells for 16 hours. IFNγ response was measured by ELISA.

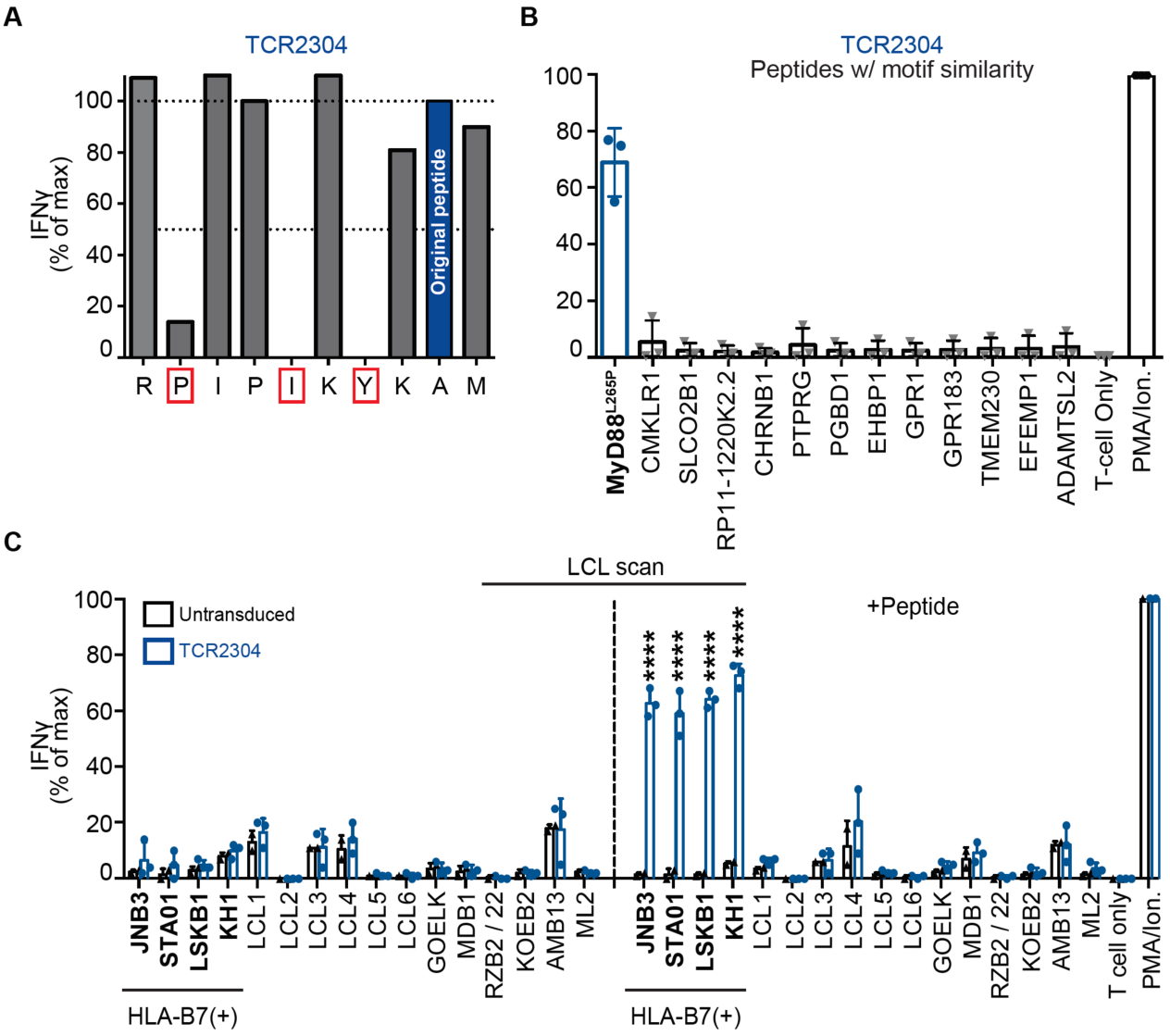

Supplementary Figure 5: Safety analysis of TCR2304

A. HLA-B*07:02 expressing K562 cells were loaded either with 10mer mutant epitope or one of the 9 alanine scan peptides at the concentration of 10 µg/ml, and co-cultured with TCR2304-T cells for 16 hours. IFNγ response was measured by ELISA. Amino acid positions that negatively affected IFNγ response more than 50% were considered vital for recognition of the mutant epitope by the TCR. *B.* Expitope online tool [19] was used to scan human proteome for peptides with sequence similarity to binding motif of TCR2304 (xPxxIxYxxx) with up to 5 mismatch positions. Resulting peptides with any binding prediction to HLA*B07:02 were loaded on target cells similarly to alanine scan (10 µg/ml), and co-cultured with TCR2304-T cells from 3 different donors for 16 hours. IFNγ response was measured by ELISA. Error bars showing SD. *C.* A library of EBV-immortalized B-LCLs were co-cultured with TCR2304-T cells from 3 different donors for 16 hours, with or without prior peptide loading. IFNγ response was measured by ELISA. Error bars showing SD. Difference between untransduced and TCR-transduced T cells in with or without peptide conditions analyzed by 2-way ANOVA: **P* < 0.05; ***P* < 0.01; ****P* < 0.001; *****P* < 0.0001.

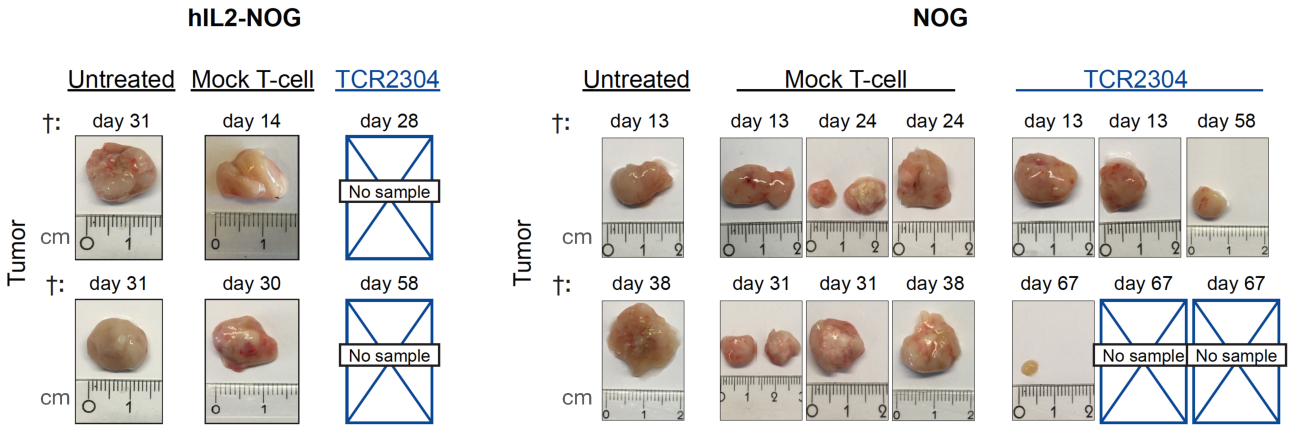

Supplementary Figure 6: OCI-Ly3 tumors from sacrificed hIL2-NOG and common NOG mice

Mice were s.c. inoculated with $5x10^6$ HLA-B*07:02 positive OCI-Ly3 cells. Once the tumors reached predetermined size of $100mm^3$ (~2weeks after injection), tumor bearing mice were treated with i.v. injection of $1x10^7$ TCR2304-T cells, or mock (untransduced) T cells of the same donor, or PBS as untreated control. Mice were sacrificed with cervical dislocation when tumor size exceeded $1500mm^3$, or or signs of distress was observed.

Supplementary Table 4: Summary of the peptides generated by the proteasome from the polypeptide substrate MyD88-L265P[256-281] in an in vitro digest.

RT alignment:		1. 180502_Cha45_Lcl_24h
identification:		2. 180502_Cha45_Ery_24h
		3. 180502_Cha45_Lcl_8h
		4. 180502_Cha45_Ery_8h

Cha-45 (MyD88$_{256-281}$ mut L265P)

LSPGAHQKRPIPIKYKAMKKEFPSIL

	m/z monoiso. Da			charge	sequence	RT	MW monoiso. Da			MS/MS
	detected	calculated	Δ	z		(min)	detected	calculated	Δ	Raw File
1	241.6578	241.6543	0.0036	2	R[9-12]P	20.3	481.3156	481.3085	0.0071	1
2	284.6687	284.6657	0.0030	2	H[6-9]R	12.6	567.3374	567.3314	0.0060	1
3	286.8528	286.8483	0.0045	3	P[10-16]K	27.2	857.5584	857.5448	0.0136	3,4
4	319.1746	319.1708	0.0038	2	P[3-8]K	18.3	636.3492	636.3416	0.0076	2,4
5	331.8578	331.8529	0.0049	3	L[1-9]R	24.1	992.5734	992.5588	0.0146	1,3,4
6	354.2118	354.2075	0.0043	3	P[10-18]M	35.0	1059.6354	1059.6224	0.0130	3,4
7	360.2266	360.2225	0.0041	2	P[12-17]A	24.2	718.4532	718.4450	0.0082	2,4
8	360.7004	360.6964	0.0041	2	K[20-25]I	39.6	719.4008	719.3927	0.0081	1-4
9	362.2473	362.2438	0.0035	2	R[9-14]K	20.6	722.4946	722.4876	0.0070	2,4
10	362.5664	362.5610	0.0054	3	R[9-17]A	24.1	1084.6992	1084.6830	0.0162	1-4
11	362.6903	362.6869	0.0034	2	S[2-8]K	19.0	723.3806	723.3737	0.0069	2,4
12	367.5489	367.5441	0.0048	3	P[3-12]P	21.8	1099.6467	1099.6322	0.0145	1,2,3
13	367.7151	367.7115	0.0036	2	K[16-21]E	14.8	733.4302	733.4229	0.0073	1-4
14	381.5725	381.5681	0.0044	3	Q[7-15]Y	26.3	1141.7175	1141.7044	0.0131	4
15	381.5854	381.5803	0.0051	3	K[8-16]K	19.2	1141.7562	1141.7408	0.0154	2-4
16	397.2250	397.2214	0.0036	2	P[3-9]R	12.3	792.4500	792.4428	0.0072	1-4
17	406.2462	406.2412	0.0050	3	R[9-18]M	25.4	1215.7386	1215.7235	0.0151	1-4
18	419.2325	419.2289	0.0036	2	L[1-8]K	20.4	836.4650	836.4577	0.0073	4
19	427.2589	427.2545	0.0044	3	H[6-15]Y	24.8	1278.7767	1278.7634	0.0133	1-4
20	429.2702	429.2708	-0.0006	1	P[23-26]L	51.4	428.2702	428.2708	-0.0006	1-4
21	440.7411	440.7374	0.0037	2	S[2-9]R	12.4	879.4822	879.4748	0.0074	2-4
22	443.7794	443.7755	0.0040	2	R[9-15]Y	30.4	885.5588	885.5509	0.0079	1-4
23	447.9404	447.9371	0.0033	3	P[3-14]K	22.1	1340.8212	1340.8114	0.0098	2-4
24	448.7730	448.7693	0.0037	2	K[14-20]K	10.9	895.5460	895.5386	0.0074	1-4
25	450.9387	450.9335	0.0052	3	A[5-15]Y	23.3	1349.8161	1349.8005	0.0156	1-4
26	463.2555	463.2551	0.0004	1	F[22-25]I	60.2	462.2555	462.2551	0.0004	1-4
27	469.9461	469.9406	0.0055	3	G[4-15]Y	27.3	1406.8383	1406.8219	0.0164	1-4
28	469.9586	469.9528	0.0058	3	H[6-16]K	20.0	1406.8758	1406.8583	0.0175	4
29	476.9536	476.9478	0.0058	3	S[2-14]K	22.7	1427.8608	1427.8434	0.0174	3,4
30	482.2897	482.2848	0.0049	2	E[1-18]M	35.2	962.5794	962.5696	0.0098	4
31	489.7760	489.7721	0.0040	2	K[16-23]P	18.9	977.5520	977.5441	0.0079	1-4
32	490.2676	490.2641	0.0036	2	M[18-25]I	33.5	978.5352	978.5281	0.0071	1-4
33	490.6119	490.6062	0.0057	3	K[14-25]I	30.4	1468.8357	1468.8185	0.0172	3,4
34	491.6313	491.6257	0.0056	3	Q[7-18]M	25.5	1471.8939	1471.8770	0.0169	4
35	491.6432	491.6378	0.0054	3	R[9-20]K	20.4	1471.9286	1471.9134	0.0162	1,2,4
36	493.6372	493.6318	0.0054	3	A[5-16]K	19.8	1477.9116	1477.8954	0.0162	4
37	493.6381	493.6318	0.0063	3	H[6-17]A	20.9	1477.9143	1477.8954	0.0189	4
38	502.2982	502.2916	0.0066	3	P[3-15]Y	27.4	1503.8946	1503.8747	0.0199	1-4
39	505.3194	505.3114	0.0080	2	I[13-20]K	14.9	1008.6388	1008.6228	0.0160	4
40	507.8265	507.8230	0.0036	2	K[8-15]Y	24.5	1013.6530	1013.6459	0.0071	1,2,4
41	507.8266	507.8230	0.0036	2	R[9-16]K	22.9	1013.6532	1013.6459	0.0073	1-4
42	512.6464	512.6390	0.0074	3	G[4-16]K	22.5	1534.9392	1534.9169	0.0223	3,4
43	520.3136	520.3130	0.0006	1	P[12-15]Y	34.4	519.3136	519.3130	0.0006	3,4
44	528.3059	528.3009	0.0050	3	K[14-26]L	34.6	1581.9177	1581.9026	0.0151	3,4
45	531.3074	531.3022	0.0052	3	S[2-15]Y	26.3	1590.9222	1590.9067	0.0155	1-4
46	533.2922	533.2881	0.0041	2	K[16-24]S	17.8	1064.5844	1064.5761	0.0083	1,3
47	534.3415	534.3361	0.0054	3	K[8-20]K	20.1	1600.0245	1600.0084	0.0161	4
48	534.6572	534.6520	0.0052	3	R[9-21]E	21.6	1600.9716	1600.9560	0.0156	2-4
49	544.9952	544.9899	0.0053	3	P[3-16]K	23.3	1631.9856	1631.9697	0.0159	2-4
50	546.8099	546.8061	0.0038	2	M[18-26]L	44.6	1091.6198	1091.6122	0.0076	1-4
51	551.3195	551.3188	0.0007	1	K[19-22]F	14.8	550.3195	550.3188	0.0007	1-4
52	551.3557	551.3552	0.0005	1	I[13-16]K	18.7	550.3557	550.3552	0.0005	1,3,4
53	553.8427	553.8378	0.0050	2	P[12-20]K	21.5	1105.6854	1105.6755	0.0099	4
54	568.6744	568.6689	0.0055	3	P[3-17]A	24.2	1703.0252	1703.0068	0.0164	2,4
55	569.8362	569.8327	0.0036	2	I[13-21]E	15.5	1137.6724	1137.6653	0.0071	3,4
56	576.3395	576.3392	0.0003	1	F[22-26]L	64.9	575.3395	575.3392	0.0003	1-4
57	577.0275	577.0223	0.0052	3	Q[7-20]K	20.2	1728.0825	1728.0669	0.0156	4
58	582.3397	582.3347	0.0041	2	A[17-26]L	47.8	1162.6574	1162.6493	0.0081	1-4
59	583.6798	583.6748	0.0050	3	R[9-22]F	30.0	1748.0394	1748.0244	0.0150	4
60	586.8276	586.8248	0.0028	2	K[14-22]F	17.9	1171.6552	1171.6496	0.0056	1-4
61	589.8353	589.8301	0.0052	2	K[16-25]I	26.1	1177.6706	1177.6602	0.0104	1-4
62	592.2981	592.2977	0.0004	1	E[21-25]I	65.8	591.2981	591.2977	0.0004	1,2
63	594.3356	594.3322	0.0034	2	S[2-12]P	21.6	1186.6712	1186.6644	0.0068	1
64	612.3531	612.3491	0.0040	3	P[3-18]M	29.7	1834.0593	1834.0473	0.0120	4
65	622.3926	622.3923	0.0003	1	I[13-17]A	15.8	621.3926	621.3923	0.0003	2-4
66	633.3966	633.3970	-0.0004	1	I[11-15]Y	39.3	632.3966	632.3970	-0.0004	1-4
67	640.3483	640.3487	-0.0004	1	K[14-18]M	14.9	639.3483	639.3487	-0.0004	3,4
68	641.3646	641.3598	0.0048	3	S[2-18]M	24.6	1921.0938	1921.0793	0.0145	4
69	646.3749	646.3722	0.0027	2	K[16-26]L	52.6	1290.7498	1290.7443	0.0055	1,3,4
70	648.3718	648.3715	0.0003	1	K[19-23]P	18.0	647.3718	647.3715	0.0003	2
71	648.4076	648.4079	-0.0003	1	P[12-16]K	18.6	647.4076	647.4079	-0.0003	1-4
72	650.8774	650.8742	0.0032	2	L[1-12]P	21.4	1299.7548	1299.7484	0.0064	1-4
73	671.3655	671.3618	0.0037	2	Y[15-25]I	33.6	1340.7310	1340.7235	0.0075	4
74	672.9124	672.9092	0.0032	2	R[9-19]K	23.7	1343.8248	1343.8184	0.0064	2,4
75	672.9127	672.9092	0.0035	2	K[8-18]M	25.3	1343.8254	1343.8184	0.0070	4
76	682.3593	682.3593	0.0000	1	M[18-22]F	18.1	681.3593	681.3593	0.0000	1-4
77	682.7376	682.7311	0.0065	3	R[9-25]I	39.0	2045.2128	2045.1933	0.0195	4
78	684.0626	684.0581	0.0045	3	S[2-19]K	22.0	2049.1878	2049.1743	0.0135	4
79	696.3897	696.3300	0.0597	1	Q[4-9]R	12.6	695.3897	695.3300	0.0597	1-4
80	705.3822	705.3818	0.0004	1	E[21-26]L	68.7	704.3822	704.3818	0.0004	1-4
81	707.4193	707.4163	0.0032	2	L[1-13]I	30.0	1412.8393	1412.8320	0.0065	4
82	727.9081	727.9038	0.0043	2	Y[15-26]L	42.6	1453.8162	1453.8076	0.0086	3,4
83	730.4495	730.4498	-0.0003	1	P[10-15]Y	39.5	729.4495	729.4498	-0.0003	1-4
84	753.3965	753.3964	0.0001	1	A[17-22]F	18.1	752.3965	752.3964	0.0001	1-4
85	753.4333	753.4328	0.0005	1	I[13-18]M	21.5	752.4333	752.4328	0.0005	2-4
86	761.4927	761.4920	0.0007	1	I[11-16]K	23.9	760.4927	760.4920	0.0007	1,3
87	768.4433	768.4437	-0.0004	1	K[14-19]K	12.8	767.4433	767.4437	-0.0004	4
88	771.4677	771.4638	0.0040	2	L[1-14]K	21.7	1540.9354	1540.9275	0.0079	1,3,4
89	833.4762	833.4767	-0.0005	1	K[20-26]L	60.2	832.4762	832.4767	-0.0005	1-4
90	848.4894	848.4876	0.0018	1	K[19-25]I	30.1	847.4894	847.4876	0.0018	1-4
91	852.9981	852.9954	0.0027	2	L[1-15]Y	26.1	1703.9962	1703.9908	0.0054	2-4
92	860.5056	860.5009	0.0047	2	S[2-16]K	20.9	1719.0112	1719.0017	0.0095	2-4
93	881.4908	881.4913	-0.0005	1	K[16-22]F	19.6	880.4908	880.4913	-0.0005	1-4
94	896.0245	896.0194	0.0051	2	S[2-17]A	21.6	1790.0490	1790.0388	0.0102	2,4
95	917.0485	917.0429	0.0056	2	L[1-16]K	24.0	1832.0970	1832.0858	0.0112	4
96	945.5517	945.5461	0.0056	2	P[10-25]I	45.1	1889.1034	1889.0921	0.0113	4
97	961.5740	961.5717	0.0023	1	K[19-26]L	43.1	960.5740	960.5717	0.0023	1-4
98	1002.0928	1002.0881	0.0047	2	P[10-26]L	51.7	2002.1856	2002.1762	0.0094	4
99	1018.0857	1018.0817	0.0040	2	L[1-18]M	29.4	2034.1714	2034.1634	0.0080	4
100	1050.5660	1050.5652	0.0008	1	A[17-25]I	34.4	1049.5660	1049.5652	0.0008	1-4

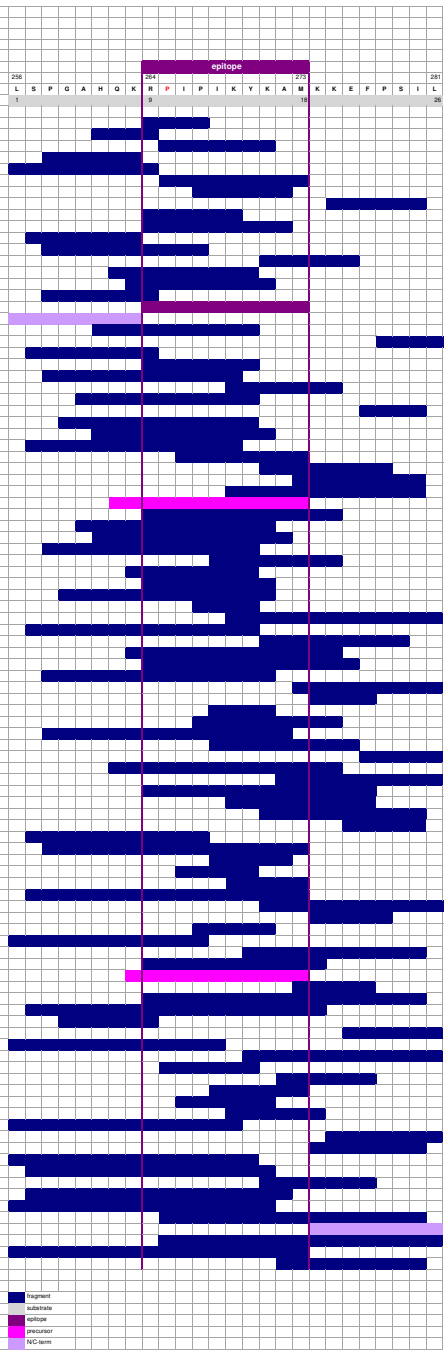

Long-term in vitro expansion ensures increased *yield of central memory T cells as perspective for manufacturing challenges*

Long-term in vitro expansion ensures increased yield of central memory T cells as perspective for manufacturing challenges

Authors: Stefanie Herda[1], Andreas Heimann[1,5], Benedikt Obermayer[2], Elisa Ciraolo[1], Stefanie Althoff[1], Josefine Ruß[1], Corinna Grunert[3], Antonia Busse[4], Lars Bullinger[4], Antonio Pezzutto[3,4,5], Thomas Blankenstein[3,5,6], Dieter Beule[2], Il-Kang Na[1,4,5,7,*]

Supplementary Material

Table of contents:

Supplementary Figures

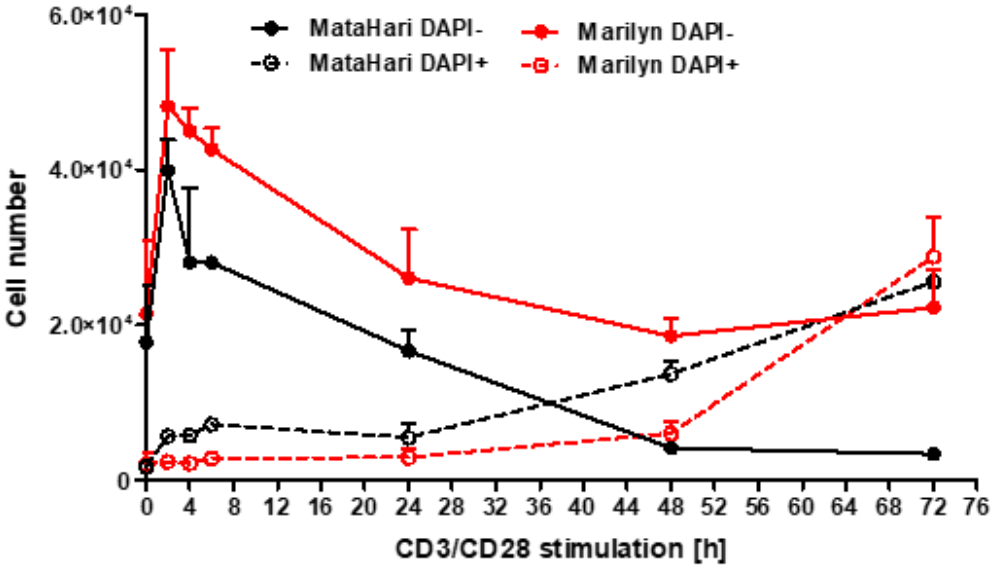

Supplemental Figure 1. Activation of HY-TCR transgenic T cells. Absolute cell numbers (y-axis) are depicted upon anti-CD3/anti-CD28 stimulation over time (x-axis). For differentiation of live and dead/apoptotic cells, the DAPI staining solution was used. Numbers of DAPI positive cells were significantly increased by 72 hours after stimulation.

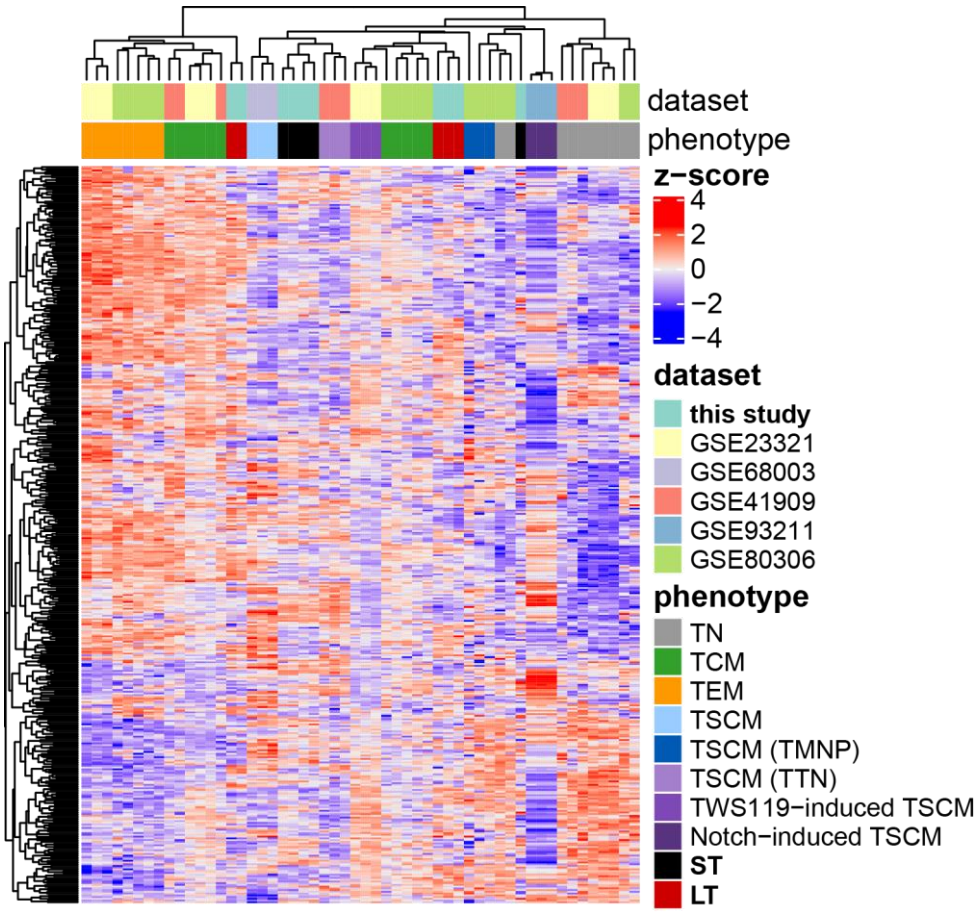

Supplemental Figure 2. Hierarchical clustering of ST and LT CD8$^+$Tcm, IL-7/IL-15-generated Tscm cells (TTN[6], GSE41909), naturally occurring CD8+ T cell subsets (TN, TEM, TCM, TSCM[11, 20, 34, 52], GSE23321), TWS119-enriched Tscm (TSCM[13], GSE68003) and Notch-induced Tscm (iTSCM[12], GSE93211), memory T cells with naïve phenotype (TMNP[23], GSE80306) based on 852 genes described by Gattinoni et al. from which 427 genes were expressed in all datasets. Each column represents a sample and each row a gene. Hierarchical clustering of ST and LT expanded Tcm, naturally occurring CD4$^+$ T cell subsets ([24], GSE61697) and Notch-induced Tscm 12 based on 447 of the Gattinoni et al. genes that are expressed in all datasets. Each column represents a sample and each row a gene.

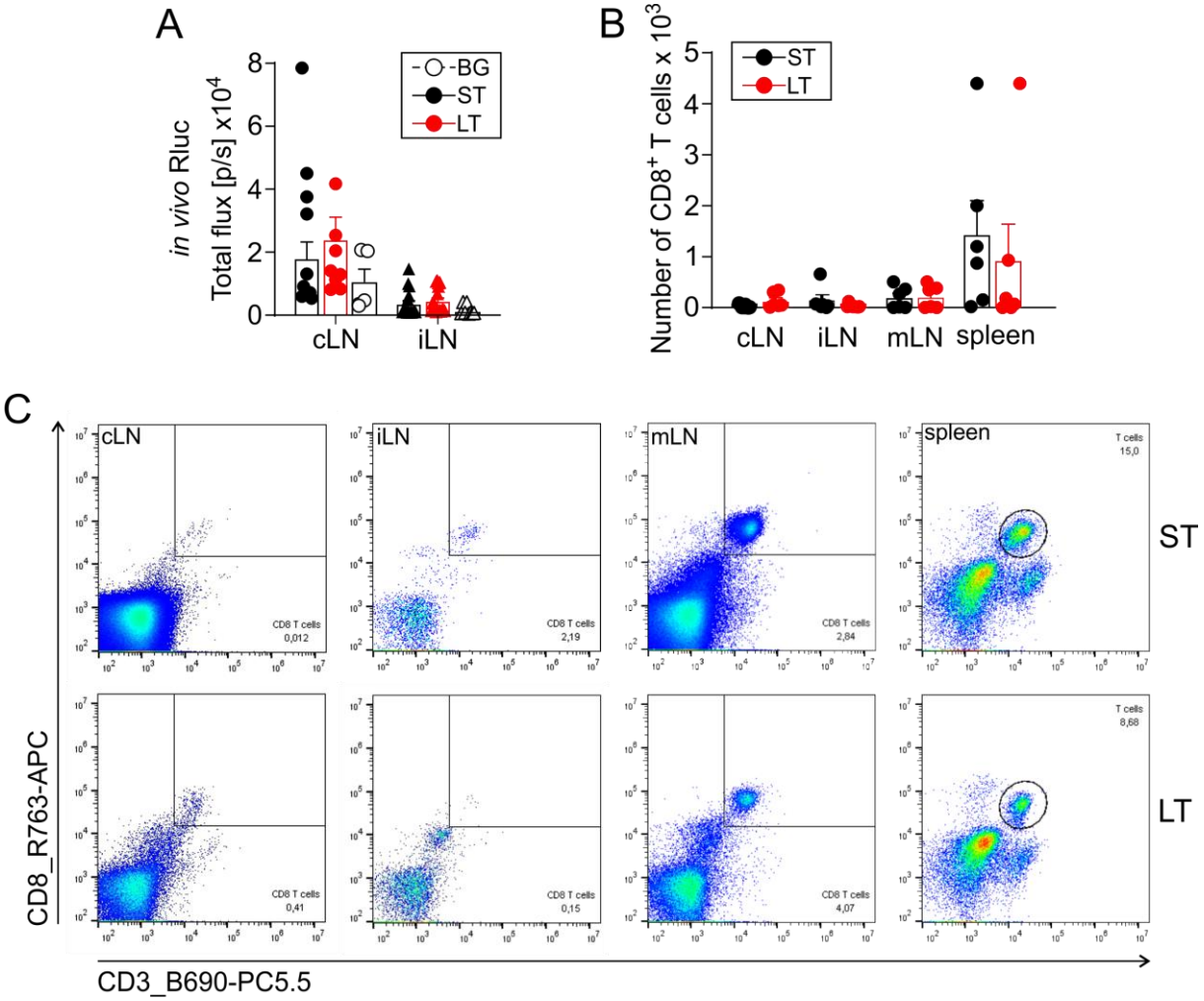

Supplemental Figure 3. Preserved Engraftment in RagKO recipients

(A) Mean ± SEM of Renilla luciferase flux values in cervical (cLN) and inguinal (iLN) one month after transfer of ST and LT T cells. BG=background (B) Number of $CD8^+$ T cell quantified by flow cytometry, *ex* vivo, in cLN, iLN, mesenteric lymph nodes (mLN) and spleen one month after transfer. The bar diagram shows mean data ± SEM of total T cell numbers. (C) Representative flow cytometry plot of $CD8^+$ isolated from cLN, iLN, mLN and spleen six months after transfer. The top row shows dot plots for the ST and the bottom row for the LT group, respectively. All data are representative of 2 independent experiments with n = 6-8 mice/group.

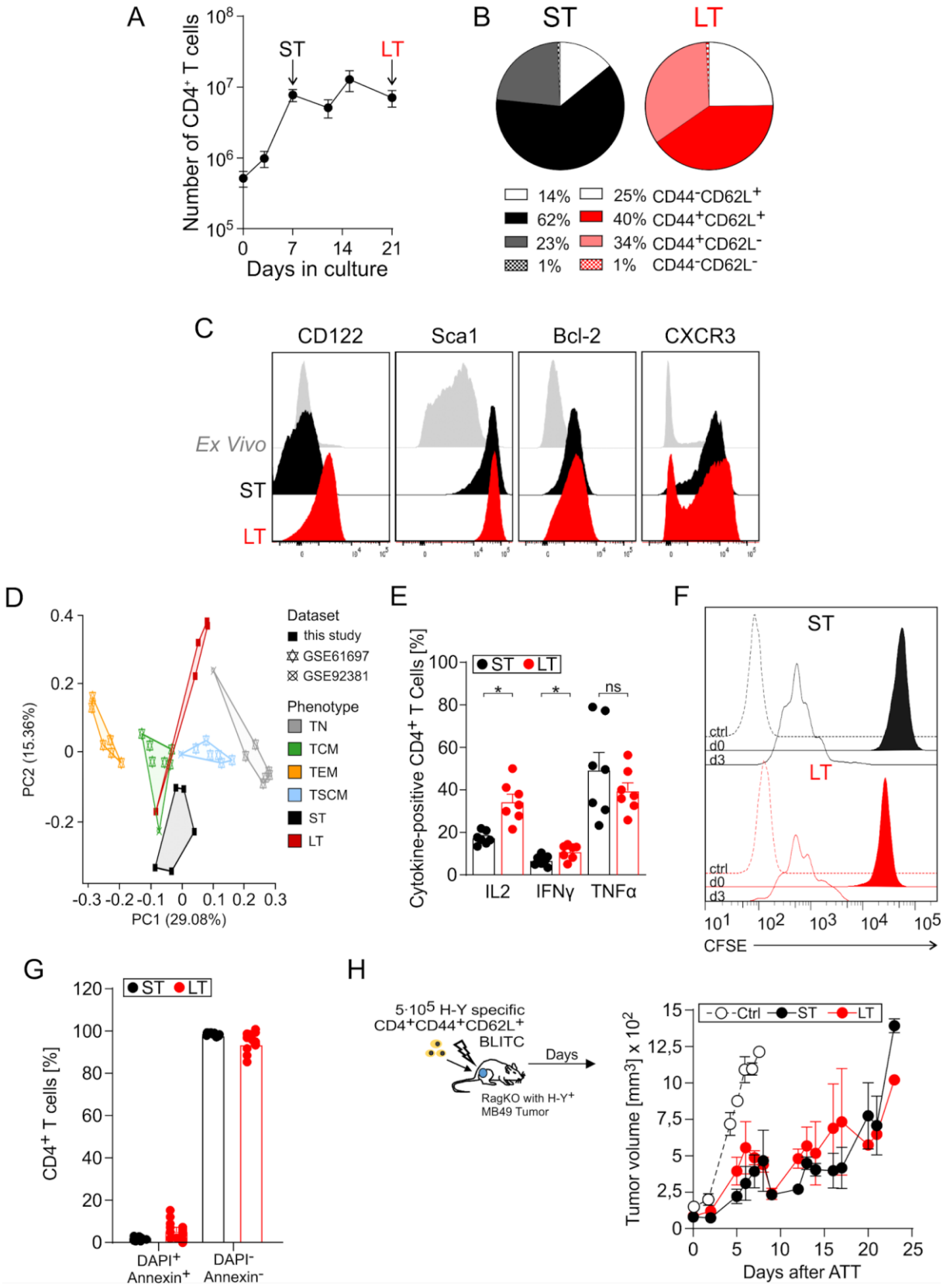

Supplemental Figure 4. ***In vitro*** **expanded CD4$^+$ T cells possesses stem-cell like and preserved functional properties**

Polyclonal murine $CD3^+$ T cells isolated from C57BL/6 mice, activated via anti-CD3/CD28 antibodies (Abs) and IL-2 for 72 hours and further cultured with IL-7/IL-15 for 4 (ST) or 18 (LT) days. (A) Cell growth over the time of $CD4^+$ T cells identified through flow cytometry. The line corresponds to the mean values ± SEM of 5-7 independent experiments with n=5-9 mice. (B) Distribution of $CD4^+$ T cell subpopulations, defined by CD44 and CD62L markers after ST and LT culture. Data were generated in 5-7 independent experiments with n = 5-9 mice. (C) Analysis of CD122, Sca-1, Bcl-2 and CXCR3 expression by flow cytometry, in $CD4^+$ Tcm subset after ST and LT culture and in comparison to *ex vivo* $CD4^+$ T cells. Each expression pick is representative of 3 independent experiments with n = 3 mice. (D) Principal component analysis (PCA) of ST and LT expanded Tcm, naturally occurring $CD4^+$ T cell subsets ([24] GSE61697) and Notch-induced Tscm ([12] GSE92381) based on 447 of the Gattinoni et al. [11, 20, 34, 52] genes that are expressed in all datasets. Each dot represents a sample. (E) Flow cytometry expression profile analysis, of IL-2, IFNγ and TNFα cytokines in ST and LT $CD4^+$ T cells stimulated with anti-CD3/CD28 Abs. Bars show mean frequencies ± SEM. *$p < 0.05$, paired *t*-test. (F) Cell proliferation of ST and LT $CD4^+$ T after stimulation for 24h with anti-CD3/CD28 Abs and after 3 days of culture. Cell proliferation was assessed by using the Carboxyfluorescein Diacetate Succinimidyl Ester (CFSE). Signal intensity of CFSE was detected through flow cytometry. Colored pick corresponds to day 0, the line to day 4 and the dot line correspond to control (ctrl) unstained cells. Pick are representative of two independent experiments, with n=2 mice. Data mean MFI ± SD for ST-d4 = 1067,5 ± 343,6 and for LT-d4 = 597,3 ± 343,6 (G) Flow cytometry analysis of DAPI and Annexin expression in cells stimulated with anti-CD3/CD28 Abs and 3 days culture. The bars show mean frequencies ± SEM of apoptotic and/or dead cells ($Annexin^+$ and/or $DAPI^+$) and living cells ($Annexin^-DAPI^-$) for two independent experiments, with n=2 mice. (H) Left, Scheme for T cell transfer into MB49-tumor bearing female RagKO mice. Right, MB49 tumor growth kinetics after transfer of ST and LT cultured $CD4^+$ cells. Data are displayed by line diagram, mean ± SEM and are generated in two independent experiments with n = 3 mice per group.

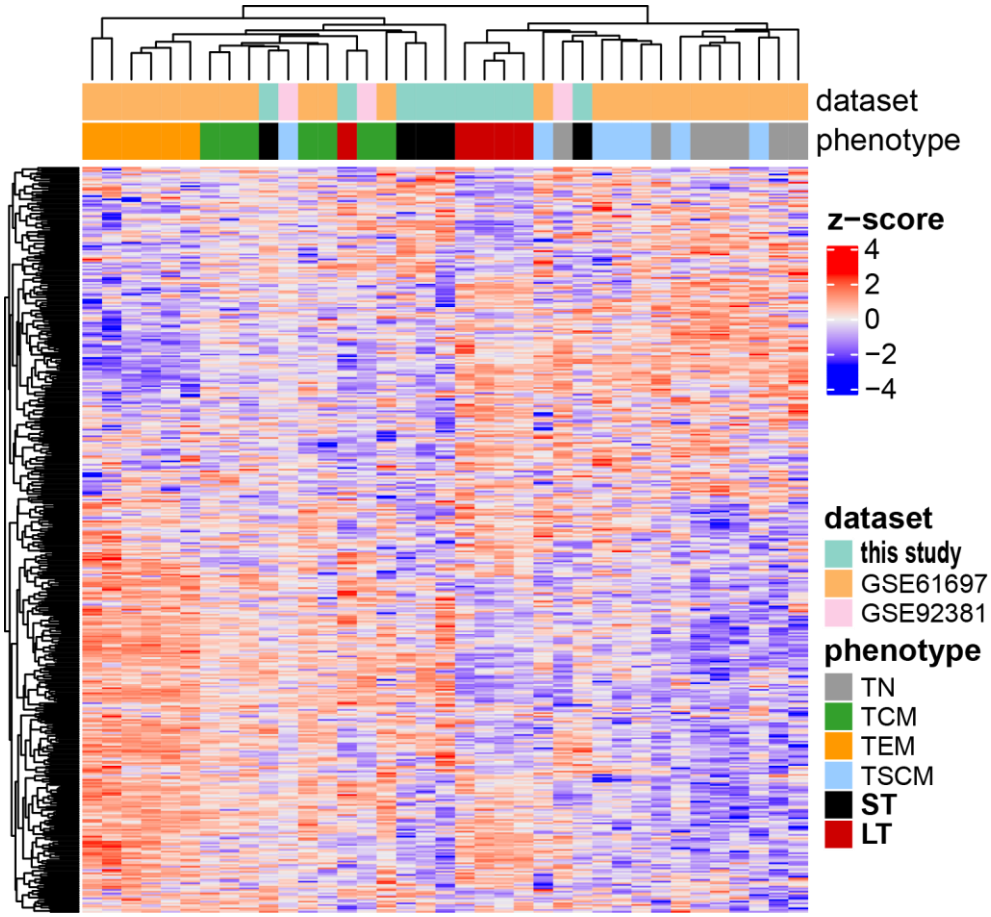

Supplemental Figure 5. Hierarchical clustering of ST and LT CD4$^+$ Tcm, Hierarchical clustering of ST and LT expanded Tcm, naturally occurring CD4$^+$ T cell subsets ([24] GSE61697) and Notch-induced Tscm ([12] GSE92381) based on 447 of the Gattinoni et al. genes that are expressed in all datasets. Each column represents a sample and each row a gene.

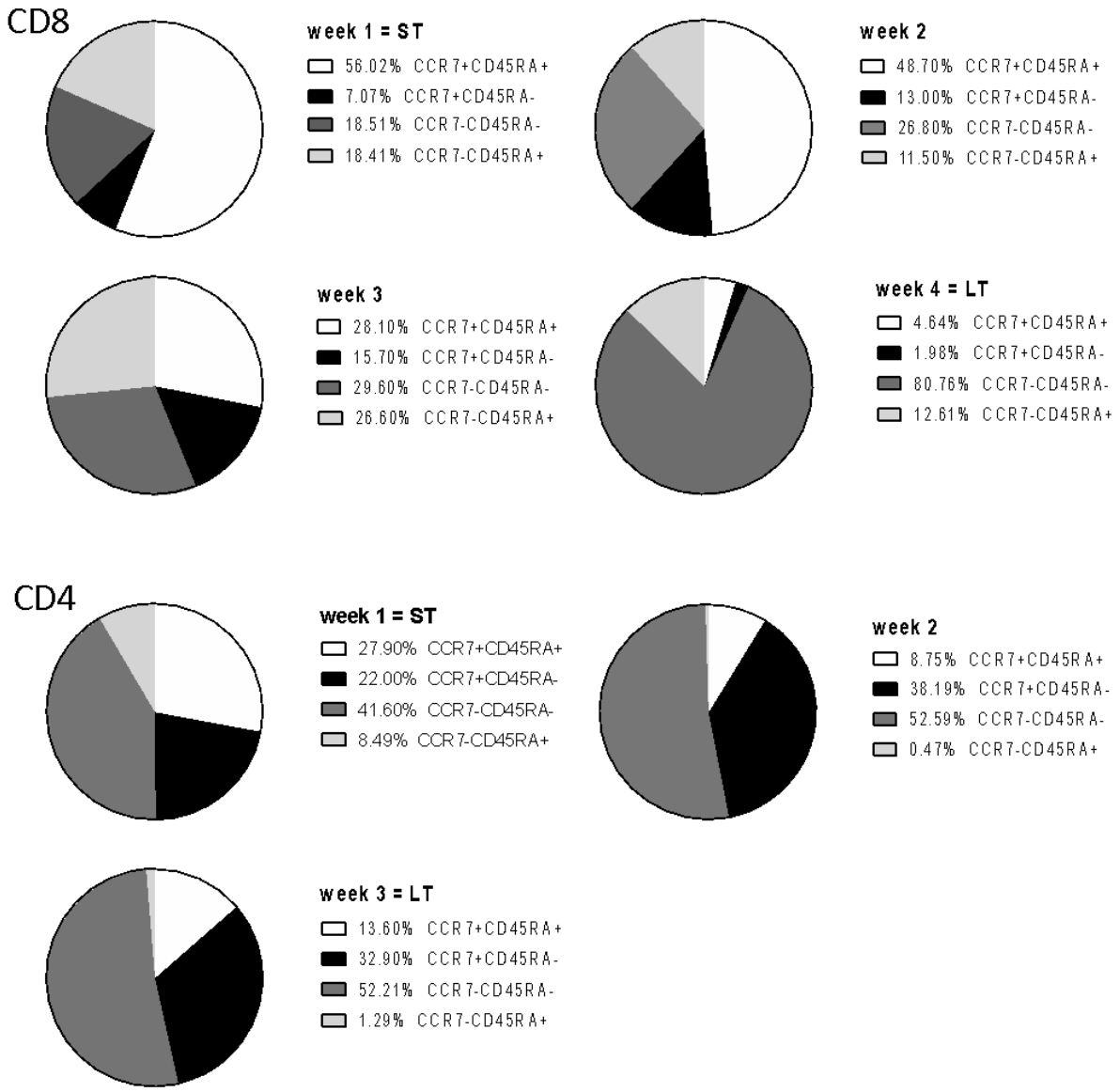

Supplemental Figure 6. Subset distribution of human T cells

Distribution of $CD8^+$ and $CD4^+$ T cell subpopulations analyzed by flow cytometry after staining with CCR7 and CD45RA antibodies.

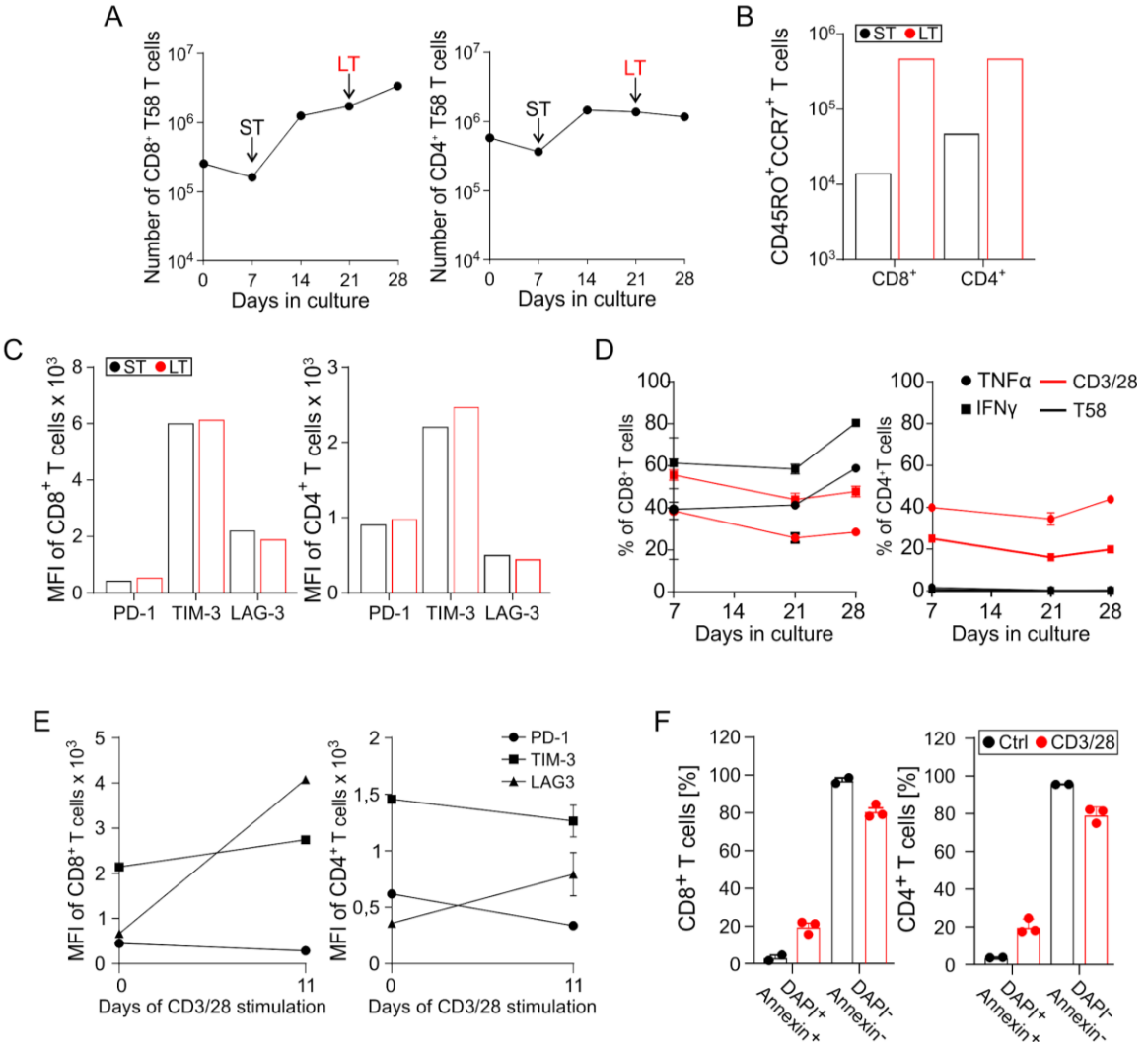

Supplemental Figure 7. Long-term expansion of T cells transduces with the tyrosinase-specific TCR (T58).

(A) Cell culture of human $CD3^+$ T cells isolated from healthy donors after transduction with a tyrosinase-specific TCR-T58 (T58) in a short-term and long-term culture setting. Proportion of $CD8^+/CD4^+$ subtype were identified through flow cytometry. Line diagram are representative of one single transduction experiment. (B) Distribution of $CD8^+/CD4^+$ T cell subpopulation, defined through flow cytometry by staining with CD45RO and CCR7 antibodies. (C) Mean fluorescence intensity (MFI) calculated through flow cytometry of inhibitory T cell receptors (TIRs) during ST and LT culture. (D) Cytokine production after 4h stimulation with anti-CD3/CD28 Abs and T58 specific peptide of $CD8^+$ and $CD4^+$. Analysis was performed through flow cytometry at day 7, 21 and 28 of culture. (E), (F) Flow cytometry expression profile analysis of TIRs, DAPI and Annexin in ST and LT transduced $CD8^+$ and $CD4^+$ after of 11 days of stimulation with anti-CD3/CD28 Abs. Line diagrams and bars are mean values ± SEM of triplicate.

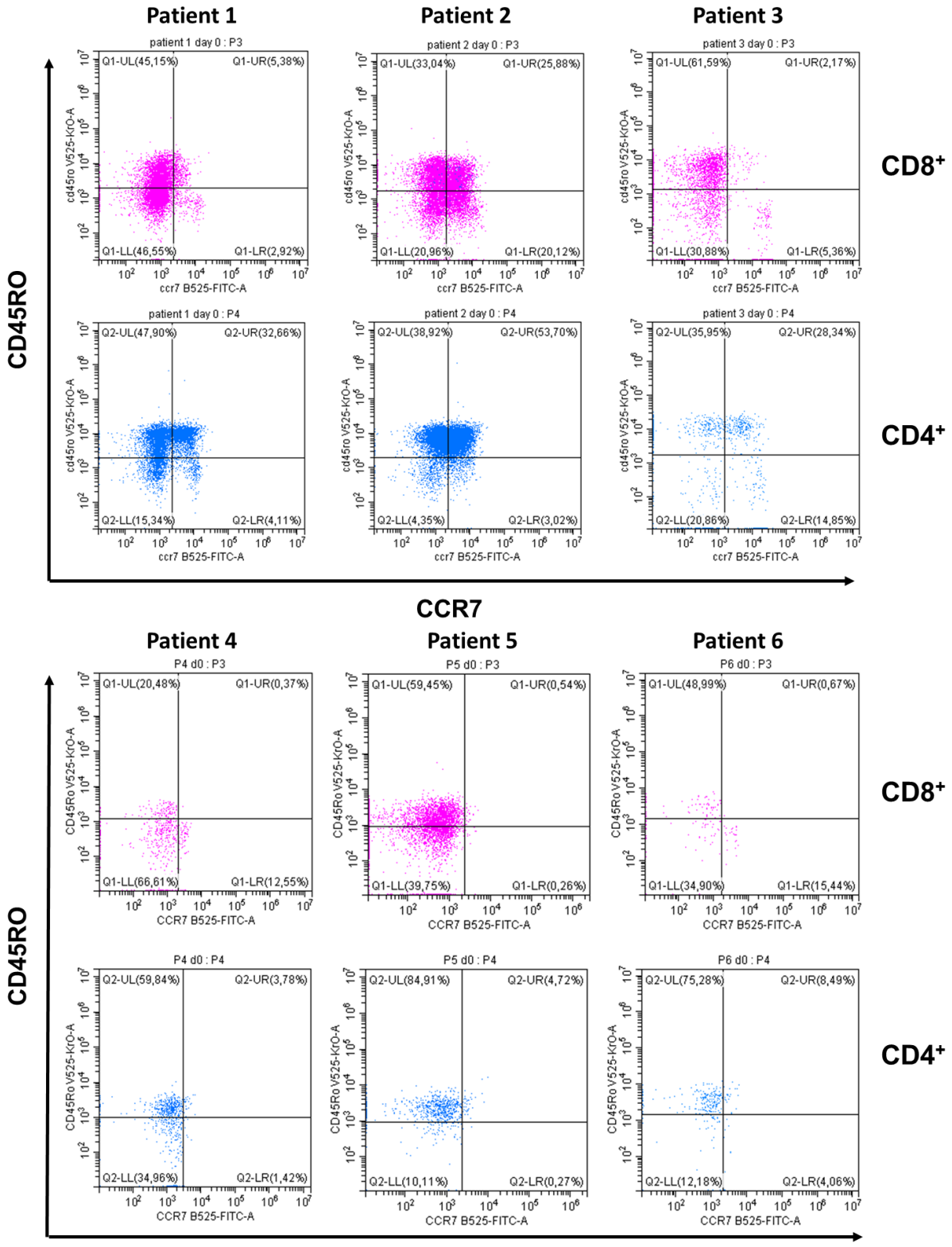

Supplemental Figure 8. CD45RO and CCR7 distribution in DLBCL patients

Representative flow cytometry plot of T cell subpopulation from 6 DLBCL patients by expression analysis of CD45RO and CCR7 for $CD8^+$ and $CD4^+$ T.

Supplementary Tables

Supplemental Table 1. List of mice

Marilyn-BLITC	Marilyn-TCR$^{+/+}$Rag1$^{-/-}$NFAT-CBR$^{+/+}$Rluc$^{+/+}$	Donor
albino B6	C57BL/6(Cg)-Tyrc-2J	Recipient
albino RagKO	B6.129S6-Rag2tm1Fwa N12-Tyrc-2J	Recipient

Supplemental Table 5. Sequencing Coverage and Quality Statistics_ RNA sequencing (RNAseq)

Sample ID	Total number of sequenced reads	Total number of uniquely mapped reads	RNA integrity number (RIN)	Ratio of all reads aligned to rRNA regions.	Expression Profile Efficiency	Total number of detected transcripts	group
Sample_456	26099881	8533815	9,3	0.0050468813	0.7628531	33331	IL.7.15_w1_batch3,
Sample_459	39724193	11998646	9,1	0.0009133729	0.75237286	33663	IL.7.15_w4_batch3
Sample_462	23566148	7600295	9,2	0.006043371999999999	0.7484026	33126	IL.7.15_w1_batch4
Sample_465	25697366	8378599	8,9	0.0052117403	0.74760145	32866	IL.7.15_w4_batch4
Sample_474	24382802	8030759	9,5	0.001497777	0.72920936	32455	IL.7.15_w1_batch6
Sample_477	28888177	9336758	9,6	0.0006676434	0.72272176	32503	IL.7.15_w4_batch6
Sample_591	37514081	11940036	9,9	0.0027670944	0.79164356	33887	IL.7.15_w1_batch8,
Sample_595	34934693	11653855	7	0.00453947	0.7498090000000001	33317	IL.7.15_w4_batch8
Sample_599	18475414	7172733	9,3	0.004400713400000001	0.76146996	32333	IL.7.15_w1_batch9
Sample_603	32568258	9635931	9,1	0.005949566	0.74925005	32956	IL.7.15_w4_batch9
Sample_1060	33210709	10807310	9,8	0.0038528538	0.76361513	32731	IL.7.15_w1_batch5
Sample_1063	31574028	10535411	9,5	0.0036153765	0.748688	32681	IL.7.15_w3_batch5
Sample_1066	31506726	10668808	9,8	0.004861978	0.7287857	32872	IL.7.15_w1_batch6
Sample_1069	31700829	10745722	10	0.0033605115000000002	0.76069397	32961	IL.7.15_w3_batch6
Sample_1072	26402533	9253255	10	0.0025941073	0.78328806	32213	IL.7.15_w1_batch7
Sample_1075	33320786	11630924	8,1	0.0077243675	0.7343028	32434	IL.7.15_w3_batch7
Sample_1078	32002243	11069523	9,9	0.0041307416	0.78739476	32630	IL.7.15_w1_batch8